博士論文

Kinetics of virus inactivation by disinfection in drinking water treatment

(浄水処理の消毒工程におけるウイルス不活化の速度論的解析)

Shotaro TORII

鳥居　将太郎

A dissertation submitted to the Graduate School of Engineering, The University of Tokyo in partial fulfillment of the requirements for the degree of

Doctor of Philosophy

Examination committee: Professor Hiroyuki KATAYAMA (chairperson)

Professor Hiroaki FURUMAI

Associate Professor Kumiko OGUMA

Assistant Professor Takashi HASHIMOTO

Associate Professor Daisuke SANO

Department of Urban Engineering

School of Engineering

The University of Tokyo

2020

Table of Contents

Abstract

Virus is one of the major microbial contaminants to cause waterborne diseases. Due to its low infectious dose, the acceptable concentration in drinking water is extremely low. This requires the regulators to achieve a high reduction through water treatment The conventional physical treatment has limited capacity to remove viruses: approximately 0 – 3-log for the activated sludge process (Hata et al., 2013; Katayama et al., 2008; Sano et al., 2016), 2-log for coagulation-sedimentation, and <1-log for rapid-sand filtration (Asami et al., 2016; Kato et al., 2018) in full-scale treatment plants. Thus, the current treatment system virtually relies on the disinfection process for reducing viruses. The allocable log reduction value (LRV) of the chemical disinfection is up to 6-log for chlorination, UV irradiation, and ozonation (Olivieri et al., 2016; Soller et al., 2018). Therefore, the efficacy and potential uncertainty of disinfection efficiency on virus reduction should be carefully examined.

In chapter 3, the inactivation kinetics of viruses were analyzed by a continuous quench flow reactor. Ozone has a strong oxidation power that allows effective inactivation of waterborne viruses. Few studies have accurately measured the kinetic relationship between virus inactivation and ozone exposure, because the high reactivity of ozone makes it difficult to measure them simultaneously. A continuous quench flow system (CQFS) is a possible solution for analyzing such a fast reaction; however, previous studies reported that CQFS provided different results of inactivation rate constants from the batch system. The objectives of this study were (1) to develop a CQFS to evaluate the kinetics of microbial inactivation accurately, (2) to evaluate the inactivation rate constants of the waterborne virus by ozone, and (3) to compare the results with previous studies. The results indicated that the simple plug flow assumption in the reaction tube of CQFS led to an underestimation of the rate constants. The accurate measurement of rate constants was achieved by the pseudo-first-order reaction model that takes the residence time distribution (RTD; i.e., the laminar flow assumption) into account. The results of inactivation experiments suggested that the resistance of viruses were getting higher in the following order: Qβ < MS2, fr, GA < CVB5 Faulkner, φX-174, PV1 Sabin, CVB3 Nancy. Predicted CT values for 4-log inactivation ranged from 0.018 mg sec L^{-1} (Qβ) to 0.16 mg sec L^{-1} (CVB3 Nancy strain). The required CT values for 4-log PV1 inactivation was 0.15 mg sec L^{-1}, which was 166-fold smaller than those reported in the United States Environmental Protection Agency guidance manuals. The overestimation in previous

studies was due to the sparse assumption of RTD in the reactor. Consequently, the required ozone CT values for virus inactivation should be reconsidered to minimize the health risks and environmental costs in water treatment.

In Chapter 4, the objectives of this study were (i) to examine a total of 35 environmental stains of F-RNA phage genotype GI collected in Tama and Sagami rivers for free chlorine resistance, and (ii) to develop the inactivation model to predict the overall inactivation efficiency of heterogeneous F-RNA phage GI strains by assuming a probability density function of free chlorine resistance. The results indicated that most environmental strains of F-RNA phage GI exhibited higher free chlorine resistance than MS2 and fr, laboratory strains of GI phage. The developed model suggested that the overall inactivation efficiency of GI phages was limited to 5.6 log and 5.3 log in Tama and Sagami river, respectively, in the case that 8 log MS2 inactivation was expected. Therefore, the heterogeneity in free chlorine resistance within specific reference pathogens should be incorporated into the model to accurately predict the inactivation efficiency in environmental water.

In chapter 5, the objectives were (1) to evaluate the variability in susceptibility to three major disinfectants (free chlorine (FC), $UV_{254,}$ and ozone) among environmental strains of coxsackievirus B5 (CVB5), (2) to characterize the genetic feature contributing to lower susceptibilities to the disinfectants, and (3) to develop a model to predict the overall inactivation efficiency of heterogeneous CVB5. A total of 12 strains of CVB5 and Faulkner strain were examined for disinfection susceptibility by bench-scale experiments. Inactivation kinetics were analyzed by the Chick-Watson model as a function of disinfectant exposure (i.e., CT value or UV dose). The whole genome was obtained by RNA sequencing. The disinfection susceptibilities were different by up to 3.4-fold in FC, 1.3-fold in UV_{254}, and 1.8-fold in ozone among CVB5 strains. Interestingly, CVB5 in genogroup B exhibited significantly lower susceptibility to FC and ozone than genogroup A, to which the Faulkner strain belongs. The capsid protein in genogroup B contained less number of sulfur-containing amino acids, which is readily reactive to oxidants. FC susceptibility showed a significantly positive correlation ($r=0.66$, $P<0.05$) with ozone susceptibility. To predict the overall inactivation efficiency of CVB5s, a probability density function (i.e. gamma distribution) of inactivation rate constants (k) were incorporated into the conventional Chick-Watson model. The modified model indicated that 4.2-fold, 1.2-fold, and 1.5-fold larger CT or dose are required to achieve 6-log overall inactivation of heterogeneous CVB5 than the prediction based only on the lab strain (i.e. Faulkner stain) in FC, UV_{254}, and ozone, respectively The disinfection susceptibilities,

especially in FC, were variable within the same genotype. Therefore, the homogeneous assumption of disinfection susceptibility should be avoided. A probability density function of disinfection susceptibility should be incorporated to predict the overall inactivation of reference pathogen.

Chapter 1

Introduction

1. Background

Virus is one of the major microbial contaminants to cause waterborne diseases. Due to its low infectious dose, the acceptable concentration in drinking water is extremely low. For instance, the virus concentration in drinking water should be less than 1 /90,000 L to achieve 10^{-6} DALYs/year/person (World Health Organization, 2011). This requires the regulators to achieve a high reduction through water treatment (e.g., 12-log reduction for indirect potable reuse in the state of California (Title 22 and 17 California Code of Regulations, 2015). The conventional physical treatment has limited capacity to remove viruses: approximately 0 – 3-log for the activated sludge process (Hata et al., 2013; Katayama et al., 2008; Sano et al., 2016), 2-log for coagulation-sedimentation, and <1-log for rapid-sand filtration (Asami et al., 2016; Kato et al., 2018) in full-scale treatment plants. Thus, the current treatment system virtually relies on the disinfection process for reducing viruses. The allocable log reduction value (LRV) of the chemical disinfection is up to 6-log for chlorination, UV irradiation, and ozonation (Olivieri et al., 2016; Soller et al., 2018). Therefore, the efficacy and potential uncertainty of disinfection efficiency on virus reduction should be carefully examined.

The efficacy of disinfectant on virus inactivation has been a great interest for researchers. Inactivation of viruses is generally evaluated as a function of disinfectant exposure (i.e, the time-dependent disinfectant concentration integrated over time) (USEPA, 1999). The disinfectant exposure is specifically described as CT values in the case of chlorination and ozonation and described as dose in case of UV irradiation. Many researchers has investigated the effect of physic-chemical parameters, temperature, pH, etc., have been studied from several decades ago (Gerba et al., 2002; Meng and Gerba, 1996; Sobsey et al., 1988). Currently, these studies has been collected and meta-analyzed in major disinfectants (free chlorine, monochloramine (Cromeans et al., 2010; Rachmadi et al., 2020), and ultraviolet irradiation (Gerba et al., 2002; Hijnen et al., 2006)). However, there are still remaining research gaps related virus inactivation with disinfectant as below.

Firstly, few studies evaluated the relationship between ozone exposure and waterborne virus inactivation. The lack of ozonation studies was mainly due to the difficulty of measuring both the CT value and the rate of virus inactivation simultaneously. Ozone is

quickly decomposed in the aqueous phase (Gardoni et al., 2012) and consumed by organic substances contained in the virus stock solution (Dunkin et al., 2017). Furthermore, measurable virus inactivation is often completed within several seconds after contact with ozone (Hall and Sobsey, 1993; Shin and Sobsey, 2003). Hence, most ozonation studies miss either information on the CT value or the rate of virus inactivation (Finch and Fairbairn, 1991; Hall and Sobsey, 1993; Herbold et al., 1989; Shin and Sobsey, 2003; Sigmon et al., 2015; Thurston-Enriquez et al., 2005).

In addition, inactivation efficiency was tested only for limited strains of viruses, mainly laboratory strain. Also, their impact on inactivation prediction was not comprehensively discussed. Most single-stranded RNA (ssRNA) viruses, including norovirus and enterovirus, are prone to mutate frequently (Sanjuan et al., 2010) due to the lack of proof-reading mechanisms during replication. The mutation in the structural protein-coding region may change the amino acid composition of the capsid. This may alter the chemical reactivity of the capsid against oxidant resulting in different inactivation kinetics since reaction rate constants between amino acids and oxidants differ among the type of amino acids. However, only a few studies discussed this topic. To fill the research gaps, in chapter 3 and 5, the disinfection susceptibility of environmental strains were investigated. Then, the conventional inactivation model was expanded to allow us to predict the overall inactivation efficiency of a specific reference pathogen, which is inherently heterogeneous.

2. Objectives

The specific objectives of this dissertation were as below.

Chapter 3 aimed to (1) to develop a continuous quench flow reactor and pseudo-first-order kinetics model that considers residence time distribution for accurate measurement of inactivation rate constants by ozone, (2) to evaluate inactivation rate constants for the waterborne virus inactivation, and (3) to compare the results with previous studies and USEPA guidance manual CT values.

Chapter 4 aimed to (1) examine a total of 35 environmental stains of F-RNA phage genotype GI collected in Tama and Sagami rivers for free chlorine resistance, and (2) to develop the inactivation model to predict the overall inactivation efficiency of heterogeneous F-RNA phage GI strains by assuming a probability density function of free chlorine resistance.

Chapter 5 aimed to (1) to evaluate the variability in susceptibility to three major disinfectants (free chlorine, UV_{254}, and ozone) among environmental strains of coxsackievirus B5 (CVB5), (2) to characterize the genetic feature contributing to lower susceptibilities to the disinfectants, and (3) to develop a model to predict the overall inactivation efficiency of heterogeneous CVB5.

3. Structure of the dissertation

This dissertation consists of six chapters and an appendix section as shown in Figure 1. Chapter 1 includes the background information and objectives of the present dissertation. Chapter 2 provides the previous studies on virus disinfection efficiency, mechanism, and prediction framework. In Chapter 3, a continuous quench flow reactor was delivered and validated to analyze the inactivation kinetics of viruses by ozone. In Chapter 4, taking the F-RNA phage GI type as an example expanded first-order inactivation model was presented to allow for predicting overall inactivation efficiency. In Chapter 5, the environmental strains of coxsackievirus B5 were disinfected by free chlorine, UV_{254}, and ozone. Then, the heterogeneity in kinetics rate constants was incorporated into first-order reaction models.

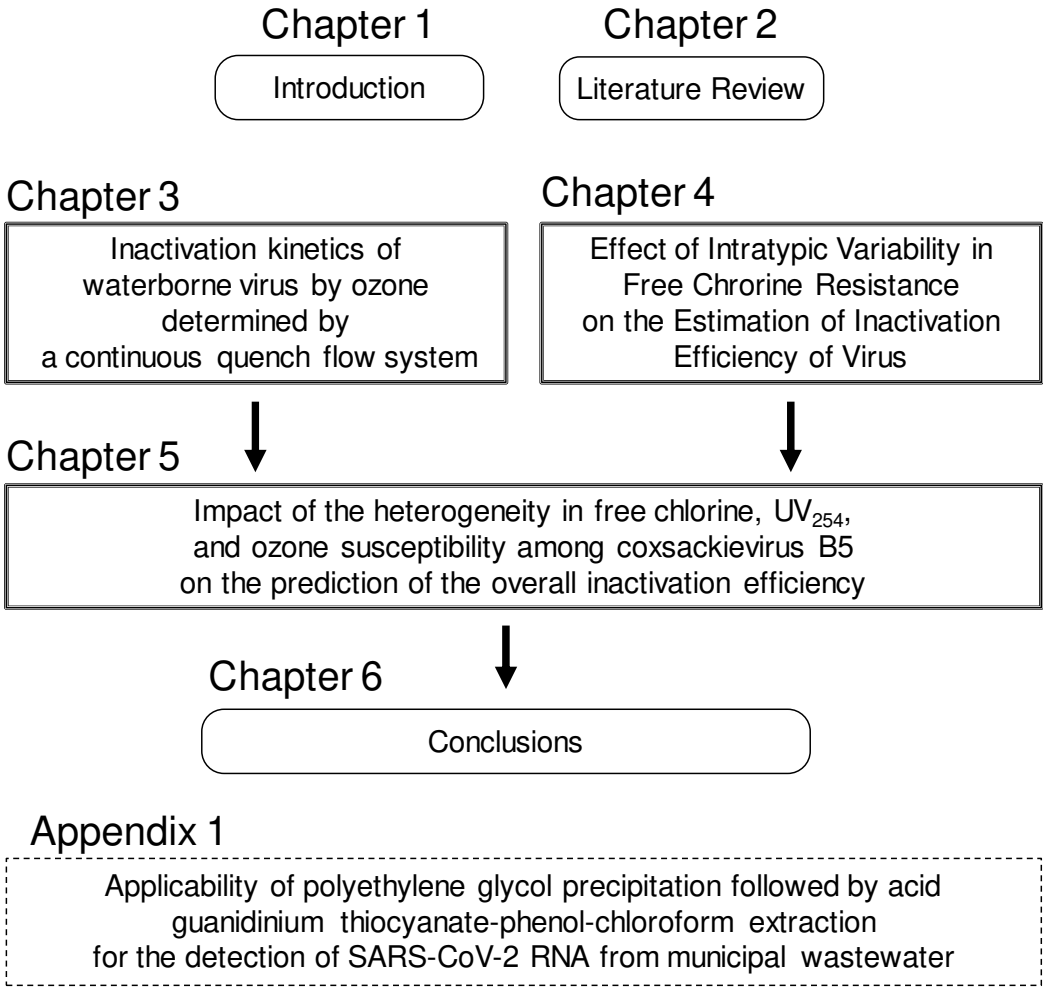

Figure 1 Structure of the dissertation

Chapter 2

Literature review

1. Importance of viruses to ensure the microbial safety of drinking water

It is fundamental to control the microbial risks stemming from the ingestion of drinking water. Around 29 % of the global population lacks access to safely-managed drinking water as of 2015 (World Health Organization, 2017). Drinking water contaminated with enteric pathogens leads to cause a variety of waterborne diseases (e.g., diarrhea). Diarrheal diseases caused 1.66 million death in 2016 and were listed in the top 10 global causes of death between 2006 and 2016 (Naghavi et al., 2017). Although waterborne outbreaks have been decreasing dramatically since the 1900s, the burden of waterborne diseases cannot be ignorable (Collier et al., 2021). According to waterborne disease outbreak (WBDO) statistics in the United States between (Craun et al., 2006), the annual number of endemic acute gastrointestinal illness cases associated with consumption of public drinking water in the United States has been estimated to range from 4.3 to 11.7 million cases and from 5.5 to 32.8 million cases. These studies highlight the importance of the continuous study on health-related water microbiology.

Enteric viruses are one of the most important causative agents of waterborne gastroenteritis. Due to their small size, the physical process, such as filtration, does not remove effectively. Specific viruses may be less sensitive to disinfection than bacteria and parasites (e.g. enterovirus is more resistant to chlorination; adenovirus more resistant to ultraviolet irradiation). Viruses can persist for long periods in water. Infective doses are typically low. Therefore, the control of viruses in drinking water is a critical issue for water treatment.

2. Enteric viruses

Enteroviruses, rotaviruses, and norovirus have been identified as potential reference pathogens (World Health Organization, 2011) under the framework of quantitative microbial risk assessment (QMRA).

2.1. Enterovirus

Enterovirus is a non-enveloped positive-sense single-stranded RNA virus and a

member of the *Picornaviridae* family. The enteroviruses were further classified into several species, such as *Poliovirus* (including genotype of poliovirus 1 (PV1), PV2, PV3), *Enterovirus A* (including genotype of coxsackievirus A2 (CVA2), CVA3 –CVA10, CVA12, CVA14, CVA16, enterovirus 71 (EV71), EV76), *Entervorius B* (including genotype of coxsackievirus B1 (CVB1), CVB2-CVB6, CVBA9, echovirus 1 (E1), E2-E7, E9, E11-E33, EV69, EV73, EV74, EV75, EV77, EV78), *Enterovirus C* (including CVA1, CVA11, CVA13, CVA17, CVA19, CVA20-CVA22, CVA24) and *Enterovirus D* (including genotype of EV68, EV70) (King et al., 2012). The virion consists of an icosahedral capsid, without an envelope, surrounding a core of single-stranded RNA. The diameter is approximately 30 nm. The capsid is composed of 60 identical units, each consisting of three surface proteins, named VP1, VP2, VP3, and an internal protein, named VP4. The single-stranded RNA has approximately 7.5 kb in size and possesses a single long open reading frame (ORF) (Figure 2). The genotyping of enterovirus is generally performed targeting the VP1 region using developed primers (Oberste et al., 2003) (Figure 2). The VP1 encodes important serotype-specific neutralization epitopes. Thus, the results of genotyping are well corresponding with those of serotyping (Oberste et al., 1999).

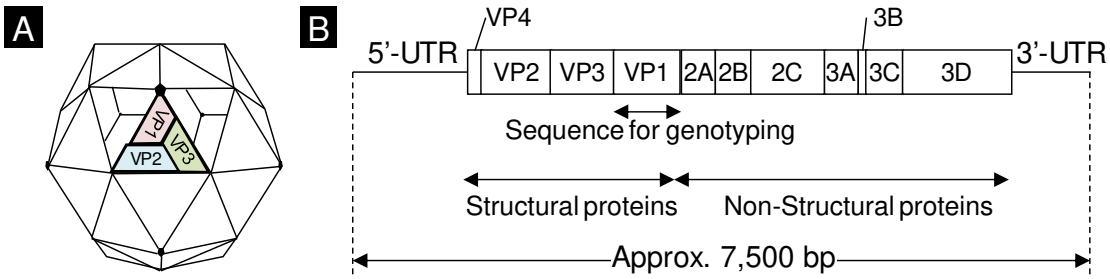

Figure 2 Basic information of enterovirus

Figure A indicates the structural illustration of enterovirus. Figure B indicates the schematic overview of the enterovirus genome.

Enterovirus can cause mild febrile illness but are also important causative agents of severe diseases, such as paralysis, meningitis and encephalitis, in children. There is a dose-response model for enteroviruses, and there is a routine culture-based analysis for measuring infective particles (Gerba and Betancourt, 2019). Due to their relatively higher availability of viral assays, Enterovirus is one of the most well-investigated agents in the academic field of health-related water microbiology.

Enteroviruses are excreted in very large numbers by infected patients, and waters contaminated by human waste could contain high concentrations.

2.2. Other important reference pathogens (rotavirus and norovirus)

Rotaviruses are the most important cause of gastrointestinal infection in children and can have severe symptoms, including hospitalization and death, with the latter being more frequent in low-income regions. There is a dose-response model for rotaviruses (Gerba et al., 1996) , but there is no routine culture-based method for quantifying infectious units. Typically, rotaviruses are excreted in very large numbers by infected patients, and waters contaminated by human waste could contain high concentrations. Occasional outbreaks of waterborne disease have been recorded.

Noroviruses are a major cause of acute gastroenteritis in all age groups. Symptoms of illness are generally mild and rarely last longer than 3 days; however, the infection does not yield lasting protective immunity. Hence, the burden of disease per case is lower than for rotaviruses. Numerous outbreaks have been attributed to drinking water. A dose–response model has been developed to estimate infectivity for several norovirus strains (Teunis et al., 2008). Although the cultivation of norovirus was recently succeeded (Ettayebi et al., 2016), no widely applicable method is available so far.

3. Inactivation of viruses by disinfection

Disinfection is commonly applied to inactivate viruses in water treatment. The disinfection method is classified into physical treatment and chemical treatment.

The physical treatment includes ultraviolet (UV) irradiation, sunlight exposure, heat, and sonic or hydrodynamic pressure. These processes inactivate viruses by causing structural change on nucleic acid, as exemplified by UV, denaturing proteins, as exemplified by heat, or structural damage (sonic or hydrodynamic pressure). Except for UV irradiation, physical disinfection is not commonly used for large-scale water treatment.

Chemical disinfectants inactivate waterborne pathogens by chemically degrading viral capsid or nucleic acids. In the context of water treatment, oxidants, such as hypochlorite, chlorine dioxide, and ozone, are widely adopted. The efficacy of chemical oxidants thus depends strongly on their reactivity with biomolecules (proteins and nucleic acids). In

addition, both the disinfectant concentration throughout the treatment, as well as the duration of the disinfection treatment (exposure time) are important parameters determining the disinfection efficiency.

3.1. Inactivation mechanism of single-stranded RNA viruses

The UV emitting light at 253.7 nm, so-called the low-pressure (LP) UV, induces photochemical reactions at pyrimidine bases of viral RNA. This reaction forms pyrimidine dimers or RNA-protein cross-links, resulting in the inhibition of RNA replication and inactivate RNA viruses (Bolton and Linden, 2003). Previous experiments have reported that the rate of genome degradation comparably matched 1:1 with the rate of infectivity loss of bacteriophage MS2 and CVB5 Faulkner (Beck et al., 2016; Pecson et al., 2011; Rockey et al., 2020; Simonet and Gantzer, 2006). These results indicate that the inactivation by LPUV can be largely explained by genome degradation in structural viewpoints and by loss of replication capacity from the functional viewpoint.

The inactivation mechanism by other UV sources emitting light of shorter wavelength (200 – 240 nm), such as KrCl excimer lamp, or that of longer wavelength (260 – 300 nm), such as UV-LED, have not been consistently discussed; For example, inactivation of MS2 by the UV light at 220 – 300 nm was mostly explained by a damage on the genome (Beck et al., 2016). Also, the inactivation of Tulane virus, single-stranded RNA virus and a cultivable surrogate for human norovirus, is explained by genome and capsid damage. These findings are different from the result of adenovirus, double-stranded DNA viruses (Beck et al., 2016; Hull and Linden, 2018; Oh et al., 2020) and rotavirus, double-stranded RNA virus (Araud et al., 2020); the inactivation by UV light emitting a shorter wavelength is mainly explained by the damage on protein. Thus, the inactivation of RNA viruses by other UV sources rather than LPUV should be further investigated.

Free chlorine is referred to as a sum of two chlorine species hypochlorous acid (HOCl) and its conjugated base, hypochlorite (OCl-). HOCl is a weak acid (pKa=7.54 at 25°C) and strong oxidant (E_0=1.49 V at 25°C;), while OCl- is a weaker oxidant compared with HOCl (E_0= 0.9 V at 25°C, (Copeland and Lytle, 2014)). The neutrally charged HOCl can penetrate the outer layers of microorganisms more readily compared to the negatively charged OCl-, and thus react with the intracellular building blocks of microorganisms. The inactivation mechanism of viruses by free chlorine has been explained from both structural and functional viewpoints. Previous studies suggested that the main component contributing to virus inactivation is the induced damage on both genome and capsid,

where the contribution to inactivation is different depending on the virus. The study using hepatitis A virus, poliovirus, echovirus 11 suggested that capsid damage contributed to virus inactivation dominantly (Nuanualsuwan and Cliver, 2003; Zhong et al., 2017a). On the other hand, the study using bacteriophage MS2, fr, GA reported the contribution of both capsid and genome damage on inactivation (Sigstam et al., 2013; Wigginton et al., 2012). From the functional viewpoint, a study employing echovirus 11 revealed that the loss of binding capacity to host cell accounted for 60% of virus inactivation (Zhong et al., 2017a). Other studies employing MS2 showed that the loss of replication and injection ability mostly explained the inactivation by free chlorine (Wigginton et al., 2012). Taken together, the virus inactivation mechanism by free chlorine is the loss of function, including either attachment, genome internalization, or replication, cause by capsid and genome damage.

Ozone is one of the strongest oxidizers, having a reduction potential of $E_0 = 2.07V$, and adopted as an advanced oxidation process in water treatment. The studies on virus inactivation have been limited and inconsistent compared with other disinfectants due to the difficulties of ozonation experiments, such as the control of exposure caused by the instability of aqueous ozone (Gardoni et al., 2012). Thus, the proposed inactivation was also inconsistent among studies. (Kim et al., 1980) employed bacteriophage f2 as a model virus and found that the ozone disrupted the capsid protein of phage f2 into subunits, liberating RNA into the solution and losing adsorption to the host pili. Their proposed mechanism was that the coat protein may be involved in the inactivation of RNA, probably by a secondary reaction of the RNA with the protein molecules modified by ozonation. Other studies employed laboratory strains belonging to the member of enteroviruses (Jiang et al., 2019; Roy et al., 1981; Torrey et al., 2019) and found that loss of genome function accounts for the majority of inactivation although ozone reacts with viral capsid as well. It should be noted that these studies evaluated the inactivation kinetics by a variety of experimental systems. Therefore, the obtained results should be further evaluated with careful consideration of the validation of the ozonation system.

3.2. Inactivation model

The inactivation process proceeds as a function of time or disinfectant exposure. The inactivation model refers to the model that captures the time-dependent inactivation. One of the most fundamental and widely used mathematical models is the first-order kinetics, according to the Chick-Watson law, proposed more than a hundred years ago (Chick and

Martin, 1908; Watson, 1908), where k is the inactivation rate constant, C is the concentration (or fluence rate) of the disinfectant, N is the concentration of infective viruses at time t, and η is the coefficient of dilution.

$$\frac{\partial N}{\partial t} = -kC^{\eta}N$$

Suppose that C was constant and η is equal to 1, the integration can be expressed as below (Meister et al., 2018).

$$\frac{N}{N_0} = e^{-kCt}$$

To adopt these models, the reactor and target organisms should meet the following requirements. First, microorganisms are genetically analogous among strains, and the inactivation to be of a single-hit and single-site type. Second, the reaction with disinfectants should be irreversible and randomly distributed among the targets leading to inactivation. Moreover, the hydraulics should be an ideal plug flow, analogous to a complete mixing batch reactor. Finally, the disinfectant concentration remains constant throughout the reaction and among the reaction points.

The simplicity and theoretical consistency of the Chick-Watson model make it attractive to analyze the rate constants of virus inactivation by disinfectants in an ideal batch reactor. Previous studies revealed that this model well fits with the virus inactivation by free chlorine (Sigstam et al., 2013; Sobsey et al., 1988; Wigginton et al., 2012), ultraviolet irradiation (Gerba et al., 2002; Pecson et al., 2011; Severin et al., 1983). Therefore, this model is applied to the Guidance Manual published by the United States Environmental Protection Agency for recommending the required CT values and UV doses (USEPA, 2010, 2006) for drinking water treatment. Other disinfectants, such as chlorine dioxide, however, do not lead to the first-order decay of viruses (Hornstra et al., 2011; Meister et al., 2018; Sigstam et al., 2014).

Under the environmental conditions, the applicability of Chick-Watson model is relatively limited because the assumption of the model does cannot be fulfilled. A lot of studies reported that the plots of log survival on contact time for disinfectant exhibited curvilinear trends. This observation was mechanically explained as follows. Each parameter may depend on other parameters or have some distributions. For example, the disinfectant concentration decays during the chlorination of wastewater effluent due to the significant amount of disinfectant demands (Buffle et al., 2006; Dunkin et al., 2018;

Haas and Karra, 1984). Another example is the inconstant k among the present viruses due to the presence of virus aggregation, as reported by a previous study (Mattle and Kohn, 2012). Moreover, the t value is not constant among the locations of the target reactor (Ducoste et al., 2001a).

Owing to the findings on the deviation of experimental data from the theory, the Chick-Watson model has been modified empirical or mechanical viewpoints, as described in the following sections.

3.3. Model modification from the empirical viewpoints

Hom model

Hom observed curvilinear plots, rather than linear, on the log survival plot as a function of contact time for chlorine disinfection of natural algal-bacterial systems (Hom, 1972). He developed an empirical generalization of the Chick-Watson pseudo-first-order rate law as below.

$$\frac{dN}{dt} = -kmNC^n t^{m-1}$$

Integration of this rate law gives the empirical Hom model.

$$\log\frac{N}{N_0} = -kC^n T^m$$

This model can describe the plots exhibiting shoulder or tailing by changing the scale factor of n and m. Haas reported that this model is consistent with the mechanistically modified Chick-Watson model, which theorized the inactivation of PV1 (Mahoney strain) considering an intermediate disinfectant-organism complex (Haas, 1980).

3.4. Model modification from the mechanistic viewpoints

3.4.1. Incorporation of decay in C

The disinfectant concentration decays throughout the reaction because demand-free conditions are rare for most oxidants and natural waters. This prompted the researcher to modified Chick-Watson model and Hom model to allow for predicting the inactivation rate during the conditions where the disinfectant concentration is decreasing.

Haas and Joffe proposed a modified Chick-Watson (MCW) model and efficiency factor Hom (EFH) model, both of which substitute the equation of first-order decay of disinfectant concentration into the parameter *C* in Chick-Watson model and Hom model, respectively (Haas and Joffe, 1994).

Suppose the disinfectant concentration decays with first-order kinetics,

$$C = C_0 \mathrm{e}^{-\mathrm{k}'\mathrm{t}}$$

C and C_0 are the disinfectant concentration at time *t* and time 0, respectively; and k' is the first-order reaction decay constant of disinfectant

Modified Chick-Watson model

$$\log \frac{\mathrm{N}}{\mathrm{N}_0} = \quad -\frac{kC_0^n}{nk'}(1 - e^{-nk't})$$

Efficiency factor Hom model

$$\log \frac{N}{N_0} = \quad -\left(\frac{m}{nk'}\right)^m kC_0^n \left(1 - e^{-\frac{nk't}{m}}\right)^m$$

Note that approximation, where Hom model was adopted, is satisfactorily provided $m > 0.4$; for values of $m < 0.4$ the efficiency factor does not accurately approximate the incomplete gamma function (Gyürék and Finch, 1998).

The advantage of The MCW and EFH models is their flexible applicability to any type of disinfection curve. These models were widely applied to analyze the virus inactivation by disinfectants (Cromeans et al., 2010; Hornstra et al., 2011; Kahler et al., 2011; Lim et al., 2010; Shirasaki et al., 2020; Thurston-Enriquez et al., 2005, 2003; Zhong et al., 2017b). The disadvantages are the difficulty of the mechanistic interpretation of the scale values, *m* and *n*. This also leads to the lack of universality of the predicted parameters; the obtained scale values *m* and *n*, were not consistently obtained. Note that the concept of the integral estimate of time-dependent residual disinfectant concentration (ICT) (Maffettone et al., 2020; Manoli et al., 2019) is analogous to the modified Chick-Watson, where *n* is set to be 1.

3.4.2. Incorporation of heterogeneity in *k*: *Cerf model*

A biphasic inactivation curve was observed when the population of target viruses consists of two subpopulations. Cerf derived a mechanistic two-fraction model that

specifically describes the inactivation of two populations with differing inactivation kinetics (Cerf, 1977). A previous study modified the preliminary model to allow for the modeling of inactivation in water treatment (Hornstra et al., 2011). The model is described below.

$$\frac{N}{N_0} = fe^{-k_1 Ct} + (1-f)e^{-k_2 Ct}$$

, where k_1 and k_2 are the inactivation rate constants for populations 1 and 2, respectively, f is the initial proportion in the less resistant fraction.

In the batch experiments, this model was utilized for the analysis of virus inactivation by chlorine dioxide (Hornstra et al., 2011; Meister et al., 2018). Also, the model predicted the *E.coli* inactivation by peracetic acid and murine norovirus inactivation by performic acid in the wastewater (Maffettone et al., 2020; Manoli et al., 2019).

3.4.3. Incorporation of heterogeneity in *t*

Most actual water treatment systems have complicated hydraulics, such as poor inlet/outlet configurations, dead zones, internal circulation, short-circulating (Ducoste et al., 2001b). Such deviations from ideal reactor configurations typically represent hydraulic inefficiencies and may result in unexpectedly poor inactivation performance. These phenomena can be interpreted as the variability in contact time (t) in the reactor, as represented by residence time distribution (RTD). Therefore, the heterogeneity in *t* also should be incorporated into the inactivation model.

The general form is as below.

$$\frac{dN}{dt} = -N(t)E(t)$$

The integrated form is

$$\frac{N}{N_0} = -\int_0^\infty N(t)E(t)dt$$

Where *N(t)* indicates the inactivation model in the batch reactor; *E(t)* indicates residence time distribution (RTD).

The derivation of closed expression of such inactivation model is possible for the typical hydraulics in the reactor, such as laminar flow or continuous stirred tank reactor

(CSTR). The derivation of these equations are described in Chapter 3.

The derivate is, however, not widely used because the RTD of the actual reactor is complicated but can be experimentally determined by tracer experiments or modeled by computational fluid dynamics (CFD). Therefore, the inactivation prediction in the actual reactor is performed coupled with CFD. The use of CFD to predict the inactivation is well documented for the UV application (Li et al., 2016; USEPA, 2006).

3.5. Inactivation kinetics of Enterovirus by disinfectants

The inactivation kinetics of Enterovirus by free chlorine has been investigated for approximately three decades ago. Previous studies indicate that coxsackievirus B5 (CVB5), one of the genotypes of *Enterovirus B*, exhibited lower susceptibility to free chlorine than other genotypes of enteroviruses, adenoviruses, hepatitis A and murine norovirus (Black et al., 2009; Cromeans et al., 2010; Kahler et al., 2011; Sobsey et al., 1988) and thus has been recognized as the most free chlorine resistant among enteric viruses. The reported values of required free chlorine CT values and required dose for 4-log inactivation of CVB5 in buffered solution or source water of drinking water were summarized in Table 1 and Table 2, respectively. The reported values of required ozone CT values were shown in Chapter 3.

Table 1 4 log CT of CVB5 Faulkner strain by free chlorine

Study	Solution	Composition	Initial FC	pH	Temp	4 log CT [$mgLs^{-1}$]	Model
(Meister et al., 2018)	PBS (-)	5 mM NaH2PO4, 10 mM NaCl	NA[c]	7.4	room	2.2	CW[a]
(Shirasaki et al., 2020)	PB	10 mM Na2HPO4 and NaH2PO4	0.1	7	20	1.19	EFH[b]
			0.5	7	20	1.15	EFH[b]
(Cromeans et al., 2010)	CDF	0.83 g of Na2HPO4 and 0.58 g of NaH2PO4 per liter	0.2	7	5	7.4	EFH[b]
(Kahler et al., 2010)	CCMWA	NA	0.2	7	5	4.3	EFH[b]
	WASH	NA	0.2	7	5	6.9	EFH[b]
	BGC	NA	0.2	7	5	4.7	EFH[b]
	CCMWA	NA	0.2	7	15	1.3	EFH[b]
	WASH	NA	0.2	7	15	2.7	EFH[b]
	BGC	NA	0.2	7	15	1.6	EFH[b]
(Black et al., 2009)	BDF	0.54 g of Na2HPO4 and 0.88 g of KH2PO4	1	7.5	5	11.5	EFH[b]
(Sobsey et al., 1988)	PB	10 mM PB unknown composition	0.5	7	5	12	CW[a]

[a] CW indicates Chick-Watson model

[b] EHF indicates: Efficiency factor Hom model

[c] NA indicates that the data is not available

Table 2 4 log dose of CVB5 Faulkner strain by UV_{254}

Study	Solution	Composition	pH	Temp	4 log Dose [mJ cm^{-2}]	Model
(Meister et al., 2018)	PBS (-)	5 mM NaH2PO4, 10 mM NaCl	7.4	room	24.8	CW[a]
(Rockey et al., 2020)	PBS	PBS; 5 mM Na2HPO4, 10 mM NaCl	7.5	20	27.9	CW[a]
(Gerba et al., 2002)	PBS	10 mM,	NA	NA	36	CW[a]

[a] CW indicates Chick-Watson model

Chapter 3

Inactivation kinetics of waterborne virus by ozone determined by a continuous quench flow system

A modified version was published as:

Torii, S., Itamochi, M., Katayama, H., 2020. Inactivation kinetics of waterborne virus by ozone determined by a continuous quench flow system. Water Res. 186. https://doi.org/10.1016/j.watres.2020.116291

1. Introduction

Ozonation is one of the advanced water treatment processes and widely applied for the control of taste, odor, and micropollutants and for microbial disinfection (von Gunten, 2018).

Viruses are major microbial contaminants that cause waterborne diseases (World Health Organization, 2011). Because of the high probability of infection with a given exposure, the acceptable concentration of viruses in drinking water is low (e.g., 1/90,000 L to achieve 10^{-6} disability-adjusted life-year/person (World Health Organization, 2011)). This requires regulators to achieve a high rate of virus reduction through water treatment (e.g., 12-log reduction for indirect potable reuse (Title 22 and 17 California Code of Regulations, 2015)). The current treatment system heavily relies on disinfection to achieve a high level of virus reduction. Log credit allocable to ozonation is up to 6-log (Olivieri et al., 2016). Therefore, the efficacy of virus reduction by ozonation should be carefully examined.

The efficiency of virus inactivation is primarily governed by the exposure to the disinfectant, the so-called CT value, which is defined as the time-dependent disinfectant concentration integrated over time (USEPA, 1999). Currently, such a dose-response relationship is critical for estimating the efficiency of microbial inactivation in a full-scale plant, as well as the information on the disinfectant decay and reactor hydraulics (Bellamy et al., 1998; Manoli et al., 2019). Although the dose-response relationship has been investigated and meta-analyzed in major disinfectants (free chlorine, monochloramine (Cromeans et al., 2010; Rachmadi et al., 2020), and ultraviolet irradiation (Gerba et al., 2002; Hijnen et al., 2006)), studies on ozonation are scarce.

The lack of ozonation studies was mainly due to the difficulty of measuring both the CT value and the rate of virus inactivation simultaneously. Ozone is quickly decomposed in the aqueous phase (Gardoni et al., 2012) and consumed by organic substances contained in the virus stock solution (Dunkin et al., 2017). Furthermore, measurable virus inactivation is often completed within several seconds after contact with ozone (Hall and Sobsey, 1993; Shin and Sobsey, 2003). Hence, most ozonation studies miss either information on the CT value or the rate of virus inactivation (Finch and Fairbairn, 1991; Hall and Sobsey, 1993; Herbold et al., 1989; Shin and Sobsey, 2003; Sigmon et al., 2015; Thurston-Enriquez et al., 2005).

The batch experiment is a golden standard for analyzing inactivation kinetics in disinfection studies; however, it is not feasible for ozonation because it is necessary to obtain samples that have reacted with a disinfectant for a few seconds. As such, several studies have modified the experimental setup to obtain both the CT value and the rate of virus inactivation. For example, early studies applied the method of continuous stirred-tank reactor (CSTR), in which the virus and ozone solution are continuously fed to the stirred tank while the solution in the tank is withdrawn at a constant flow rate (Roy et al., 1982). A recent study developed a unique experimental batch system that enables the simultaneous determination of the CT value and virus inactivation (Wolf et al., 2018). Despite the researchers' efforts to improve the experimental setup, the reported inactivation rate constants were inconsistent among available studies.

One of the underlying causes of the inconsistency is the sparse approximations of exposure time of collected samples. For example, Roy et al. (1982) conducted virus ozonation in CSTR and reported the required time for 2-log virus inactivation under a certain ozone concentration. The United States Environmental Protection Agency (USEPA) simply multiplied the required time with the ozone concentration and reported it as required CT values for 2-log virus inactivation (USEPA, 2010, 1991). However, the required time represents just an average residence time (τ) in CSTR. In other words, not every virus travels the reactor for time τ. Theoretically, the short-circuiting flow, which travels in the reactor for a shorter time than the mean residence time in which much greater portion of viruses remains infective, affects the average virus concentration at a given time. Therefore, the currently proposed values do not represent the actual CT value but rather the "Cτ" value, which virtually includes the effect of the heterogeneity of hydraulics. Another cause is the reduced mixing efficiency of the disinfectant solution with the virus solution. Wolf et al. (2018) noted that their system might underestimate the rate constants because a large portion of inactivation had occurred before the system

reached a state of complete mixing.

The continuous quench flow system (CQFS) is a bench-scale experiment technique that comprises a pump, small mixer, and reaction tube. It was developed to analyze the kinetics of fast reactions. Several studies have applied this system to evaluate the degradation of chemicals, such as carbamazepine (Buffle et al., 2006) and textile dyes (Gomes et al., 2010). Generally, the system drives the test solution and ozone solution separately, mixes them in a small reactor, and facilitates the mixture to flow in the reaction tube continuously. The exposure time is controlled by changing the length of the tube or flow rate. This setup makes it possible to obtain the samples reacting for a few seconds. Therefore, CQFS is a potential solution to measure both the ozone CT value and the rate of virus inactivation simultaneously.

In this study, we introduced a CQFS in which the flow regime is laminar to evaluate the first-order rate constants for the waterborne virus inactivation with ozone. The challenge for CQFS used in previous studies was a tacit assumption of flow hydraulics in reaction tubes. Several studies assumed the flow regime in the reaction tube to be a plug flow, although it was actually laminar flow (Buffle et al., 2006; Hunt and Mariñas, 1997) or not described (Czekalski et al., 2016; Gomes et al., 2010; Wolf et al., 2018). Moreover, scattered or biphasic data were observed in a single dose-response relationship determined by CQFS, possibly because the flow regime was not controlled among data points (Hunt and Mariñas, 1997; Wolf et al., 2018). These properties required researchers to develop more solid experimental protocols. Specifically, it is necessary to develop a pseudo–first-order kinetic model that takes the residence time distribution (RTD) function into account and to control the flow regime throughout the entire experiment.

The objectives of this study were (1) to develop a CQFS and pseudo–first-order kinetics model that considers RTD for an accurate measurement of inactivation rate constants by ozone, (2) to evaluate inactivation rate constants for the waterborne virus inactivation, and (3) to compare the results with previous studies and USEPA guidance manual CT values.

2. Materials and methods

2.1. Virus propagation, purification and enumeration

F-RNA coliphages (MS2, fr, GA, Qβ) and somatic coliphage φX-174 were propagated by *E.coli* K12A/λ(F+) and *E.coli* C (NBRC13898), respectively. Coxsackievirus B3 (CVB3) Nancy strain, coxsackievirus B5 (CVB5) Faulkner strain, and poliovirus type 1 (PV1) Sabin strain were propagated by buffalo green monkey kidney (BGM) cells.

The propagated stocks were centrifuged at 3,500*g* for 15 min to remove cell debris. The supernatant was filtered through a cellulose acetate membrane (0.2 μm, DISMIC-25CS, Advantec, Tokyo, Japan). Then, 10 mL of the filtrate was washed with 10 mM phosphate buffer (PB) and concentrated to approximately 600 μL by a Centriprep YM-50 filter unit (Merck Millipore, Tokyo, Japan).

Density-gradient centrifugation was performed as described elsewhere (Loison et al., 2016; Torii et al., 2019a). For the coliphages, iodixanol (60% OptiPrep; Axis-Shield, Dundee, Scotland) was used as a gradient. Briefly, 3 mL of 40% iodixanol solution prepared in PB was placed in an ultracentrifuge tube. Subsequently, 2 mL of 20% iodixanol prepared in the coliphage concentrate was layered on the 40% iodixanol solution. Then, the tubes were centrifuged at 160,000*g* for 7 hr at 15 °C. For the mammalian viruses, cesium chloride was selected as a gradient. In brief, 500 μL of the concentrated virus was layered on 4.5 mL of cesium chloride solution prepared in 10 mM PB in centrifuge tubes and centrifuged at 160,000 g for 18 hr at 15 °C. After the centrifugation, 1 mL of aliquot positioned for the buoyant density of each virus was collected. The collected virus suspensions were desalted with 10 mM PB three times by Amicon Ultra 100 kDa (Merck Millipore). The purified virus stock was kept at 4 °C until ozone disinfection experiments.

The number of infective coliphages were quantified by a single agar layer (SAL) procedure. For each sample, a series of 10-fold dilutions was prepared in 10 mM phosphate buffer (PB) at pH 7.0. Then, 0.1 or 1 mL samples were added to Petri dishes and mixed with LB agar containing propagated host *E. coli* and incubated at 37 °C overnight. Each dilution was enumerated in duplicate. The concentrations of coliphages were reported as PFU/mL.

The number of infective CVB3, CVB5, and PV1 was enumerated by most probable number (MPN) assay using BGM cells on 96-well plates, with five replicates and four

dilutions per sample (Meister et al., 2018). The samples to be quantified were serially diluted 10-fold by maintenance medium, supplemented with 1% fetal bovine serum. Each well was inoculated with 150 μL of diluted samples. After the incubation at 37 °C with 5% CO_2 for 5 to 6 days, the presence of cytopathic effects was monitored by microscope. The number of positive wells of each dilution was counted and analyzed by an R package (Ferguson and Ihrie, 2019). The concentrations of CVB3, CVB5, and PV1 were reported as MPN/mL.

2.2. Setup of continuous quench flow system (CQFS)

The CQFS was set up as shown in Figure 3. The reactor comprised two peristaltic pumps (Perista pump AC-2110II, ATTO Co. Ltd., Japan) to drive two solutions (virus solution and disinfectant solution), a T-connector mixer (VRFT6, ISIS Co. Ltd., Japan) in which the magnetic ball was stirred, and a silicone tube (outer diameter: 4 mm, inner diameter: 2 mm) to facilitate the reaction with disinfectant.

The virus solution was driven at 0.31 mL/s and mixed at a 1:1 ratio with a disinfectant solution, resulting in the mixed solution flowing at 0.62 mL/s in the silicone tube. The velocity of the mixed solution was 20 cm/s. The flow rate was not changed for any of CQFS experiments to maintain the flow regime, at a Reynolds number (*Re*) of 395, in the silicone tube. The reaction time can be controlled by selecting different tube lengths, $l = 20\tau$ (s), where l (cm) represents the length of the silicone tube and τ (s) represents the desired retention time. A preliminary experiment showed that virus loss by the attachment to the reaction tube was negligible even when using the tube length of 180 cm. At the outlet of the reaction tube, an exceeded amount of sodium thiosulfate ($Na_2S_2O_3$) was prepared in a Petri dish to stop the reaction immediately. In this study, the disinfected sample at the outlet of the mixer was regarded as the 0 s sample. This was because this CQFS has a dead volume from mixing point to the point at which the first data point was collectable. The average dead time (i.e., residence time of the mixer) was estimated to be 0.24 seconds. All of the experiments were conducted at 22 ± 1 °C. The mixer and each reaction tube were rinsed thoroughly with MilliQ before and after the CQFS operation.

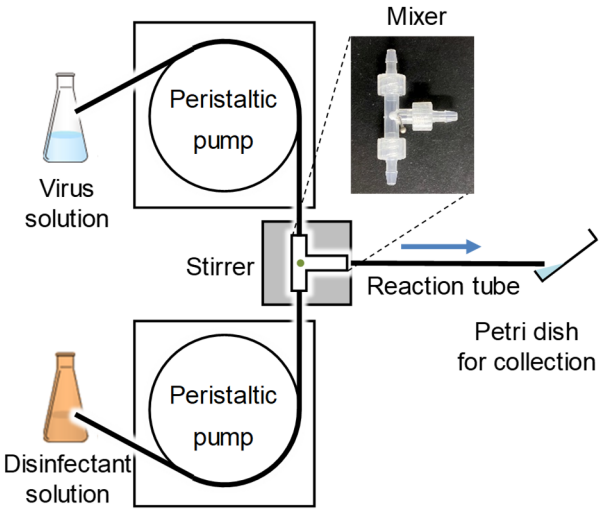

Figure 3 Setup of the continuous quench flow system

2.3. Ozone production and measurement

An ozone generator (Ebara; OZSD-3000A, Japan) was used to produce ozone gas from oxygen. The obtained gas was bubbled through chilled MilliQ pre-acidified by phosphoric acid (pH 3.5) to prepare the ozone stock solution at a final concentration of >5 mg L^{-1}.

The concentration of the stock solution was determined by direct spectrophotometry with an absorption coefficient of ozone, ε_{260} = 3,200 M^{-1} cm^{-1} (von Sonntag and von Gunten, 2012). In ozonation experiments, the concentration was determined by the decolorization of indigo trisulfonate, with an adsorption coefficient ε_{600} = 20,000 M^{-1} cm^{-1} (Bader and Hoigné, 1981) according to the Standard Methods for the Examination of Water and Wastewater Indigo Colorimetric Method, with slight modification.

Ozone concentration was calculated based on the Beer-Lambert law as follows.

$$c = \frac{\Delta A}{\varepsilon_{600} l} \times M \times 1000 \times \frac{V_{indigo} + V_{collected}}{V_{collected}}$$

$$\Delta A = A_{blank} \times \frac{V_{blank}}{V_{indigo} + V_{collected}} - A_{sample}$$

where A is the absorbance at 600 nm (cm^{-1}), c (mg L^{-1}) is the ozone concentration, ε_{600} = 20,000 (M^{-1} cm^{-1}) is the molar attenuation coefficient of ozone at 600 nm, M = 48 (g

mol^{-1}) is the molecular weight of ozone, l is the path length of the cell, $V_{collected}$ (mL) is the volume of samples collected for measurement of ozone concentration, V_{indigo} (mL) is the volume of indigo reagent, and, V_{blank} (mL) is the volume of the blank sample.

In the ozonation of phenol (see 2.5.3), the absorbance at 600 nm (A_{600}) was measured using a 1-cm glass cell. The blank sample was prepared by adding 6 mL of Indigo reagent II into 5 mL of MilliQ (V_{blank} = 11 (mL))

In the ozone disinfection experiment (see 2.6), the absorbance at 600 nm (A_{600}) was measured using a 5-cm glass cell. The blank sample was prepared by adding 1.08 mL (=V_{indigo}) of Indigo reagent I into 9.72 mL of MilliQ. (V_{blank} = 10.8 (mL))

2.4. Calculation of ozone Cτ values

The calculation of the Cτ value is shown in Figure 4. In this study, the ozone concentration was measured at each time point. The Cτ value was given by the following equation.

$$C\tau = \int_0^{\tau_3} C d\tau = \frac{C_0 + C_1}{2}(\tau_1 - \tau_0) + \frac{C_1 + C_2}{2}(\tau_2 - \tau_1) + \frac{C_2 + C_3}{2}(\tau_3 - \tau_2)$$

This is corresponding to the area in Figure 4. Herein, a linear decay of ozone between time points was assumed

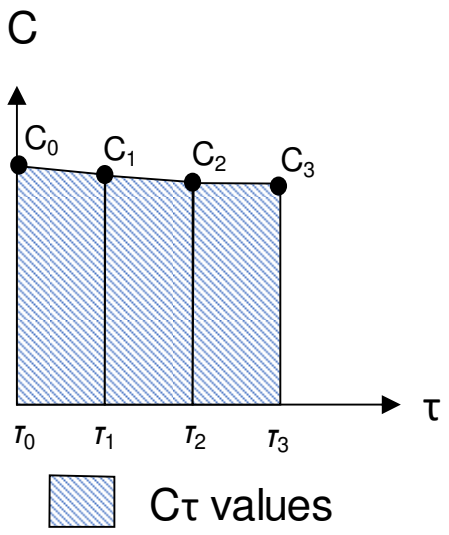

Figure 4 Example of calculation of Cτ value

τ_0, τ_1, τ_2 and τ_3: time points of sampling

C_0, C_1, C_2 and C_3: ozone concentration at each time point

2.5. Validation of CQFS

2.5.1. Chlorination of MS2 in the batch system

Batch chlorination of MS2 was conducted in a 50 mL glass beaker. A free chlorine working solution was prepared by diluting sodium hypochlorite with 10 mM PB at pH 7.0 to obtain a final concentration of 7.8 to 7.9 mg L^{-1} as Cl_2. Free chlorine was measured by the spectrophotometric method using N,N-diethyl-*p*-phenylene-diamine (DPD) with a DR890 colorimeter (Hach Company, Loveland, CO). Before each experiment, the glass beaker was washed with MilliQ and the working solution. Then, 20 μL of purified MS2 stocks were spiked into 20 mL of stirred working solution. One milliliter of aliquot was harvested and directly mixed with 50 μL of $Na_2S_2O_3$ at a concentration of 5,000 mg/L at 6 s and 12 s. The initial virus concentration was sampled from 20 mL of PB spiked with 20 μL virus stock. The initial virus concentration was 10^{6-7} PFU/mL. Note that the concentration of free chlorine was not decayed at 30 s for the whole experiment (data not shown). This batch experiment was conducted four times.

2.5.2. Chlorination of MS2 in the CQFS

MS2 chlorination was conducted by the developed CQFS. MS2 was suspended in 10 mM PB at pH 7.0 as the virus solution, and free chlorine at a concentration of 15 to 16 mg L^{-1} as Cl_2 in 10 mM PB was prepared as the disinfectant solution. Then, different lengths of reaction tubes (60, 120, 180 cm) were installed on the outlet of the mixer depending on the desired retention time (3, 6, 9 s) of the samples. The sample at 0 s was taken at the outlet of the mixer. For a single experiment, 6.2 mL of samples at 0 s, 3 s, 6 s, and 9 s were taken in Petri dishes with $Na_2S_2O_3$ for enumeration of MS2. Additional samples (3.1 mL) were taken in Petri dishes without $Na_2S_2O_3$ in the collection of 0 s and 9 s samples. A 1 mL of the sample on the Petri dish was taken immediately, mixed with 9 mL of DPD solution and examined for free chlorine. The free chlorine concentration of the mixed solution at time 0 s ranged from 7.6 to 8.1 mg L^{-1} as Cl_2. The MS2 concentration at time 0s ranged from 3.0×10^5 to 5.0×10^5 PFU/mL. The decay in free chlorine was <0.1 mg/L as Cl_2 (data not shown). The experiment was run four times.

2.5.3. Ozonation of phenol in the batch system

An ozone solution was prepared at a final concentration of 2.9 mg L^{-1}. Before each experiment, the glass beaker was washed with MilliQ and the ozone solution. The ozone solution was acidified to pH 3.0 by phosphoric acid and spiked with *tert*-butanol (at a

final concentration of 10 mM) as a radical scavenger. Then, 150 μL of phenol stocks (25 mg L^{-1}) were spiked into 15 mL of the stirred ozone solution. The reaction was stopped at 10 s by adding the excess amount of $Na_2S_2O_3$ (at the final concentration of 100 mg L^{-1}). The initial phenol concentration was determined by sampling from 15 mL of MilliQ spiked with 150 μL phenol stock. The concentration of phenol was determined by the spectrophotometric method using 4-Aminoantipyrine described in USEPA method 420.1. This batch experiment was conducted at 22 ± 1 °C in triplicate. In the batch system, we could not measure the phenol and ozone concentration simultaneously. Thus, we measured the ozone decay during the reaction above separately. The ozone concentration was maintained at 59 ± 7% during the reaction of phenol and ozone (n=2) (data not shown). The CT value was calculated by multiplying the time-dependent concentration integrated over time.

2.5.4. Ozonation of phenol in the CQFS

Phenol was suspended at the final concentration of 500 μg/L in pre-acidified MilliQ at pH 3.0 with *tert*-butanol at a final concentration of 10 mM. The ozone solution was prepared at the concentration of at pH 3.0. Then, reaction tubes were prepared to achieve the retention time of 0, 2, 4, 6 s. The sample at 0 s was taken at the outlet of the mixer. For a single experiment, approximately 12 mL of samples were taken in Petri dishes with $Na_2S_2O_3$ at each time point to measure the phenol concentration. Additional samples were collected on a Petri dish with 6 mL of Indigo solution II for approximately 8 s at each time point. The collected volume was measured by a balance and ranged from 5.1 to 5.8 mL. The solution was used to measure the residual ozone concentration. (see 2.3). The concentration of ozone at time 0s was 2.4 to 3.3 mg L^{-1}. The ozone concentration at 6s was maintained at 72 ± 10% compared with 0 s. The Cτ value was calculated by multiplying the τ-dependent concentration integrated over τ (see Figure 4). The ozonation of phenol in the CQFS was performed in triplicate.

2.5.5. Analysis of inactivation rate constants

The inactivation rate constants determined by the batch system (k_{batch}) were modeled by the following equation.

$$\frac{N_T}{N_0} = e^{-kCT}$$

where N_T is the infective virus concentration at time T (PFU mL^{-1} or MPN mL^{-1}), N_0 is the infective virus concentration at time 0 (PFU mL^{-1} or MPN mL^{-1}), k is the first-order inactivation rate constant (mg^{-1} sec^{-1} L), C is the disinfectant concentration (mg L^{-1}), and T is time (s).

The inactivation rate constants determined by CQFS (k_{CQFS}) were determined by two models in which the assumption of flow regime in the reaction tube was different, plug flow or laminar flow. In the plug flow assumption, the velocity profile was constant, depending on the location of the reaction tube; in the laminar flow assumption, it was parabolic, as determined by the Hagen-Poiseuille law.

Under the plug flow assumption, the pseudo–first-order reaction is described as Model 1.

$$\frac{N_\tau}{N_0} = e^{-kC\tau} \quad \text{(Model 1)}$$

where τ is the average residence time in the reaction tube (seconds), which is given by l/v (where l is the length of the reaction tube [cm] and v is the mean velocity [cm s^{-1}])

Under the laminar flow assumption, the pseudo–first-order reaction is modeled as Eq. (1). The model considers the RTD in the reaction tube (Fogler, 2008; Hilder, 1979)

$$\frac{N_\tau}{N_0} = \int_0^\infty e^{-kCT} E(T) dT \qquad (1)$$

where $E(T)$ is the RTD function.

For laminar flow, the RTD function is expressed as Eq. (2) (Fogler, 2008).

$$\mathrm{E}(T) = \begin{cases} 0 \text{ for } (T \le \frac{\tau}{2}) \\ \frac{\tau^2}{2T^3} \text{ for } (T \ge \frac{\tau}{2}) \end{cases} \qquad (2)$$

The dimensionless form of Eq. (2) is

$$E(\Theta) = \tau E(T) = \begin{cases} 0 \text{ for } (\Theta \leq 0.5) \\ \dfrac{1}{2\Theta^3} \text{ for } (\Theta \geq 0.5) \end{cases} \text{ with } \Theta = \frac{T}{\tau} \qquad (3)$$

Eq. (1) can be transformed as Eq. (4) by partial integration.

$$\frac{N_\tau}{N_0} = \int_0^\infty e^{-kCT} E(T) dT = \int_0^\infty e^{-kC\Theta} E(\Theta) d\Theta = \int_{0.5}^\infty \frac{e^{-kC\Theta}}{2\Theta^3} d\Theta$$

$$= \quad (1 - 0.5kC)e^{-0.5kC} + (0.5kC)^2 \int_{0.5}^\infty \frac{e^{kC\Theta}}{\Theta} d\Theta \qquad (4)$$

Then, Eq. (4) was approximated by Hilder's equation (Fogler, 2008; Hilder, 1979).

$$\frac{N_\tau}{N_0} = \frac{1}{(1 + 0.25kC\tau)e^{0.5kC\tau} + 0.25kC\tau} \text{ (Model 2)}$$

Note that the errors of this algebraic expression (Model 2) from the exact solution of Eq. (4) were less than 0.04 log (Hilder, 1979).

$$\frac{N_\tau}{N_0} = \frac{1}{(1 + 0.25kC\tau)e^{0.5kC\tau} + 0.25kC\tau} \text{ (Model 2)}$$

The abatement of phenol was also modeled as above. N_τ/N_0 was replaced with $[\text{phenol}]_\tau/[\text{phenol}]_0$.

2.6. Ozone disinfection experiments

Ozone disinfection was conducted by the developed CQFS. Purified coliphage or mammalian viruses suspended in 20 mM PB at pH 7.0 and an ozone solution in MilliQ were prepared as the virus solution and disinfectant solution, respectively. The ozone concentration before mixing was 0.03 – 0.12 mg L^{-1} when testing coliphages and 0.24 – 0.30 mg L^{-1} when testing enteroviruses. It should be noted that the *tert*-butanol was not added to mimic inactivation during ozonation in water treatment. The resultant mixed solution had a pH of 7. Reaction tubes were then installed to the outlet of the mixer. The length of the reaction tube was set depending on the desired retention time, 0.5, 1, 1.5 s or 1, 2, 3 s. For a single ozonation experiment, samples were taken at four time points, including the 0 s sample. First, the reacting solution was collected on a Petri dish with 1.08 mL of Indigo solution I for approximately 15 s. The collected volume was measured by a balance and ranged from 8.9 to 9.5 mL. The solution was used to measure the residual ozone concentration. (see the 2.3). The concentration of ozone at time 0 s was 0.01 to 0.06 mg L^{-1} for coliphages and 0.07 to 0.13 mg L^{-1} for enteroviruses. The ozone concentration was maintained at 80% ± 8% for coliphages and 92% ± 3.5% for enteroviruses during the reaction. The $C\tau$ value was calculated by multiplying the τ-dependent concentration integrated over τ (see 2.4). Furthermore, an approximately 5 mL of sample was collected in Petri dishes with an excessive amount of quenching solution (50 µL of 5,000 mg L^{-1} of $Na_2S_2O_3$) for virus enumeration. The ozonation experiment was performed in triplicate for each virus.

2.7. Calculation of 4-log CT value from of previous studies

The 4-log CT value of each study was determined as follows.

Roy et al. (1982) AWWA

The calculation was done by following the report (USEPA, 1991). The data of the time to achieve 2-log PV1 inactivation (0.5 min) was adopted from table 1 of Roy et al. (1982). Then, time was multiplied by the residual ozone concentration (0.15 mg L^{-1}). The CT value (0.075 mg min L^{-1} = 4.5 mg sec L^{-1}) was adopted as the 2-log CT value. The 4-log CT value was obtained by multiplying the 2-log CT values by 2. Thus, the 4-log CT value was given as 9.0 mg sec L^{-1}.

Wolf et al. (2018) Environ Sci Technol

The 4-log CT values were predicted as in the same manner as in the current study, namely, $4/k\log_{10}e$. The inactivation rate constants (k) were taken from Table 2.

Hall et al. (1993) Appl Environ Microbiol

Hall et al. reported that a >4.9-log reduction was achieved with a CT value of <0.98 mg min L^{-1} under pH 6.0. Based on this, we determined to be <5.88 mg sec L^{-1} as the 4-log CT values.

Finch et al. (1991) Appl Environ Microbiol

Finch et al. reported ozone inactivation of MS2 with a change in the ozone dose for a contact time of 20 sec. They reported a 5-log reduction of MS2 under the conditions of 0.08 mg L^{-1} of ozone. Thus, the 4-log CT in this study was determined to be <1.6 mg s L^{-1}.

Sigmon et al. (2015) Environmental Engineering Science

They conducted MS2 ozonation in batch system. The minimum applied ozone concentration was 0.10 mg/L. Also, the minimum contact time was 10 s. Under the conditions, they observed > 4-log MS2 inactivation. Hence, the 4-log CT in this study was determined to be <1.0 mg s L^{-1}.

USEPA Guidance Manual

The ozone CT values for 4-log inactivation of viruses at 22°C were obtained from CT calculator provided by USEPA. (https://www.epa.gov/dwreginfo/ground-water-rule-

compliance-help-water-system-owners-and-operators) (Access available as of Jun. 9th. 2020).

2.8. Statistical analysis

All statistical analyses were performed with R. Model fitting was conducted using the function nls(). Multiple comparisons were performed with the Tukey-Kramer test after checking the homogeneity of the variances by Bartlett test. A *P*-value of <0.05 was considered to be statistically significant.

3. Results

3.1. Validation of the CQFS

The validation of the CQFS was performed as follows. Firstly, we validated the hydraulics of the CQFS by comparing the two models, which consider different flow regimes in the reaction tubes; Model 1 assumes plug flow, whereas Model 2 assumes it as a laminar flow. To this end, the first-order rate constant of MS2 inactivation with free chlorine ($k_{MS2,\,FC}$) was investigated by the batch experiment. Then, MS2 inactivation was also performed in CQFS at the comparable physico-chemical conditions. Free chlorine was chosen as a model disinfectant because of its slower reaction compared with ozone, allowing us to analyze the kinetics by both the batch system and CQFS. Moreover, we checked if the CQFS can accurately analyze the rate constant of ozone reaction. For this purpose, we analyzed the abatement of phenol in CQFS by applying the selected pseudo-first-order reaction model.

The log inactivation rate of MS2 in the batch system was plotted in Figure 5 as a function of CT value.

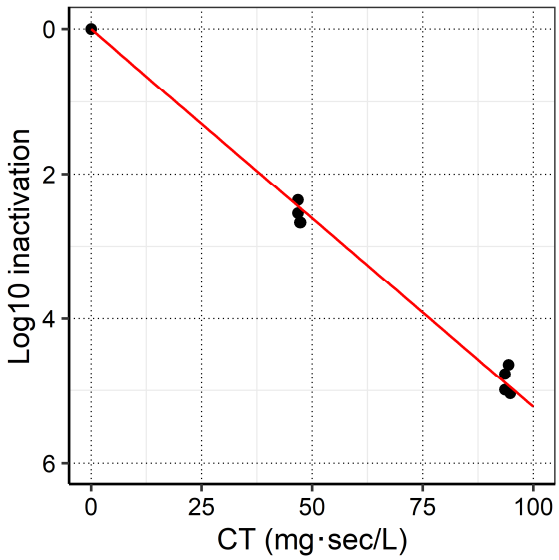

Figure 5 MS2 inactivation with free chlorine as a function of CT value

The red line indicates the regression line.

The determined $k_{MS2,\,FC}$ was 0.120 ± 0.002 mg^{-1} sec^{-1} L (mean ± standard error [SE]). This was comparable with a previous report (0.130 ± 0.010 mg^{-1} min^{-1} L) that performed MS2 inactivation with free chlorine under similar physico-chemical conditions (Sigstam et al., 2013).

The log inactivation rate of MS2 in CQFS was plotted in Figure 6 as a function of Cτ value. The root-mean-square error (RMSE) of the two models, in which 0.120 ($k_{MS2,\,FC}$ determined by the batch system) was substituted for k, were described in Table 3. Excellent agreement between experimental data and Model 2 predictions was achieved. The RMSE was smaller in Model 2 compared with Model 1, indicating that Model 2 fitted better to the experimental data. Moreover, the $k_{MS2,\,FC}$ was determined to be 0.080 ± 0.002 or 0.124 ± 0.004 (mg^{-1} sec^{-1} L) if we fit Model 1 or Model 2 to the experimental data, respectively. Hence, Model 2 was able to provide inactivation rate constant comparable to that determined by the batch system.

For the following experiments using CQFS, we maintained the same flow regime, namely, the same Reynolds number, and adopted Model 2 to analyze the rate constants.

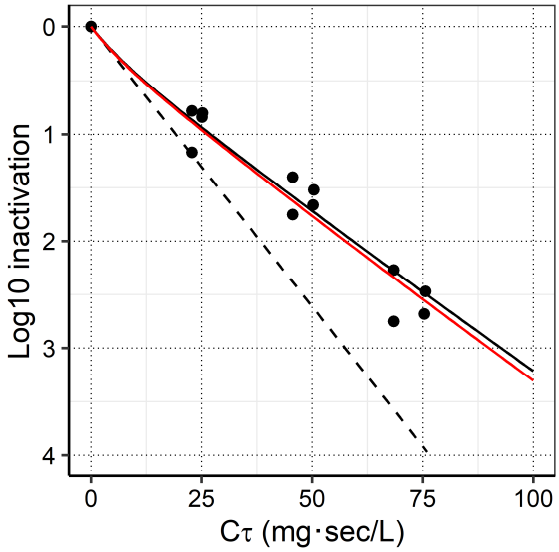

Figure 6 MS2 inactivation with free chlorine performed by CQFS

The dashed black line and solid black line show the prediction by Model 1 and Model 2, where 0.120 ($k_{MS2,\,FC}$) was substituted for k, respectively. The red line shows the regression line, where Model 2 was fitted to the experimental data.

Table 3 Comparison of inactivation models in CQFS

Model	Equation	Order of reaction	Flow regime assumption	RMSE
1	$\frac{N_\tau}{N_0} = e^{-kC\tau}$	Pseudo first order	Plug flow	1.85
2	$\frac{N_\tau}{N_0} = \frac{1}{(1+0.25kC\tau)e^{0.5kC\tau} + 0.25kC\tau}$	Pseudo first order	Laminar flow	0.41

Where N_τ, virus concentration at time τ (PFU mL^{-1} or MPN mL^{-1}), N_0, virus concentration at time 0 (PFU mL^{-1} or MPN mL^{-1}), k, first-order inactivation rate constants (mg^{-1} sec^{-1} L), C, disinfectant concentration (mg L^{-1}); τ, average residence time (sec).

The abatement rate of phenol was plotted in Figure 7 as a function of Cτ. The reaction rate constant of $k_{phenol,\ ozone}$ was determined to be 839 ± 23 (M^{-1} sec^{-1}) using Model 2. This was nearly comparable (1.2-fold difference) to $k_{phenol,\ ozone}$ determined by the batch system (993 ± 75 M^{-1} sec^{-1}) in this study. Moreover, $k_{phenol,\ ozone}$ in this study was consistent with the reported value (1300 ± 300 M^{-1} sec^{-1}) in previous research (Hoigné and Bader, 1983). These results suggest that the developed CQFS combining with Model 2 can be applicable to analyze the rate constants of ozone reaction.

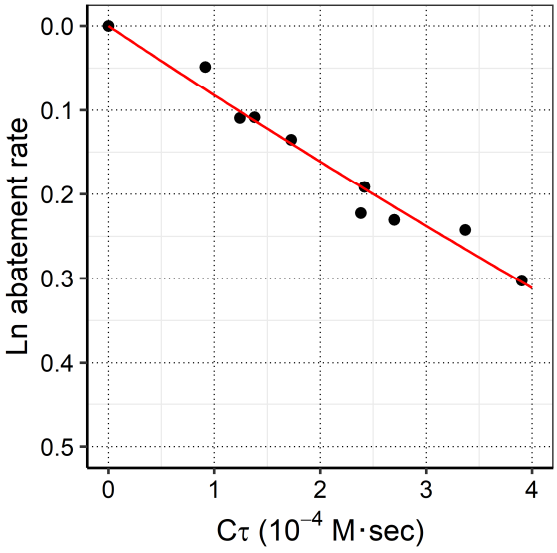

Figure 7 The natural log abatement rate of phenol as a function of Cτ value

The red line indicates the regression line of Model 2

3.2. Ozone inactivation rate constants of various type of viruses

Log virus inactivation as a function of Cτ was plotted in Figure 8. The inactivation rate constants (k) were estimated by fitting Model 2 to the experimental data. The predicted 4-log CT value was given by $4/k\log_{10}e$. These results are summarized in Table 4. The inactivation rate constants ranged from 58 to 511 mg^{-1} sec^{-1} L. The predicted 4-log CT values from 0.018 to 0.16 mg sec L^{-1}. Statistically significant differences in ozone resistance were observed, namely, Qβ < MS2, fr, GA < φX-174, PV1 Sabin, CVB3 Nancy, CVB5 Faulkner.

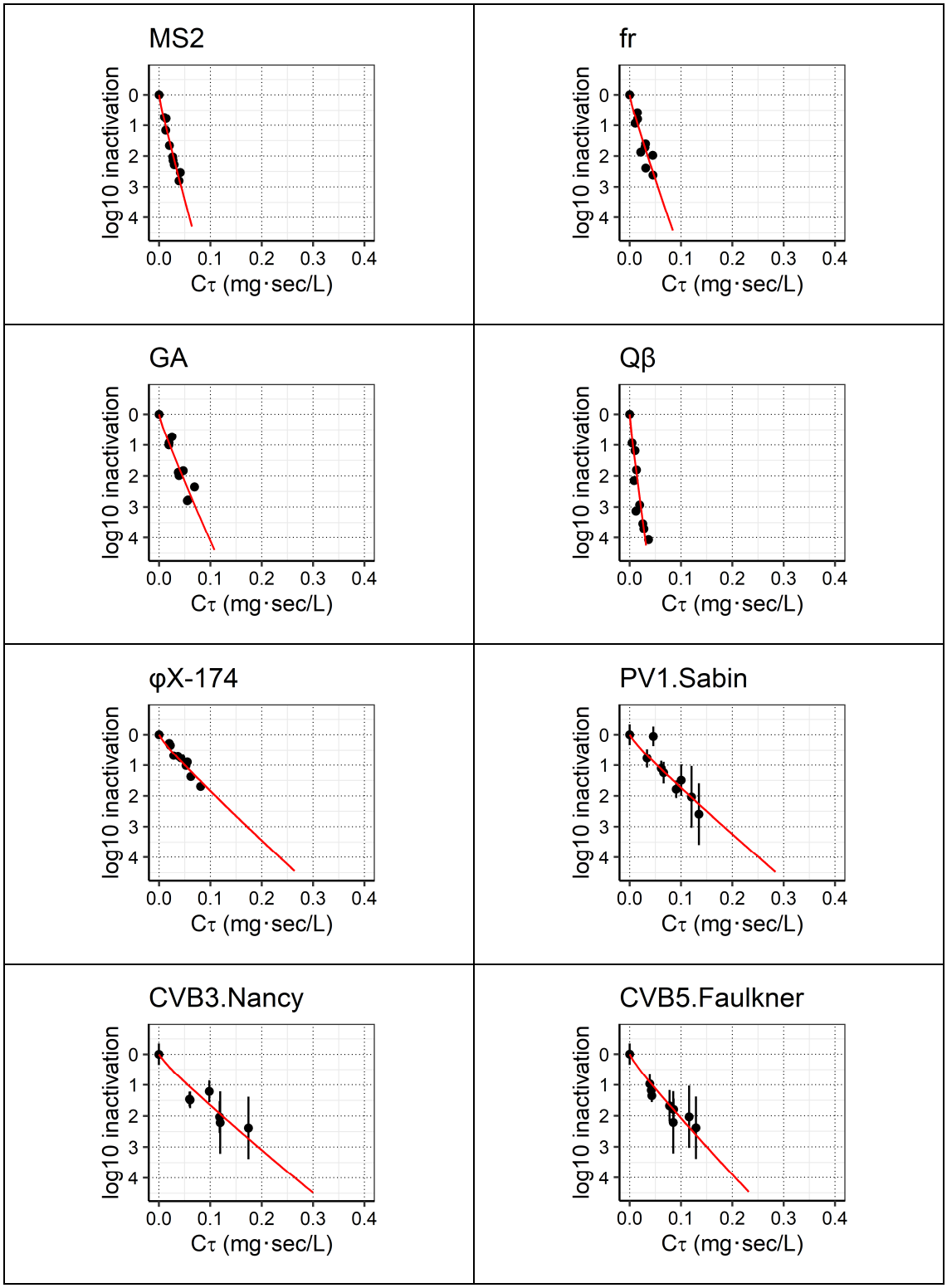

Figure 8 Log inactivation of viruses as a function of Cτ values

The red line showed the regression curve. For PV1.Sabin, CVB3.Nancy, and CVB5.Faulkner, the log inactivation rate was plotted along with error bars representing theoretical standard errors of MPN values.

Table 4 Inactivation rate constants for viruses by ozone, with corresponding standard errors (SE) and predicted 4-log CT values

Virus	k (mg^{-1} s^{-1} L)	SE (mg^{-1} s^{-1} L)	4-log CT (mg sec L^{-1})
Qβ	511	37	0.018
MS2	259	8.8	0.036
fr	203	15	0.045
GA	157	9.1	0.059
CVB5.Faulkner	74	3.9	0.12
φX-174	65	3.2	0.14
PV1.Sabin	61	4.7	0.15
CVB3.Nancy	58	4.3	0.16

4. Discussion

4.1. Agreement between CQFS and batch experiments

The inactivation rate constants are theoretically specific to the type of virus and should not change depending on the experimental system. However, a previous ozonation study reported different inactivation rate constants of MS2 between the CQFS and batch system (<5-fold) (Wolf et al., 2018). Others did not compare their testing system with another experimental system (Finch and Fairbairn, 1991; Roy et al., 1982). We hypothesized that the observed difference among the experimental system was due to the inappropriate assumption on reactor hydraulics. For example, some studies tacitly regarded it as plug flow and considered the hydraulic residence time as uniform distribution, even though the flow regime was actually laminar (Re = 460) (Buffle et al., 2006) or not clear (Gomes et al., 2010). Thus, we first validated the CQFS to check if the inactivation rate constants can be consistently obtained by both the batch experiment and the CQFS.

Our experimental results did not agree with Model 1. This indicates that the assumption on plug flow leads to inaccurate measurement of inactivation rate constants. In our CQFS, the flow regime was laminar (Re = 395), where the velocity is twice as fast as the average velocity at the center of the tube. This means that the reaction time is half at the center, resulting in the presence of more infective viruses. Thus, Model 2, which considers the effect of short-circuiting flow, predicted the experimental data better than Model 1 did.

It should be noted that Buffle et al. (2006) and Wolf et al. (2018) reported that the kinetics of the abatement of phenol and carbamazepine were <10% different between the CQFS and batch experiment, although they adopted Model 1 in the CQFS (Buffle et al., 2006; Wolf et al., 2018). This contradiction was due to the difference in the extent of the achieved rate of abatement/inactivation between the chemical and microbial experiments. In a typical bench-scale experiment, the achieved rate of chemical abatement is up to 1 log (90%), whereas that of microbial inactivation is >2-3 log. Hence, for the chemical abatement experiment, the assumption of hydraulics has little effect on the analysis of inactivation kinetics. The extent of degradation taking place in the bulk of the water was so small that small volumes with little degradation have a tiny effect on the average concentration after ozonation. This is highlighted in Figure 6. The gap between Model 1 and Model 2 was smaller until 1-log (i.e., 90%) reduction, whereas it became larger as the rate of inactivation increased. As a result, the appropriateness of Model 2 was apparent in this study. Therefore, it is important to consider the RTD in CQFS, especially in the

case of the microbial inactivation experiment.

4.2. Comparison of inactivation rate constants with previous studies

The observed ozone resistance trend was similar to that reported by previous studies, which investigated in buffered water (Wolf et al., 2018), namely, Qβ < MS2 < φX-174 < CVB5, and which examined in secondary effluent of municipal wastewater (Sigmon et al., 2015), namely, MS2 < φX-174 < CVB5. Coliphage MS2, Qβ, and φX-174 are typical surrogates to assess the removability of enteric viruses through water treatment, such as coagulation sedimentation (Kato et al., 2018), membrane filtration (Torii et al., 2019b), and chlorination (Sano et al., 2016). However, our results showed that they were more susceptible than all the tested poliovirus and coxsackievirus except CVB5 Faulkner (Table 4). Thus, MS2, Qβ and φX-174 are not the conservative indicators in the assessment of enteric virus reduction by ozonation systems.

Inactivation rate constants of all of the tested viruses (58-511 mg^{-1} sec^{-1} L), were larger than those of *E. coli* WR1 strain (19.1 mg^{-1} sec^{-1} L at 22 °C, (Smeets et al., 2006)), suggesting that viruses were >1.5-fold more susceptible to ozonation than the *E. coli* strain. This result supports a previous suggestion (Sigmon et al., 2015) that *E. coli* could be used as a surrogate to ensure virus reduction through ozonation.

The predicted 4-log CT values were compared with the previous studies which conducted ozonation under the comparable physico-chemical conditions (Figure 9) (Finch and Fairbairn, 1991; Hall and Sobsey, 1993; Roy et al., 1982; Sigmon et al., 2015; Wolf et al., 2018). The 4-log CT value of MS2 in this study was similar (1.2-fold difference) to the previous investigation using CQFS (Wolf et al., 2018). The slight difference was partially due to the choice of the inactivation model (discussed above). The 4-log CT values of MS2 determined by the unique batch system (Wolf et al., 2018) were 5-fold larger than ours. This was because a large portion of the inactivation had proceeded before the system reached the state of complete mixing in their experimental system (Wolf et al., 2018). This effect contributed to the discrepancies of other viruses between Wolf et al. (2018) and our study; We reported smaller 4-log CT values by 7.4-fold in Qβ, 2.6-fold in φX-174, and 8.4-fold in CVB5, respectively. Note that a further consideration on the impact of hydroxyl radicals is required to explain the difference. between Wolf et al., (2018) and ours. They added a radical scavenger (i.e., *tert*-butanol) into their experimental system, which largely reduced the formation of hydroxyl radicals. This also may lead to slower reaction compared to ours. Although the contribution of

hydroxyl radicals on virus inactivation was estimated to be negligible in lake water and wastewater (Wolf et al., 2018), it might be larger in pure water, such as buffer solution.

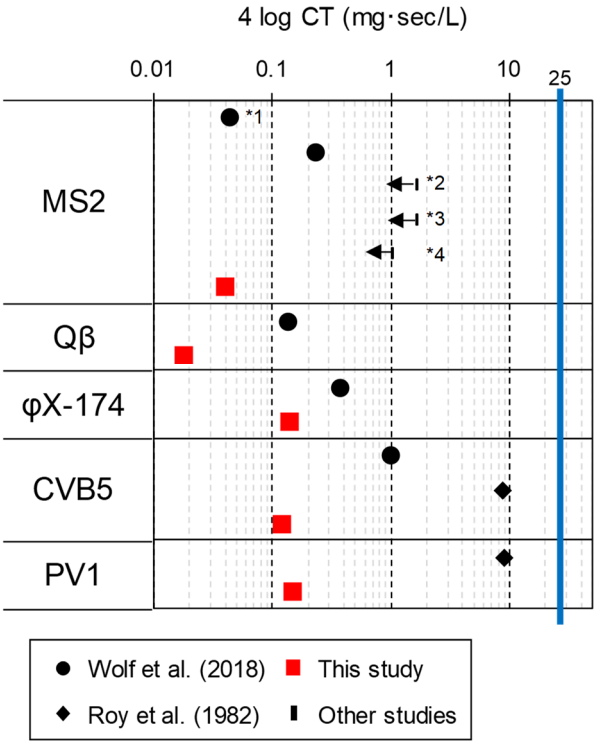

Figure 9 Comparison of 4-log CT value among available studies

Plots with arrows indicate left-censored values. The bolded blue line shows 4-log CT values at 22 °C applied in USEPA guidance manual CT values. Note that all of the ozonation studies cited herein were conducted in phosphate buffer or PBS under the following physicochemical conditions: temperature 16 to 22 °C, pH 6.5 to 7.96.

*1 determined by CQFS in Wolf et al. (2018) study *2 Hall et al. (1993)

*3 Finch et al. (1991) *4 Sigmon et al. (2015)

The 4-log CT values of CVB5 and PV1 in this study were 72-fold and 60-fold smaller than those of Roy et al. (1982). This is due to the difference in the assumption of exposure time. They assumed the average hydraulic retention time to be the exposure time in CSTR without any adjustment of hydraulics (Roy et al., 1982), suggesting that the impact of short-circuiting flow on the CT value was not considered. Thus, we re-calculated the 4-log CT values by incorporating the effect of hydraulics as below.

The first-order reaction in the CSTR can be also modeled as in the case of Eq. (1) in

this supporting information.

$$\frac{N_\tau}{N_0} = \int_0^\infty e^{-kCT} E(T) dT \qquad (4)$$

The residence time distribution (RTD) function in CSTR, namely E(T), is as follows (Fogler, 2008).

$$\mathrm{E(T)} = \frac{1}{\tau} e^{-\frac{T}{\tau}}$$

Eq. (4) can be transformed to

$$\frac{N_\tau}{N_0} = \int_0^\infty e^{-kCT} E(T) dT = \int_0^\infty \frac{e^{-\left(\frac{1}{\tau}+kC\right)T}}{\tau} dT = -\frac{1}{\frac{1}{\tau}+kC} \cdot \frac{1}{\tau} \cdot \left[e^{-\left(\frac{1}{\tau}+kC\right)T}\right]_0^\infty$$

$$= \frac{1}{1+\mathrm{kC\tau}} \quad \text{(Model 3)}$$

Then, the log inactivation as a function of Cτ value in Models 1 and Model 3, are shown in Figure 10, where 61 ($k_{\mathrm{PV1,\,ozone}}$) was substituted for k.

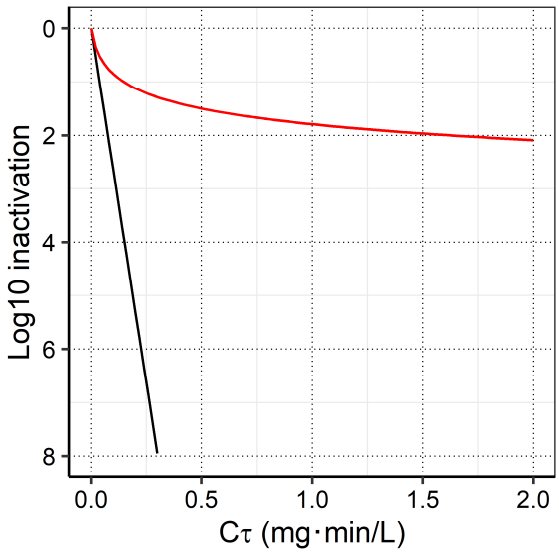

Figure 10 Comparison of theoretical PV1 inactivation under batch reactor and CSTR

The black line indicates the theoretical inactivation in the batch reactor, whereas the red line shows the inactivation in the CSTR.

For example, the required Cτ value to achieve 2-log inactivation is calculated to be 4.6/*k* and 99/*k* in the batch reactor and CSTR, respectively. Therefore, the CT value is theoretically overestimated by 22-fold when the Cτ value was directly reported as the CT value without any adjustment of reactor hydraulics. The remaining difference might be explained by the incomplete mixing of ozone over the water volume, which made streamlines with little ozone in the reactor.

4.3. Implications for the ozone dose management

The current USEPA guidance manual CT values are given by multiplying the required CT value for PV1 inactivation from Roy et al. (1982) with a safety factor of 3× (USEPA, 2010, 1999, 1991). This value has been widely cited in the literature on bench-scale inactivation (Lim et al., 2010; Thurston-Enriquez et al., 2005) and in the prediction of virus inactivation in full-scale treatment (Amoueyan et al., 2019; Smeets et al., 2006). However, 4-log CT values in our study were 166-fold smaller than USEPA guidance manual CT values. Hence, the required CT value for virus inactivation should be reconsidered to accurately predict the virus inactivation by ozonation

It should be noted that the required CT values for the 4-$\log_{10}$ virus inactivation shown in this study were determined by extrapolating the pseudo–first-order relation between CT and inactivation rate. Thus, caution should be taken before interpreting these results. A recent pilot-scale experiment reported that the linear relationship between log virus inactivation and the ozone CT value were observed only at lower rate of virus inactivation (until the initial 4- to 5-log inactivation in surface water or 1- to 2-log inactivation in secondary effluent (Wolf et al., 2019)). They did not observe a log-linear trend but rather a tailing-trend versus CT value at a higher rate of virus inactivation. This is assumingly because a small portion of the virus was protected by the water matrix, which enhanced the virus resistance against ozone (i.e., tailing effect). Therefore, the dose-response relationship in this study can only be applied to predict virus inactivation up to the reported range in the actual ozonation system. To predict the upper range of inactivation (e.g., >6-log inactivation in surface water and >3-log inactivation in secondary effluent), further research is required to consider how to incorporate such a protective effect of the water matrix into the inactivation model.

5. Conclusions

- A simple plug flow assumption in the reaction tube of CQFS leads to underestimating the first-order rate constants of virus inactivation under laminar flow conditions.
- The pseudo–first-order inactivation model that takes into account the RTD (i.e., laminar flow assumption) in the reaction tubes of CQFS made it possible to determine the inactivation rate constants equivalently to those determined by conventional batch system.
- Coliphage MS2, Qβ, which are common surrogates to assess the efficiency of virus reduction through water treatment, were more susceptible to ozonation than poliovirus and coxsackievirus. This indicates that they are not conservative indicators to assess the inactivation of enteric viruses by the ozonation system.
- We predicted that the ozone CT values for 4-log reduction of PV1 (0.15 mg sec L^{-1}), CVB3 Nancy (0.16 mg sec L^{-1}), and CVB5 Faulkner (0.12 mg sec L^{-1}), which were 166-, 156-, and 208-fold smaller than USEPA guidance manual CT values, respectively.

.

Chapter 4

Effect of Intratypic Variability in Free Chrorine Resistance on the Estimation of Overall Inactivation Efficiency of FRNA-phage GI type

A modified version was published as:

鳥居将太郎、片山浩之、ウイルス種内の遊離塩素耐性分布幅が全体不活化率の推定に及ぼす影響、環境工学研究論文集、土木学会環境工学委員会、GS3-0884、2020

1. Introduction

Viruses are major microbial contaminants that cause waterborne diseases (World Health Organization, 2011). Because of the high probability of infection with a given exposure, the acceptable concentration of viruses in drinking water is low (e.g., 1/90,000 L to achieve 10^{-6} disability-adjusted life-year/person (World Health Organization, 2011)). This makes it difficult to assure the viral safety by monitoring the concentration of finished water. Therefore, we need an alternative framework, which is to guarantee the reduction or inactivation efficiency based on the virus concentration in source water.

In urbanized water, the treated wastewater in upstream flows into a source of drinking water supply located at downstream. This situation is referred to as unplanned potable reuse, also known as *de facto* reuse (Soller et al., 2019) and recognized to pose a higher microbial risk. However, the specific regulation framework was not generally implemented. For example, in the United States, no federal regulations specifically address the co-location of drinking water treatment plants in relation to wastewater treatment plant discharge sites upstream of the same water source (Rice and Westerhoff, 2015). However, based on the theoretical background of the risk assessment, the regulators of drinking water may choose to implement potable reuse practices. One of the most known potable reuse practices is the 12/10/10 rules of IPR projects in California (Title 22 and 17 California Code of Regulations, 2015). This rule requires to the regulators who discharges treated wastewater into groundwater for the purpose of indirect potable reuse to reduce virus concentration by 12-log through the whole treatment.

In Japan, *de facto* water reuse is a general implementation and thus its risk should be investigated. Here, as an example, we consider the viral risk of a typical water treatment

train, including activated sludge process as wastewater treatment, and coagulation-sedimentation followed by rapid sand filtration as a drinking water treatment. Previous measurements of virus reduction in full-scale treatment indicated that approximately 2 log reduction of F-specific bacteriophage was observed for activated sludge process and no significant reduction in the chlorination of effluent (Hata et al., 2013). The coagulation-sedimentation provided 2 log removal of pepper mild mottle virus, behaving similarly with enteric viruses in this process, and the rapid sand filtration achieved no significant reduction (Kato et al., 2018).These studies suggest that a total of 8-log reduction of viruses are required during the following disinfection process.

Chlorination (as free chlorine disinfection) is the only disinfectant in the typical drinking water treatment and regarded as a final barrier for the control of pathogens in Japan. This suggests that 8-log inactivation viruses should be achieved only by chlorination. Note that allocable log credit values per single treatment is up to 6-log in California. This suggests that the viral control relying on chlorination is inappropriate in terms of multiple-barriers concept.

The efficacy of chemical disinfection against viruses and the effect of physic-chemical parameters, temperature, pH, etc., have been studied from several decades ago (Gerba et al., 2002; Meng and Gerba, 1996; Sobsey et al., 1988). In the case of chlorination, these studies helped U.S Environment Protection Agency (USEPA) to develop the table of required CT values depending on pH, temperature, and target LRV. Specifically, the required CT values were obtained from LRV of monodispersed hepatitis A virus (HAV) as the representative virus in buffered demand free water with incorporating a safety factor of 3 (USEPA, 2016). Previous research investigated the impact of water matrix and the species or genotype of viruses on the inactivation efficiency by free chlorine.

Only a few studies, however, evaluated the disinfection susceptibilities among closely related strains. Single-stranded RNA (ssRNA) viruses are prone to mutate frequently (Sanjuan et al., 2010) due to the lack of proof-reading mechanisms during replication. For example, the capsid coding region, VP1, of CVB5 was reported to mutate at 0.008 substitutions/site/year. (Hicks and Duffy, 2011). This leads to genetic discreteness of currently circulating viruses from the lab strain in case of Enterovirus (Lukashev et al., 2018) and F-specific RNA coliphage (Hartard et al., 2015). These reports indicate that the amino acid sequence in capsid structure are diverse within the same genotype. The reactivity of amino acids with free chlorine has been reported to differ up to 10,000-fold (Dodd, 2012; Wigginton and Kohn, 2012). Considering that the damage on capsid protein

leads to virus inactivation(Torrey et al., 2019; Wigginton et al., 2012; Zhong et al., 2017b) , it can be hypothesized that the disinfection susceptibility differs between laboratory and environmental strains. In fact, Meister et al., examined the inactivation of environmental strains of CVB5 with free chlorine. They tested a total of 6 environmental strains of CVB5 and reported variabilities in disinfection susceptibilities. For instance, they reported an environmental strain possessing a 5-fold lower susceptibility against free chlorine than Faulkner strain. Therefore, the reliance on the inactivation data of laboratory strain might overestimate the inactivation of indigenous viruses. However, few studies proposed the framework to determine the required CT values under the existence of strains exhibiting different susceptibilities.

The objective of this chapter is to compare the free chlorine susceptibilities of environmental strains, isolated in the river affected by the chlorinated wastewater effluent and laboratory strain of F-specific RNA phage GI type. Moreover, we developed the inactivation model to predict the overall inactivation efficiency of heterogeneous F-RNA phage GI strains by assuming a probability density function of free chlorine resistance. Note that F-specific RNA phage belongs to ssRNA viruses and thus can work as an indicator of biological diversity within the same species of ssRNA viruses.

2. Materials and methods

2.1. Field survey

The field survey was conducted at Tama river in May 23rd, 2018 and at Sagami River at September 11th, 2018. The sampling point at Tama river was located at 1 km downstream of Kitatamaichigo wastewater treatment plant. The sampling point in Sagami river was located at 300 m downstream of Samukawa drinking water treatment plant. The physicochemical and microbiological water quality is shown in Table 5.

Table 5 Physicochemical and microbiological water quality in sampling point

River	Temperature (°C)	pH	Conductivity (mS/m)	Turbidity (NTU)	*E.coli* (CFU/mL)	F-specific bacteriophage (PFU/mL)
Tama river	19.5	8.09	26.4	1.13	11	0.95
Sagami river	22.6	7.75	11.3	12.8	3	0.17

2.2. Detection and isolation of environmental strains of F-specific RNA phages

F-specific phages were determined from a 100 mL of sample by a single-agar-layer method (Grabow, 2004) using *Salmonella enterica* serovar Typhimurium WG49 as a host. Brierfly, a 100 mL of water sample pre-warmed at 37 °C was added into 2x trypton glucose agar and well mixed. Then, the mixture was poured into ten pieces of plates and incubated overnight. The number of plaques was enumerated and reported as plaque-forming units (PFU/mL).

The plaques were randomly isolated from agar plates using a sterilized toothpick and inoculated in a 1.5-ml microtube containing 500 µl of autoclaved phosphate buffer)10 mM, pH 7.0). The microtubes were vigorously vortexed and stored as a plaque suspension at 4 °C until further analysis.

2.3. Genotype of environmental F-specific phage by RT-qPCR

RNA was extracted from 2 µl of plaque suspension by heating at 95 °C for 5 min. The heat treated suspension was subjected to one-step RT-qPCR using Quantitect Probe RT-PCR kit (QIAGEN), The primers and probe specific to F-specific RNA phage GI type

designed by a previous study (Wolf et al., 2010) were adopted. According to the previous study, the samples showing Ct of < 20 were identified as GI type. This genotyping procedure was conducted in singlicate. The RT-qPCR runs were performed under the following temperature conditions: 50 °C for 15 min, 95 °C for 5 min, and 40 cycles of 95°C for 15 sec and 60°C for 60 sec.

2.4. Determination of free chlorine inactivation rate constants of each strain

A total of 37 environmental strains (18 strains from Tama river, 17 strains from Sagami river, and 2 laboratory strain, including MS2 and fr) were examined for their free chlorine susceptibilities.

2.4.1. Propagation of environmental and laboratory strains.

The environmental and laboratory strains of GI type were propagated using *E.coli* K12A/λ (F^+) as a host. The LB broth inoculated with *E.coli* K12A/λ (F^+) at a final concentration of 10^5 CFU/mL were incubated in shaker at 37 °C for 2 hrs. Then, 50 μL of phage suspension was added into the *E.coli* suspension and incubated overnight. After propagation, the phage suspensions were centrifuged at 5000g for 15 min and filtered through a cellulose acetate filter (0.2 μm, DISMIC-25CS, Advantec, Tokyo, Japan) to obtain a crude stock. The concentration of each crude stock was 10^{9-11} PFU/mL. The crude stocks were diluted by 100-fold with 10 mM phosphate buffer (referred to diluted stock) and used for disinfection experiments.

2.4.2. Disinfection experiments

Each GI strain propagated in 2.4.1 were subjected to the disinfection experiments in duplicate. All the glassware, including conical beaker, stirrer bar, and glass bottle, used for disinfection experiments were soaked with 50 mg/L of sodium hypochlorite prepare din 10 mM phosphate buffer and incubated overnight to quench any free chlorine demand.

The free chlorine stock solution was prepared at the final concentration of approximately 100 mg/L. The concentration was measure by DPD method using DR890 colorimeter (Hach Company, Loveland, CO).

Free chlorine disinfection experiment was performed in a batch system at 21 ± 1 °C. Previous studies showed that the virus inactivation with free chlorine proceeds with pseudo-first order with respect to exposure (Sigstam et al., 2013; Wigginton et al., 2012). Our pre-experiments indicated that the inactivation of MS2 proceeded with pseudo-first

kinetics manner (R^2=0.97). Thus, we assumed that all the tested isolates followed the psedo-first order kinetics with respect to CT values.

The 20 μL of diluted stock was inoculated with 20 mL of phosphate buffer and mixed with stirrer for 1 min. A 1-ml of aliquot was collected and added into the 1,5 mltube containing 10 μL of sodium thiosulfate at a concentration of 5,000 mg/L. This sample was used to measure the initial virus concentration.

After the collection of initial sample, a 200 μL of free chlorine stock solution was added into the reactor. A 1 mL of chlorinated sample was collected and quenched in 1.5 mL tube, containing 10 μL of sodium thiosulfate at a concentration of 5,000 mg/L at 60 seconds. Then, the concentration of free chlorine was immediately measure after the sample collection. The decay in free chlorine was less than 5.6 %.

The concentration of GI phage was enumerated by single agar layer method.

2.5. Estimation of inactivation rate constants

The inactivation rate constants were estimated by Chick-Watson model (Chick and Martin, 1908; Watson, 1908) as shown below.

$$\frac{\partial N}{\partial T} = -kC^{\eta}N$$

N: Phage concentration (PFU mL^{-1}) *k*: inactivation rate constnats (mg^{-1} sec^{-1} L)
C: Free chlorine concentration (mg L^{-1}) *T*: time (sec) η: Coefficienct of dilution

Suppose coefficient of dilution can be set to be 1, The equantion can be transformed as follows.

$$N = N_0 e^{-kCT}$$

N_0: Initial phage concentration (PFU mL^{-1})

The inactivation rate constants *k* was determined by the following equation. The arithmetic mean of two determined values were reported.

$$\frac{N_{60}}{N_0} = \mathrm{e}^{-kCT}$$

N_0: Initial phage concentration (PFU mL^{-1}) N_{60}: Phage concentration at time 60 seconds

(PFU mL^{-1})

k: inactivation rate constants (mg^{-1} sec^{-1} L) C: Free chlorine concentration (mg L^{-1})

T: Time (seconds), Required CT values for 4 log inactivation of virus

$$4\log CT \ \ (mg \ \ sec \ \ L^{-1}) = \frac{4}{klog_{10}e}$$

2.6. Parameter inference of the probability density function

In this study, Two types of probability distributions (log-normal and gamma distributions) were assumed for the inactivation rate constant k

$$k \sim lognormal \ (\mu, \sigma)$$

$$k \sim gamma \ (\alpha, \beta)$$

The parameters of gamma distribution (α, β) and lognormal distribution (μ, σ) were inferred by moment matching estimation and maximum likelihood estimation, by fitting each distribution to the set of disinfection rate constants estimated in the section 2.5. The parameters inference, Kolmogorov-Smirnov test and the calculation of Akaike information criterion (AIC) were performed with an R package {fitdistrplus} (Delignette-Muller and Dutang, 2015).

2.7. Inactivation model incorporating the distribution of inactivation rate constants

The overall inactivation of GI phage was modeled as follows. Firstly, the inactivation rate of a GI strain, whose inactivation rate constant is *k*, can be formulated by a pseudo-first-order model.

$$\frac{N_k}{N_{k,0}} = e^{-kD} \quad \cdots (4)$$

where $N_k/N_{k,0}$ indicates the inactivation rate, *D* indicates the CT values, and *k* indicates the inactivation rate constant. We can interpret *k* as the level of susceptibility to disinfectants; for instance, if $k = 2$, the strain inactivates twice faster compared with the strain that has $k = 1$.

Therefore, we can predict the overall inactivation rate of the GI type as follows if we use the inactivation rate constant of MS2 for laboratory strains,

$$\frac{N}{N_0} = e^{-k_{MS2}CT}$$

k_{MS2}: Inactivation rate constants for MS2 (mg^{-1} sec^{-1} L)

Suppose that the inactivation rate constant, *k*, differs and distributes as *f*(*k*). The overall inactivation can be given by the arithmetic mean of the inactivation rate weighted by the probability density function.

$$\frac{N}{N_0} = \int_0^\infty \frac{N_k}{N_{k,0}} \cdot f(k)dk = \int_0^\infty e^{-kD} \cdot f(k)dk$$

where N/N_0 indicates the overall inactivation rate of CVB5. $N_k/N_{k,0}$ is the inactivation rate of the strain whose constant is *k*.

If *k* distributes in log-normal manner, the equation above does not have a closed-form expression. The overall survival rate of CVB5 was described as eq. (8) and numerically simulated by summing the survival rate weighted by the probability density function. The numerical simulation was conducted, where *n* was set to be 10^7.

We initially generated a total of 10^7 random numbers following lognormal distribution. Then, we assigned the obtained *k* to e^{-kCT} individually and calculate the arithmetic mean of all the e^{-kCT}.

$$k \sim lognormal(\mu, \sigma)$$

$$\frac{N}{N_0} = \lim_{n\to\infty} \sum_{z=1}^{n} \frac{e^{-CTx_z}}{n} \quad \cdots (8)$$

where x_z is the susceptibility randomly sampled from the lognormal distribution

3. Results and discussion

3.1. Free chlorine disinfection experiments

A total of 37 strains of F-specific RNA phage GI type (35 environmental strains isolated in the Tama river and Sagami river and two laboratory strains) were tested for free chlorine resistance, and the CT values required for the inactivation of 4 logs of each strain are shown in Figure 11.

First, the inactivation rate constant *k* of the laboratory strain MS2 was 0.14 ± 0.01 (mg-1 sec-1 L), and the 95% confidence interval of the CT value required for 4 log inactivation was [56.7, 74.5 (mg sec L^{-1})]. These values were comparable to those reported in previous studies22, 23) in which MS2 inactivation experiments were conducted (Sigstam et al., 2013).

Secondly, 13 out of 18 strains in the Tama River and all the strains (17 out of 17) in Sagami River were found to be resistant compared to 74.5, the upper limit of the 95% confidence interval for the 4 log inactivated CT value of MS2. The required CT value of most resistant strain for 4 log inactivation was 1.6 times higher than that of laboratory strain MS2. In other words, predicting the inactivation rate using laboratory strains may overestimate the chlorine disinfection inactivation rate.

In addition, the inactivation rate constant of the GI environmental strains in the Sagami River was significantly lower than in the Tama River (Wilcoxon rank sum test: $P < 0.05$). A previous study suggested that environmental strains belonging to the GI type have different gene sequences in the capsid region depending on the type of fecal contamination (Hartard et al., 2015). Therefore, the free chlorine disinfection resistance of GI wild-type strains may differ with geographic differences.

Future analysis of the genetic information of each wild strain is expected to reveal the differences in disinfection resistance between strains and between rivers.

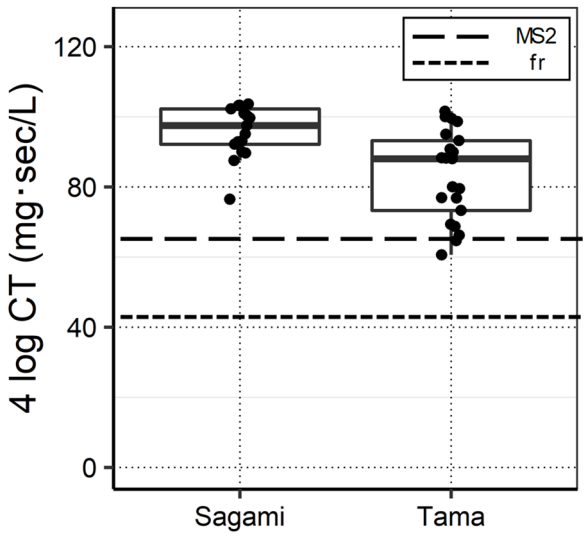

Figure 11 4 log CTvalues for each environmental strain

The environmental strain in each river are marked with black circles. The value of laboratory strain MS2 was shown with long dashed lines and fr was shown with short dashed lines.

3.2. Estimation of probability distribution of inactivation rate constants

The probability distributions of the inactivation rate constants of environmental strains of GI-type were estimated.

First, the AIC was used to determine the appropriate assumption of probabilities distribution fitting better to the experimental results (the log-normal or gamma distributions) The AICs for the Tamagawa river were -107.4 and -106.9, assuming log-normal and gamma distributions, respectively. In the Sagami River, the values were -113.8 and -113.2, respectively. Therefore, the log-normal distribution fitter better in both rivers.

The parameters for the log-normal distribution of the inactivation rate constant were estimated to be (μ, σ) = (-2.18, 0.15) and (-2.33, 0.07) for the Tama and Sagami rivers, respectively. The distribution of the generated random numbers for k is shown in Figure 12. The P value of the Kolmogorov-Smirnov test was more than 0.05 for both, suggesting that they may follow a log-normal distribution. The generated random numbers for k were

used in the numerical calculation of the overall inactivation rate using Model 2.

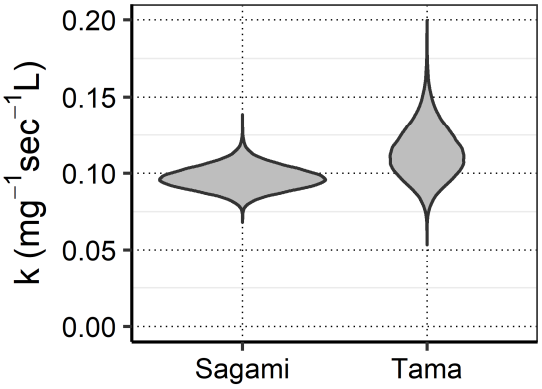

Figure 12 Violin plot of inactivation rate constants

3.3. Impact of distribution of inactivation rate constants on the prediction of inactivation rate

Previous studies have examined the effects of physicochemical water quality (e.g., water temperature and pH) on the inactivation rate constant (Cromeans et al., 2010; Kahler et al., 2011; Sobsey et al., 1988). However, there is no model that accounts for the variability due to biological differences within species. This study suggested that GI environmental strains in the water environment had a higher free chlorine resistance than laboratory strains and that the free chlorine resistance were different among strains. Therefore, the overall GI-type inactivation rate should be predicted by Model 2, which accounts for biological variation. On the other hand, in actual water quality control, the overall inactivation rate is estimated based on the laboratory strains (Model 1). Therefore, a comparison between the two models to reveal problems with current water quality management that do not account for the distribution of inactivation rate constants.

Figure 13 shows the relationship between CT values and overall inactivation rates for Model 1 and Model 2. The CT values required for 4 log and 8 log inactivation were predicted to be 65 and 129 (mg sec L^{-1}) for Model 1, respectively. On the other hand, Model 2 predicted values of 90, 197 (Tama River), 98, and 201 (Sagami River) (mg sec L^{-1}), respectively. It was suggested that a large CT value should be applied to achieve the

same degree of inactivation in actual water treatment. In other words, the microbial cotrol based on the inactivation rate of the GI laboratory strain, MS2, overestimates the inactivation of various GI types in the actual treatment The deviations are larger at higher assumed inactivation rates. For example, when GI-type phages in the Tama and Sagami rivers were disinfected with the CT value which achieves 8 log inactivation of laboratory strain MS2, the overall inactivation rate was limited to be 5.6 and 5.3 log, respectively. The information on the variation in free chlorine resistance within species should be taken into account when estimating the inactivation rate of actual environmental samples.

The next point is the need for further investigation of the uncertainties in the assumptions of the log-normal distribution and the limit calculations. In predicting high inactivation rates, the estimation of the skirts of the distribution of the inactivation rate constants affects the overall inactivation rate. Therefore, it is necessary to carefully evaluate the validity of the parameter estimation method and the setting of n in the limit calculation (e.g., how large n should be estimated for the predicted inactivation rate to fully reflect the assumptions of the lognormal distribution) when the model is used in practice.

Further studies are required in terms of two viewpoints. First, it is necessary to investigate the variability in inactivation rate constants of enteric viruses, which are risk factors in actual water treatment. The results of this study suggest that the free chlorine resistance of noroviruses and enteroviruses, possessing single-stranded RNA, may have a variability in free chlorine resistance. Existing inactivation models need to be developed by investigating the tolerance distribution range of wild strains.

The next point is the need for further investigation of the uncertainties in the assumptions of the log-normal distribution and the limit calculations. In predicting high inactivation rates, the estimation of the lower-tail of the distribution affects the overall inactivation rate, especially at the higher inactivation rate. Therefore, it is necessary to carefully evaluate the variability of the parameter estimation method and the setting of n in the limit calculation (e.g., how large n should be estimated for the predicted inactivation rate to fully reflect the assumptions of the lognormal distribution) when the model is used in practice.

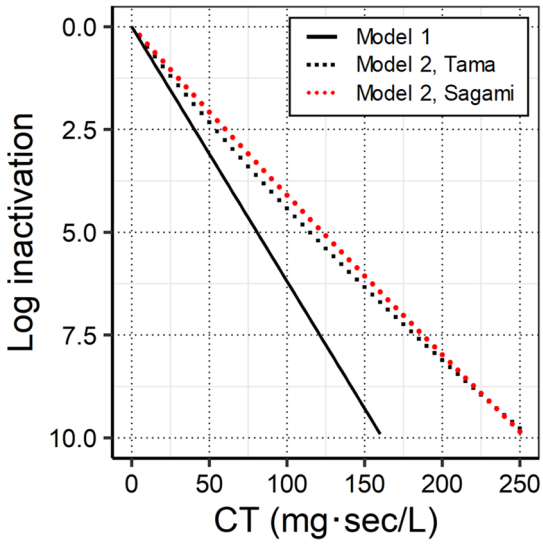

Figure 13 Overall inactivation of GI phage

Model 2, Tama: Overall inactivation in Tama river

Model 2, Sagami: Overall inactivation in Sagami river

4. Conclusions

Environmental strains belonging to the F-specific RNA bacteriophage type GI were isolated and tested for free chlorine resistance in the Tama and Sagami rivers, where the chlorinated secondary effluent occupied a large part of flowing. The results showed that (i) the chlorine resistance of 13 of 18 environmental strains in the Tama River and all 17 straubs in the Sagami River was significantly higher than that of laboratory strain MS2. (ii) when GI wild-type strains in the Tama and Sagami rivers were disinfected with CT values that achieves 8 log inactivation of laboratory strain MS2, the overall inactivation rate was estimated to be only 5.6 and 5.3 logs, respectively. Therefore, the estimation of the inactivation efficiency based on the laboratory strain MS2 may overestimate the actual inactivation rate by 2.4 - 2.7 log. Considering that the findings of experiments with laboratory strains are generally used to discuss the disinfection effect of viruses, the information on the variation in free chlorine resistance within species should be taken into account when estimating the inactivation rate of actual environmental samples.

Chapter 6

Conclusions

Virus is one of the major causative agents of waterborne diseases. Due to its low infectious dose, the acceptable concentration in drinking water is extremely low. This requires the regulators to achieve a high reduction through water treatment The conventional physical treatment has limited capacity to remove viruses in full-scale treatment plants. Thus, the current treatment system virtually relies on the disinfection process, such as chlorination, ultraviolet irradiation, and ozonation, for reducing viruses. Therefore, the efficacy and potential uncertainty of disinfection efficiency on virus reduction should be carefully examined.

The present dissertation filled the research gaps related to the kinetics of virus inactivation by disinfection in drinking water and also highlighted the importance of the reconsideration on inactivation kinetics of viruses by disinfectants.

1. Inactivation kinetics of waterborne virus by ozone

- A simple plug flow assumption in the reaction tube of CQFS leads to underestimating the first-order rate constants of virus inactivation under laminar flow conditions.
- The pseudo–first-order inactivation model that takes into account the RTD (i.e., laminar flow assumption) in the reaction tubes of CQFS made it possible to determine the inactivation rate constants equivalently to those determined by the conventional batch system.
- Coliphage MS2, Qβ, which are common surrogates to assess the efficiency of virus reduction through water treatment, were more susceptible to ozonation than poliovirus and coxsackievirus. This indicates that they are not conservative indicators to assess the inactivation of enteric viruses by the ozonation system.
- We predicted that the ozone CT values for 4-log reduction of PV1 (0.15 mg sec L^{-1}), CVB3 Nancy (0.16 mg sec L^{-1}), and CVB5 Faulkner (0.12 mg sec L^{-1}), which were 166-, 156-, and 208-fold smaller than USEPA guidance manual CT values, respectively. The required CT values should be reconsidered to minimize the health risks and operational costs simultaneously.

2. Effect of Intratypic Variability in Free Chrorine Resistance on the Estimation of Overall Inactivation Efficiency of FRNA-phage GI type

- A total of 30 strains (out of 35 strains) of F-RNA phage GI exhibited higher free chlorine resistance than MS2 and fr, laboratory strains of GI phage.
- The developed model, incorporating the heterogeneity in free chlorine susceptibility, suggested that the overall inactivation efficiency of GI phages was limited to 5.6 log and 5.3 log in Tama and Sagami river, respectively, in the case that 8 log MS2 inactivation was expected.
- The heterogeneity in free chlorine resistance within specific reference pathogens should be incorporated into the model to accurately predict the inactivation efficiency in environmental water.

3. Impact of the heterogeneity in free chlorine, UV254, and ozone susceptibility among coxsackievirus B5 on the prediction of the overall inactivation efficiency

- Environmental strains of coxsackievirus B5 (CVB5) in genogroup B exhibited significantly lower susceptibility against free chlorine and ozone than CVB5 genogroup A, to which the laboratory strain of CVB5 (Faulkner strain) belong. This indicates that CVB5 Faulkner should not be regarded as the “most” chlorine or ozone resistant virus”.
- The lower susceptibility in genogroup B may be attributable to the low reactivity of capsid protein. The free chlorine and ozone susceptibility were associated with the number of sulfur-containing amino acid (i.e. cysteine and methionine), which are readily reacted with oxidants.
- The disinfection susceptibilities among CVB5 strains were variable in free chlorine and, by contrast, nearly constant in UV_{254}. This difference in variability among disinfectants provided a novel viewpoint; The prediction of inactivation efficiency by UV_{254} is not likely to be affected by the biological heterogeneity while that by free chlorine might fail due to the variety in susceptibilities within CVB5 strains.
- Free chlorine susceptibility was positively correlated with ozone susceptibility. This was attributable to the similarity in the inactivation mechanism (i.e., oxidation

of the capsid). This means that the infective viruses that remained after ozonation may exhibit lower free chlorine susceptibility. This leads to overestimating the inactivation efficiency by the free chlorine that follows ozonation in actual water treatment train because the microbial inactivation credit is allocated to each water treatment independently. Moreover, this suggested a potentially robust multiple-barrier treatment, such as UV_{254} and one of FC or ozone, not the combination of free chlorine and ozone.

- We expanded the Chick-Watson model to predict the inactivation efficiency of heterogeneous CVB5 by assuming a probability density function (gamma or lognormal) of inactivation rate constants (k). The model showed how dangerous it is to assume the homogeneous susceptibility when predicting the virus inactivation of a specific reference pathogen. For example, the model indicated that 2.8 – 4.2-fold of free chlorine CT is required to fulfill the 6-log overall inactivation of heterogeneous CVB5 strains compared to that for CVB5 Faulkner. This effect is striking in free chlorine due to the higher variability in susceptibility than UV_{254} and ozone.

4. Overall conclusions

The findings of this dissertation provided two implications for the more accurate determination of inactivation efficiency during disinfection process.

- Implications for meta-analysis of inactivation rate constants

The findings on the inactivation kinetics of viruses by disinfectants have been accumulated since the 1980s. Currently, several studies tried to wrap up these studies by systematic review and meta-analysis (Boehm et al., 2019; Espinosa et al., 2020; Hijnen et al., 2006; Kadoya et al., 2020; Rachmadi et al., 2020). However, they also observed great inter-study variability in the inactivation kinetics. Although the standpoint of the meta-analysis is to accept the inconsistency among studies as the inherent variability that the disinfectants originally have, the understanding of the fundamental factors producing the variability can contribute to more precise prediction. For example, Chapter 3 in this dissertation pointed out that the observed discrepancy (up to 72-fold) of virus inactivation kinetics by ozone was due to the inappropriate calculation of CT values of previous studies; the heterogeneity in t in the CSTR was not taken into account. This finding can improve the criteria for data extraction (whether the reviewer of meta-analysis includes

the corresponding data or not) during a systematic review process.

■ Implications for advanced disinfection control

The overdosing of disinfectants is accepted as a safer approach from the viewpoint of microbial risks; however, it results in increased operational cost. The integrated disinfection design framework aims to control the disinfectant exposure time by time to appropriately balance under-treatment and over-treatment, resulting in providing environmental and economic benefits in water treatment (Bellamy et al., 1998; Manoli et al., 2019).

The precisely meta-analyze inactivation rate constants and their distribution can be incorporated into IDDF. The IDDF concept was created to determine the required disinfectant dose and contact time site-specifically. The main three components include,

1. Disinfectant demand and decay rate
2. Inactivation kinetics of target pathogen
3. Hydraulics of disinfection contactor

The comprehensive consideration of these factors can theoretically predict the virus inactivation at the actual treatment (Bellamy et al., 2000a).

The outcomes of this dissertation can be also interpreted as a further improvement in the IDDF concept. Specifically, Chapter 3 recommended the reconsideration of k values adopted in the ozone disinfection of viruses. Chapter 4 and 5 proposed other models that allow for incorporating the distribution of k in which the target pathogen inherently has. The upgraded IDDF was proposed in Figure 25.

Further studies thus should identify the fundamental factors affecting the existing discrepancy among studies. The accumulation and summarization of factors affecting heterogeneity are expected to contribute to more precise and flexible prediction of inactivation efficiency.

Consequently, the application of the proposed IDDF provides the mechanistic rationale on the current empirical-based disinfection in water treatment. This leads to the more precise prediction of virus inactivation efficiency and the optimization of water treatment.

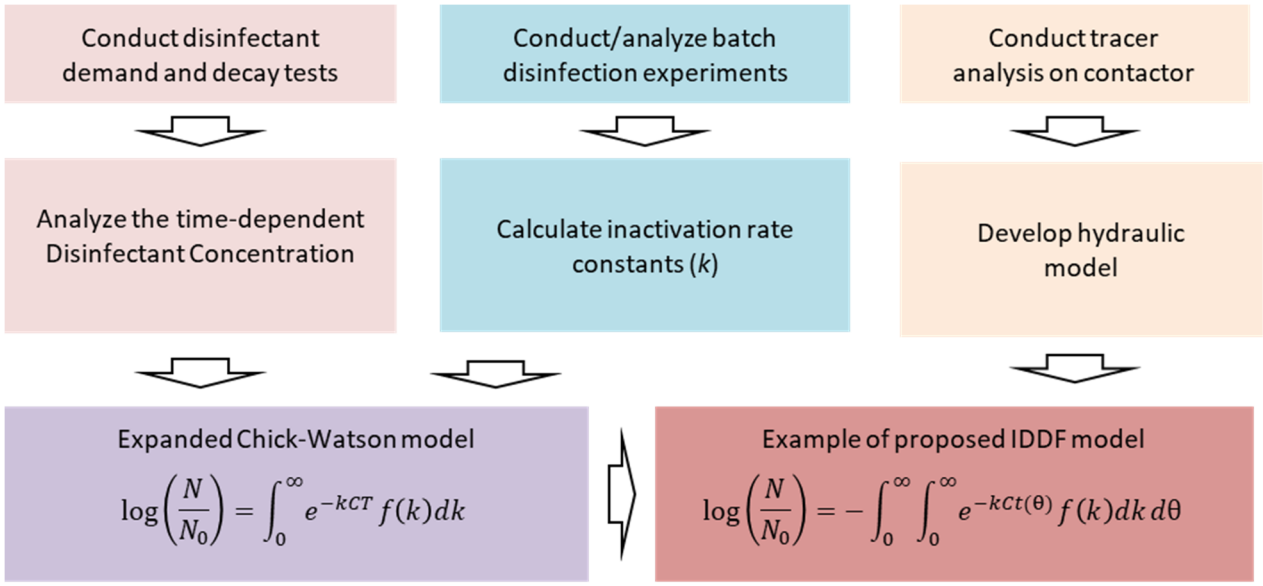

Figure 25 Integrated disinfection design framework (IDDF) modeling approach

Appendix

Applicability of polyethylene glycol precipitation followed by acid guanidinium thiocyanate-phenol-chloroform extraction for the detection of SARS-CoV-2 RNA from municipal wastewater

A modified version was published as:

Torii, S., Furumai, H., Katayama, H., 2020. Applicability of polyethylene glycol precipitation followed by acid guanidinium thiocyanate-phenol-chloroform extraction for the detection of SARS-CoV-2 RNA from municipal wastewater. Sci. Total Environ. 143067.

1. Introduction

The ongoing disease outbreaks caused by severe acute respiratory syndrome coronavirus 2 (SARS-CoV-2) have tremendous damage to global health and world economics. The main transmission of the respiratory viruses is via close contact with respiratory secretions expelled by an infected person (World Health Organization, 2020). Although the respiratory viruses predominantly caused respiratory diseases, the SARS-CoV-2 genome was detected not only from the respiratory tract but also from stools (Chan et al., 2011; Wölfel et al., 2020). Therefore, the detection of human pathogenic viruses from wastewater suggests the presence of infected people in the catchment area. This approach has been expected to be feasible to evaluate the eradication of poliovirus in the community (Lodder et al., 2012) and the prevalence of norovirus, (Kazama et al., 2016) known as wastewater-based epidemiology (WBE). Currently, the monitoring of the SARS-CoV-2 concentration is expected to be a powerful tool for the early detection of outbreaks and the prediction of prevalence in the catchment (Kitajima et al., 2020; Murakami et al., 2020; Rusiñol et al., 2020).

Recent studies have detected SARS-CoV-2 in the raw sewage or secondary effluent by applying primary concentration methods followed by RNA extraction and reverse transcription (RT)-quantitative polymerase chain reaction (qPCR) (Ahmed et al., 2020a; Haramoto et al., 2020; Medema et al., 2020; Randazzo et al., 2020; Sherchan et al., 2020). The adopted primary concentration methods included polyethylene glycol precipitation (PEG) (Lewis and Metcalf, 1988), ultrafiltration (UF) (Ikner et al., 2011), electronegative

membrane vortex (EMV) (Haramoto et al., 2020), and adsorption–extraction methods (Ahmed et al., 2020a). Toward a broad application of WBE, the whole process for the quantification of viruses should be cost effective with high efficiency.

The conventional primary concentration has been optimized to detect waterborne enteric viruses, which are mostly nonenveloped. Enveloped viruses possess a lipid membrane at the outermost layer, thus exhibiting different physical properties (i.e., more hydrophobic) from nonenveloped viruses (Lytle and Routson, 1995). Few studies have evaluated the applicability to the recovery of enveloped viruses from water. A previous study adopted the filter-lysis method and struggled with efficient recovery of enveloped viruses: poliovirus (nonenveloped) for 45% versus koi herpes virus (enveloped) for 3.6% (Haramoto et al., 2009). Thus, the conventional process should be optimized for the efficient recovery of enveloped viruses.

A recent study compared a variety of concentration methods for the recovery of murine hepatitis virus (MHV), a surrogate of SARS-CoV-2, from raw sewage (Ahmed et al., 2020b). They reported the highest MHV recovery rate for the adsorption–extraction methods with $MgCl_2$ pretreatment (65.7%). They also reported a 56.0% recovery for the UF using Amicon Ultra-15 centrifugal filter device. Although these methods achieved a recovery efficiency high enough for detecting enveloped viruses in the raw sewage, expensive equipment (e.g., bead-beating system) and costly consumable supplies (e.g., centrifugal device) are needed for sample processing. Hence, the primary concentration methods that can be used in low-resource settings should be developed. Moreover, previous studies did not investigate how the water quality and the type of the molecular process affect the whole recovery efficiency of enveloped viruses. Thus, the recovery efficiency of enveloped viruses from the raw sewage should be further validated.

Bacteriophage φ6 is an enveloped double-stranded RNA virus, with a diameter of 85 nm, belonging to *Cystoviridae*, infecting gram-negative *Pseudomonas syringae*. To evaluate the recovery efficiency during primary concentration and the persistence in the aqueous phase, this virus has been frequently used as a surrogate for pathogenic enveloped viruses (i.e., human coronavirus and influenza virus) (Casanova and Weaver, 2015a; Ye et al., 2016). A recent study adopted it as a molecular process control (MPC) (Sherchan et al., 2020). Moreover, φ6 and its host, *Pseudomonas syringae*, are not pathogenic to humans and require minimal containment for laboratory facilities (i.e., BSL1) (Casanova and Weaver, 2015b). Finally, φ6 can be propagated within 1 day with high titers (up to 10^{10} PFU/mL); thus, it can be practically used as a surrogate for the

human pathogenic enveloped viruses.

This study aims (1) to compare the combination of primary concentration (UF, EMV, and PEG) and RNA extraction (QIAamp Viral RNA Mini Kit and TRIzol) for the whole process recovery of nonenveloped and enveloped virus surrogates and (2) to test the applicability of the method providing the highest φ6 recovery to detect SARS-CoV-2 RNA from the raw sewage. In this study, F-specific coliphage MS2, as a surrogate of nonenveloped viruses, and *Pseudomonas* phage φ6, as a surrogate of enveloped viruses, were adopted as a whole process control (WPC) (Haramoto et al., 2018). Furthermore, the murine norovirus (MNV) was used as an MPC to evaluate the inhibitory effects or recovery loss during the RNA extraction and RT-qPCR process.

2. Materials and Methods

2.1. Preparation of coliphage MS2, *Pseudomonas* phage φ6, and murine norovirus

Bacteriophage MS2 (NBRC 102619, National Institute of Technology and Evaluation (NITE), Tokyo, Japan) was propagated as described elsewhere (Torii et al., 2019a). *Pseudomonas* phage φ6 (NBRC 105899, NITE) was propagated using *Pseudomonas syringae* (NBRC14084, NITE) as a host strain. Briefly, 3 mL of phosphate buffer (PB) (10 mM, pH 7.0) was added on the soft LB plates (0.7% agar) semiconfluent with φ6 plaques (approximately 1000 plaques/plates) and incubated at room temperature for 5 h. The suspension and soft agar were then removed from the plate and transferred to a centrifuge tube. Next, 10 mL of recovered viruses were clarified by centrifugation at 3500 g for 15 min and filtered through a cellulose acetate filter (0.2 μm, DISMIC-25CS, Advantec, Tokyo, Japan). MNV S7-PP3 strain was propagated using RAW.264.7 cell as a host (Kitajima et al., 2008). The concentrations of propagated stocks were approximately 10^{11} PFU/mL, 5×10^{9} PFU/mL, and 10^{11} copies/mL for MS2, φ6, and MNV, respectively. The propagated stocks were stored at 4°C. Before the primary concentration, the MS2 and φ6 stocks were diluted by 1000-fold and 100-fold, respectively, to prepare the diluted stocks.

2.2. Raw sewage

Three raw sewages were used for the comparison: raw sewage A was a grab sample collected from the influent of a wastewater treatment plant (WWTP) located in Niigata

Prefecture, raw sewage B was a composite sample collected from the influent of a WWTP located in Kanagawa Prefecture, and raw sewage C was a composite sample collected from the influent of WWTP located in Tokyo metropolis. The composite samples of raw sewage at wastewater treatment plants B and C were generated as below. At wastewater treatment B, raw sewage was collected on May 11, 13, 18, 25, and 27 and June 1 and 3. An approximately 200 mL of each raw sewage was stored at −20°C before compositing. At wastewater treatment C, raw sewage was collected on May 13, 18, 22, 25, and 28 and June 1, 4, 10, 24, and 30. An approximately 150 mL aliquot of each raw sewage was stored at −20°C. The stored aliquots were thawed and mixed well to generate composite samples. The resultant composite samples were stored at −20°C before the primary concentration. The physicochemical water qualities of each raw sewage is shown in Table 18. All the samples were stored at −20°C until the primary concentration.

Table 18 Physicochemical water quality parameters of each raw sewage

Raw sewage	pH	Total suspended solids (TSS) (mg/L)[a]	UV_{260}
A	7.56	225 ± 27	0.231
B	8.19	344 ± 41	0.583
C	8.45	334 ± 49	0.529

[a]TSS was measured three times. Average and standard deviation are described.

2.3. Primary concentration

Three primary concentration methods were tested: ultrafiltration after pre-centrifugation (**UF**), electronegative membrane vortex (**EMV**), and polyethylene glycol precipitation after pre-centrifugation (**PEG**).

A 50-mL (for **UF** and **EMV**) or 40-mL (for **PEG**) of raw sewage was inoculated with 1/1000 amount of diluted stocks of MS2 and φ6 (i.e., 50 μL for **UF** and **EMV**, 40 μL for **PEG**) and incubated at 4 °C for 1.5 h – 2.5 h. For a single day, ranging from 4 to 14 of aliquots of spiked raw sewage were prepared. As a control, 50 mL of MilliQ water spiked with 50 μL of diluted stocks of MS2 and φ6 were prepared in duplicate every single day. The incubation of raw sewage for 1.5–2.5 h is expected to reach the liquid–solid partitioning of spiked viruses at equilibrium, which allows for mimicking the actual partitioning conditions of viruses in raw sewage (Ye et al., 2016). The procedure of each primary concentration method was conducted four times per type of raw sewage (i.e., raw sewages A, B, and C).

UF: A 50-mL aliquot of raw sewage was centrifuged at 3500 g for 15 min to remove large particles. The supernatant was further centrifuged at 3500 g for 20 min to filter through the Centricon Plus-70 centrifugal device with a molecular cutoff of 30 kDa (Merck Millipore, Billerica, MA, USA). The final volume of the concentrates ranged from 0.17 to 0.21 mL. Thus, the concentration factor in UF ranged from 237- to 294-fold.

EMV: EMV was performed based on a previous study (Haramoto et al., 2020). A 50 mL aliquot of raw sewage inoculated with 500 µL of 2.5 M $MgCl_2$ was filtered through a mixed cellulose-ester membrane (HAWP04700, pore size, 0.45 µm; diameter, 47 mm; Merck Millipore) by vacuum aspiration. Subsequently, 10 mL of elution buffer, containing 0.2 g/L of sodium polyphosphate, 0.3 g/L of ethylenediaminetetraacetic acid trisodium salt trihydrate ($C_{10}H_{13}N_2O_8Na_3$ $3H_2O$), and 0.1 mL/L of Tween 80, was added to the filtered membrane in a 50-mL centrifuge tube. Elution was performed by vigorous vortexing using a football-shaped stirring bar. This step was repeated using a 5 mL of elution buffer after transferring a 10-mL of eluent to a different centrifuge tube. The resultant eluent (approximately 15 mL) was centrifuged at 2,000 g for 10 min at 4°C. The supernatant was filtered through a cellulose acetate filter (0.2 µm, DISMIC-25CS, Advantec, Tokyo, Japan). The filtrate was centrifuged at 1,500 g for 10 min twice followed by 5 min in a Centriprep YM-50 UF device (Merck Millipore) for concentration. The final volume of the concentrate ranged from 0.64 to 4.38 mL. Thus, the concentration factor in EMV ranged from 11.4- to 78.1-fold.

PEG: A 40-mL aliquot of raw sewage was centrifuged at 3,500 g for 5 min to remove large particles. The supernatant was supplemented with 4 g of PEG8000 (Sigma-Aldrich , MO, USA) and 2.35 g of NaCl (Wako, Osaka, Japan) to the final concentrations of 10% (w/v) and 1.0 M, respectively, and incubated at 4 °C overnight in a shaker (Hata et al., 2020). Thereafter, the mixture was centrifuged at 10,000 g for 30 min. The pellet was resuspended with 10 mM PB. The final volume of the concentrate ranged from 0.42 to 0.8 mL. Thus, the concentration factor in PEG ranged from 50- to 95-fold.

After each primary concentration, the resultant concentrate and control samples were stored at -20 °C until the molecular process. Freeze-thawing of primary concentrates was limited up to once.

2.4. RNA extraction

For the section 3.1, two types of viral RNA extraction methods were tested: spin

column-based nucleic acid purification using QIAamp Viral RNA Mini Kit (QIAGEN, Hilden, Germany) and acid guanidinium thiocyanate–phenol–chloroform extraction (Chomczynski and Sacchi, 1987) using TRIzol reagent (Thermo Fisher Scientific, MA, USA). First, a 140-μL aliquot of the virus concentrate was seeded with 5 μL of nonenveloped MNV (corresponding to 4.32 ± 0.19 copies) as an MPC. As a control, a 140-μL aliquot of MilliQ spiked with the same amount of MNV was prepared in duplicate. The comparison of MNV concentrations between concentrated samples and control samples allows to evaluate the molecular process recovery ratio as described in 2.6. The spiked concentrates were processed following the manufacturer's instruction to obtain an RNA extract with a final volume of 60 μL. Thus, the concentration factor in the RNA extraction process was 2.3-fold. The extracted RNA was subjected to the RT process within the same day.

2.5. RT-qPCR

Before the RT-qPCR step, the RNA was incubated at 95°C for 5 min followed by 4°C for 1 min (Mijatovic-Rustempasic et al., 2013) to denature dsRNA of φ6. A preliminary investigation indicates that the heating step did not significantly affect the quantification results of MS2 suspended in MilliQ water (data not indicated).

First, 20 μL of the RNA extract was subjected to the RT step. A High-Capacity cDNA RT Kit (Thermo Fisher Scientific) was used to obtain cDNA with a final volume of 40 μL. The concentration factor in RT process was 0.5-fold. The obtained cDNA was stored at 4°C and subjected to qPCR within 2 days.

Then, TaqMan™ Gene Expression Master Mix was used to perform qPCR following the manufacturer's protocol. A 5 μL of the cDNA was mixed with 15 μL of the reaction mixture containing 10 μL of the master mix, virus-specific forward primers and reverse primers, and TaqMan probe. The sequence of primers and the probe (Gendron et al., 2010; Kitajima et al., 2008; Wolf et al., 2010) were described in Table 19. The conditions of thermal cycling were as follows: 50°C for 2 min and 95°C for 10 min, followed by 45 cycles of 94°C for 15 sec and 60°C for 60 sec (for quantification of MS2 and φ6), or followed by 94°C for 15 sec and 56°C for 60 sec (for MNV quantification).

Table 19 The primers and probes for qPCR assays

Assay	Function	Name	Sequence (5' – 3')	Product length	Citation
MS2	F	VTB4-FphGIf	GTCCTGCTCRACTTCCTGT	91	(Wolf et al., 2010)
	R	VTB4-FphGIr	ATGGAATTSCGGCTACCTACA		
	P	VTB4-FphGIprobe	FAM-CGAGACGCTACCWTGGCTATCGC-BHQ1		
φ6	F	φ6Tfor	TGGCGGCGGTCAAGAGC	100	(Gendron et al., 2010)
	R	φ6Trev	GGATGATTCTCCAGAAGCTGCTG		
	P	φ6Tprobe	FAM-CGGTCGTCGCAGGTCTGACACTCGC-BHQ1		
MNV	F	MKMNVF	CGGTGAAGTGCTTCTGAGGTT	60	(Kitajima et al., 2008)
	R	MKMNVR	GCAGCGTCAGTGCTGTCAA		
	P	MKMNVP	FAM-CGAACCTACATGCGTCAG-MGB-NFQ		
NIID_2019-nCOV_n	F	NIID_2019-nCOV_N_F2	AAATTTTGGGGACCAGGAAC	158	(Shirato et al., 2020)
	R	NIID_2019-nCOV_N_R2ver3	TGGCACCTGTGTAGGTCAAC		
	P	NIID_2019-nCOV_N_P2	FAM-		

			ATGTCGCGCATTGGCATGGA -BHQ1		
CDC N1	F	2019-nCoV_N1-F	GACCCCAAAATCAGCGAAAT	73	(Centers for Disease Control and Prevention, 2020)
	R	2019-nCoV_N1-R	TCTGGTTACTGCCAGTTGAATCTG		
	P	2019-nCoV_N1-P	FAM-ACCCCGCATTACGTTTGGTGGACC-BHQ1		
CDC N2	F	2019-nCoV_N2-F	TTACAAACATTGGCCGCAAA	67	(Centers for Disease Control and Prevention, 2020)
	R	2019-nCoV_N2-R	GCGCGACATTCCGAAGAA		
	P	2019-nCoV_N2-P	FAM-ACAATTTGCCCCCAGCGCTTCAG -BHQ1		
CDC N3	F	2019-nCoV_N3-F	GGGAGCCTTGAATACACCAAAA	72	(Centers for Disease Control and Prevention, 2020)
	R	2019-nCoV_N3-R	TGTAGCACGATTGCAGCATTG		
	P	2019-nCoV_N3-P	FAM-AYCACATTGGCACCCGCAATCCTG -BHQ1		

A standard curve generated from tenfold serial dilution of standard DNA (plasmid DNA or oligo DNA) containing the target sequence (10^5–10^1 or 5×10^5 to 5×10^0 copies/reaction) was used to determine the number of viral genome copies per qPCR reaction. A negative control was included in all qPCR assays. The amplification efficiencies for MS2, φ6, and MNV averaged 93.5%, 97.2%, and 99.8%, respectively. The coefficient of determination (R^2) for MS2, φ6, and MNV assay averaged 0.998, 0.999, and 0.999.

To test the impact of RT-qPCR kit on the whole or molecular process recovery (see section 3.3), the RT-qPCR steps described earlier (referred to Method 1) was compared with one-step RT-qPCR using QuantiTect Probe RT-PCR kit (QIAGEN) (Method 2). Method 2 was performed following the manufacturer's instruction. A 5 µL of the RNA extract was mixed with 15 µL of the reaction mixture, containing 10 µL of master mix (QIAGEN), 0.2 µL of QuantiTect RT mix, virus-specific forward primers and reverse primers, and TaqMan probe. The conditions of thermal cycling were as follows: 50°C for 30 min and 95°C for 15 min, followed by 45 cycles of 94°C for 15 sec and 60°C for 60 sec (for quantification of MS2 and φ6), or followed by 94°C for 15 sec and 56°C for 60 sec (for MNV quantification).

2.6. Calculation of whole process recovery and molecular process recovery

The whole process recovery ratio (*W*), molecular process recovery ratio (*M*), and sample limit of detection (*SLOD*) (copies/mL) were presented as Eq. (1), (2), and (3), respectively. The cDNA concentration of MS2 and φ6 in control were measured by QIAamp Viral RNA Mini Kit, followed by RT-qPCR and were 5.55 ± 0.31 log and 5.61 ± 0.27 log copies/mL, respectively. The comparison of virus concentrations between concentrated samples and control allows for the evaluation of the whole process recovery ratio as described below.

$$W = \frac{C_{obs\_WPC}}{C_{ini\_WPC} \cdot x} \qquad \text{Eq. (1)}$$

$$M = \frac{C_{obs\_MPC}}{C_{ini\_MPC}} \qquad \text{Eq. (2)}$$

$$SLOD = \frac{ALOD}{W \cdot x} \qquad \text{Eq. (3)}$$

where C_{obs_WPC} indicates the cDNA concentration of WPC in concentrated samples (copies/mL), C_{ini_WPC} indicates the cDNA concentration of WPC in the control sample (copies/mL), x the concentration factor during the whole process (primary concentration, RNA extraction, and RT), C_{obs_MPC} indicates the cDNA concentration of MPC in concentrated samples (copies/mL), C_{ini_MPC} indicates the cDNA concentration of MPC in the control sample (copies/mL) and *ALOD* indicates the assay limit of detection defined as the minimum copy number with a 95% probability detection (copies/mL).

The concentrated samples and corresponding control samples were always subjected to RT-qPCR simultaneously to avoid the potential bias on the whole and molecular process recovery ratio. Furthermore, the number of freeze-thawing (i.e., none or once) was made consistent between concentrated and control samples.

2.7. Detection of SARS-CoV-2 RNA from raw sewage

2.7.1. Refinement of PEG+TRIzol by RNeasy PowerMicrobiome Kit

The PEG + TRIzol method was slightly modified by combining TRIzol LS reagent (Thermo Fisher Scientific) with RNeasy PowerMicrobiome Kit (QIAGEN) (TRIzol + RNeasy PowerMicrobiome Kit). This method contains two steps: sample lysis by TRIzol LS reagent and RNA precipitation, purification and elution using RNeasy PowerMicrobiome Kit. The theoretical advantages of this method are to increase the input volume for RNA extraction, which contribute to minimize the SLOD, and to reduce the sample processing time compared to TRIzol.

Specifically, a 250 µL aliquot of PEG concentrate was mixed with 750 µL of TRIzol LS reagent and vigorously vortexed for 30 s. After a 5 min incubation, 200 µL of chloroform was added to the mixture and vigorously vortexed for 15 s. The mixture was then centrifuged at 12,000 g for 15 min at 4°C. A colorless upper aqueous phase was mixed with 150 µL of solution IRS, which is designed to effectively remove PCR inhibitors (Ahmed et al., 2020b). Thereafter, the RNA was precipitated and filtered through a silica-based column followed by washing and elution, as described in the manufacturer's instructions, without DNase treatment. The final volume of eluted RNA was 60 µL. Thus, the concentration factor of this process was 4.2-fold.

The applicability of PEG + TRIzol + RNeasy PowerMicrobiome Kit was confirmed by raw sewages A, B, and C. The whole process recovery of φ6 was evaluated in duplicate for each raw sewage. The RT-qPCR process follows method 1 (two-step RT-qPCR using

High-Capacity cDNA Reverse Transcription Kit and TaqMan™ Gene Expression Master Mix).

2.7.2. Processing of raw sewage from COVID-19 epidemic areas

A 400–500 mL of grab sample of raw sewage was collected on June 30, July 6, 16, 22, and 29; and August 5, 2020 at municipal WWTPs D and E, located in Tokyo Metropolis, Japan. The samples were stored at −20°C until processing. A total of 12 samples were further processed as below.

A 40-mL aliquot of each raw sewage was concentrated by PEG. Then, a 250 μL of the concentrate was processed by TRIzol + RNeasy PowerMicrobiome Kit to obtain a 60 μL of RNA extract.

Then, 35 μL of RNA extract was subjected to RT to obtain 70 μL of cDNA as a final volume. Four published assays (NIID_2019-nCOV_n, CDC N1, CDC N2, and CDC N3 assays(Centers for Disease Control and Prevention, 2020; Shirato et al., 2020)) were performed to detect the SARS-CoV-2 RNA from raw sewage. We also tested the whole process recovery ratio of φ6.

A standard curve generated from tenfold serial dilution of standard DNA [plasmid DNA (Integrated DNA Technologies) for CDC assays and gBlocks for NIID assay] containing the target sequence (5×10^4 to 5×10^0 copies/reaction) was used to determine the number of viral genome copies per qPCR reaction. Negative control was included in duplicate in all qPCR assays. The amplification efficiencies for NIID_2019-nCOV_n, CDC N1, CDC N2, and CDC N3 averaged 97.1%, 94.5%, 92.2%, and 95.2%, respectively. The coefficient of determination (R^2) for NIID_2019-nCOV_n, CDC N1, CDC N2, and CDC N3 averaged 0.995, 0.995, 0.999, and 0.998, respectively. The assay limit of quantification (ALOQ) (i.e., lowest copy number detected at 100%) was 1 copies/μL.

2.8. Statistical analysis

Paired *t*-test and analysis of variance (ANOVA) were conducted using R (R Core Team, 2019).

3. Results and discussion

3.1. Whole process recovery ratio of MS2 and φ6

The comparisons among the combination of primary concentration and RNA extraction methods were performed as shown in Figure 26. For each type of raw sewage, three primary concentration methods were performed four times. Each primary concentrate was then subjected to two types of RNA extraction methods. Note that UF concentration was performed separately to conduct both RNA extraction methods; The limited volume of single UF concentrate (i.e., 170 – 210 µL) did not allow for conducting both methods, which requires a total of 280 µL of concentrate. UF+TRIzol was not performed for raw sewage A due to the limited amount of the sample.

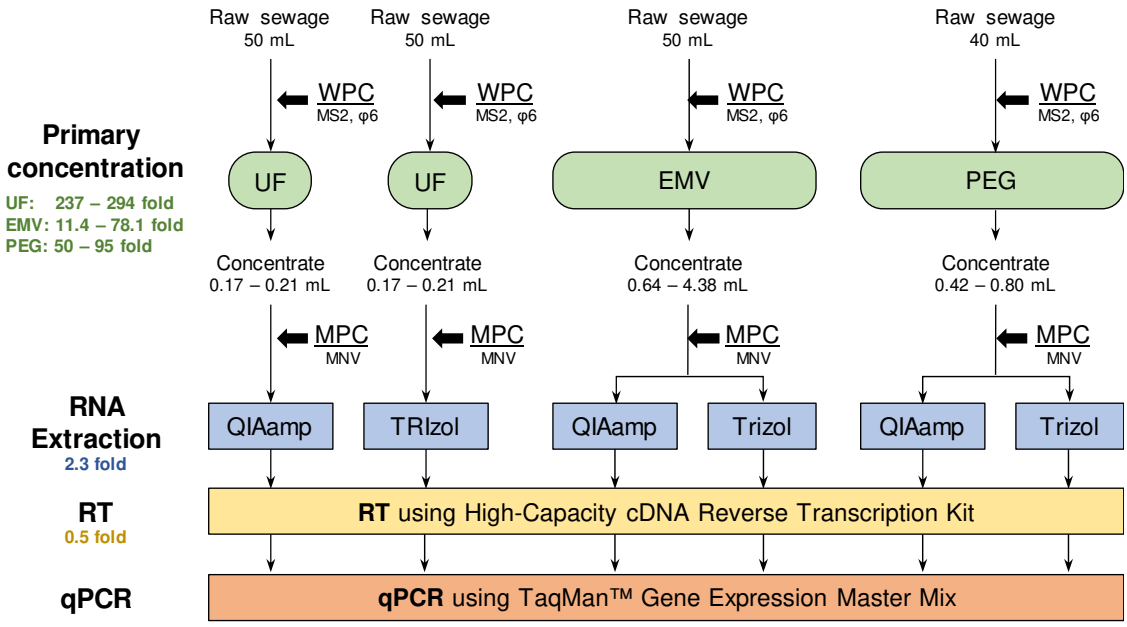

Figure 26 Flow diagram of sample processing for the comparison of whole process recovery ratio

The concentration factor in each process was described as **-fold, below the name of the processing.

The whole process recovery ratio of MS2 and φ6 by each method (primary concentration + RNA extraction) as a function of the type of raw sewage is shown in **Figure 27Figure 27**. The mean log whole process recovery ratio along with its corresponding standard deviation (SD) is shown in Table 20.

PEG + TRIzol provided the highest mean φ6 recovery ratio of −0.38 ± 0.13 log (41.6%), −0.53 ± 0.23 log (29.8%), and −0.30 ± 0.31 log (49.8%) for raw sewages A, B, and C, respectively. The second highest recovery was achieved by UF + QIAamp Viral RNA Mini Kit [−0.60 ± 0.25 log (25.0%) for B, −0.45 ± 0.20 log (35.8%) for C] or EMV + QIAamp Viral RNA Mini Kit [−0.68 ± 0.40 log (21.0%)] for A. Two methods (PEG + QIAamp Viral RNA Mini Kit and EMV + TRIzol) did not provide >−1.0 log (>10%) recovery for φ6. These results suggested that PEG + TRIzol can be an efficient recovery method of enveloped viruses from a variety of raw sewages.

PEG + TRIzol showed the highest φ6 recovery among the five combinations. A similar approach was performed for the detection of SARS-CoV-2 from the raw sewage (Wu et al., 2020b). A previous study reported a comparable whole process recovery ratio of MHV [−0.39 log (44%)] with our results (Ahmed et al., 2020b). These studies further confirmed the applicability of PEG + TRIzol for the efficient recovery of enveloped viruses.

PEG + QIAamp Viral RNA Mini Kit provided significantly lower φ6 recoveries than PEG +TRIzol by averaged 1.2 log (paired *t*-test, $P < 0.001$), whereas the MS2 recoveries were comparable (paired *t*-test, $P > 0.05$). This might be because the particles in the PEG concentrate might hamper the extraction of φ6 by QIAamp Viral RNA Mini Kit. A previous study also reported the lower RNA extraction efficiency for enveloped influenza virus than QIAamp Viral RNA Mini Kit under the presence of particles (Fabian et al., 2009). TRIzol was originally designed to extract isolate RNA from cell and tissue samples, whereas QIAamp Viral RNA Mini Kit was designed to extract from relatively turbid-free samples (i.e., plasma, serum, and other cell-free body fluids) according to the manufacturer. These results may contribute to the superior performance of TRIzol over QIAamp Viral RNA Mini Kit.

UF was chosen as a primary concentration method in several studies (Medema et al., 2020; Sherchan et al., 2020) for the detection of SARS-CoV-2 from raw sewage. Our results indicated that UF concentration provided ranging from -1.19 to -0.45 log (6.4 – 35.8 %) and from -0.86 to -0.52 log (13.8 – 30.0 %) when combined with QIAamp Viral RNA Mini Kit and TRIzol, respectively. These results were comparable with Ahmed et al. (2020b), which have reported MHV recovery of −0.55 log (28%) using UF [i.e.,

Centricon Plus-70 (10 kDa)]. A slightly lower recovery of UF+ QIAamp Viral RNA Mini Kit in raw sewage A was due to the outlier (φ6 recovery of −2.06 log) (see **Figure 27**). Interestingly, the use of TRIzol did not significantly improved the whole process φ6 recovery of UF, contrary to the results observed in PEG. This was possibly because the positive effect of using TRIzol for φ6 extraction was offset by the inhibition during molecular process. The MNV recovery was lower in UF+TRIzol than UF+QIAamp Viral RNA Mini Kit by 0.37 to 1.09 log (see Figure 28 and **Table 21**). Accordingly, the MS2 recovery was lower in TRIzol than QIAamp Viral RNA Mini Kit, as shown in **Figure 27**. Thus, the both effects, higher extraction efficiency but stronger inhibition, leads to the comparable whole φ6 recovery ratio of UF + TRIzol to UF + QIAamp Viral RNA Mini Kit.

EMV + QIAamp Viral RNA Mini Kit has been originally developed to concentrate viruses and protozoa simultaneously (Haramoto et al., 2012). This method provided favorable φ6 recovery ratio for raw sewage A. However, the φ6 recovery was decreased to −1.01 ± 0.42 (9.7%) for B and −1.80 ± 0.22 (1.6%) for C. Interestingly, the result of ANOVA suggested that the water matrix significantly affected the recovery ratio of MS2 ($P < 0.05$) and φ6 ($P < 0.01$). The lower recovery in raw sewages B and C might be due to the lower elution efficiency, caused by the higher turbidity and organic concentration in wastewater matrix (higher TSS and UV_{260}) (see **Table 18**)). The turbid water matrix promoted membrane fouling, which prevented the elution buffer from contacting with the surface of the membrane, where viruses attached, during the vigorous vortex. In the filtration of raw sewage supplemented with Mg^{2+} ions through negatively charged membranes, not only viruses but also various components of feed water (e.g., humic acids, silica, and clays) are co-deposited on the membrane surface (Hata et al., 2011). Previous research also reported the negative impact of membrane fouling on the elution efficiency (Shi et al., 2016). In fact, the original work developing EMV + QIAamp Viral RNA Mini Kit validated the whole process recovery ratio of nonenveloped coliphage Qβ and poliovirus for river water and tap water, but did not test for raw sewage (Haramoto et al., 2012). A recent work detected SARS-CoV-2 RNA from the secondary effluent and did not detect from the raw sewage (Haramoto et al., 2020). These results suggest that EMV + QIAamp Viral RNA Mini Kit can be applied only to concentrate enveloped viruses for relatively clean water samples (e.g., secondary effluent or raw sewage containing low TSS and UV_{260}, such as A) and not universally recommended for raw sewage.

EMV + TRIzol provided a lower recovery of both MS2 and φ6 (<5%). This was possibly because the combination of a low recovery in primary concentration and low

recovery in the molecular process. The MNV recovery ranged from −1.33 to −0.54 log (4.7%–29%), suggesting a significant loss in the molecular process (Figure 28 and **Table 21**). The reason of low MNV recovery by TRIzol is the inappropriate physicochemical conditions for guanidinium thiocyanate–phenol–chloroform extraction. This RNA extraction should be performed at pH 4 (Chomczynski and Sacchi, 1987), whereas the EMV elution buffer has pH 9.5 (due to the sodium polyphosphate and ethylenediaminetetraacetic acid trisodium salt trihydrate) and includes surfactant (due to Tween 80). Hence, this effect might contribute to the lower recovery of EMV + TRIzol.

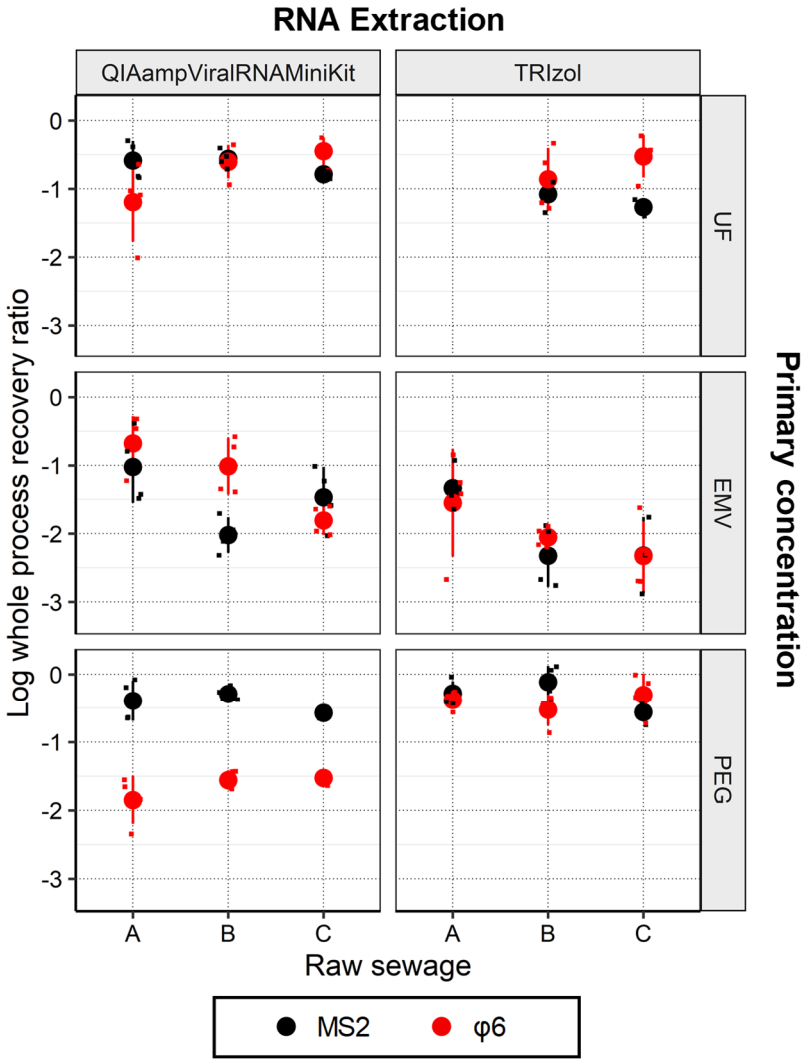

Figure 27 Whole process recovery ratio of MS2 and φ6 by each method (primary concentration + RNA extraction) as a function of the type of raw sewage

Each panel shows the MS2 and φ6 recovery with respect to the type of raw sewage. Black color indicates MS2 recovery, whereas red color indicates φ6 recovery. Circles with error bar indicate mean values and standard deviation. Smaller square is jittered plots, indicating each data of recovery ratio. Note that the whole process recovery ratio by UF+TRIzol (raw sewage A) was not available.

Table 20 MS2 and φ6 recovery ratio of each method (primary concentration + RNA extraction)

Raw sewage	Primary concentration	RNA extraction kit	MS2			φ6		
			Mean[a]	SD[b]	Mean[c] (%)	Mean[a]	SD[b]	Mean[c] (%)
A	UF	QIAamp Viral RNA Mini Kit	-0.58	0.53	26.1	-1.19	0.58	6.4
	EMV	QIAamp Viral RNA Mini Kit	-1.02	0.30	9.5	-0.68	0.40	21.0
	EMV	TRIzol	-1.33	0.30	4.6	-1.55	0.79	2.8
	PEG	QIAamp Viral RNA Mini Kit	-0.39	0.18	40.8	-1.85	0.35	1.4
	PEG	**TRIzol**	**-0.28**	**0.28**	**52.4**	**-0.38**	**0.13**	**41.6**
B	UF	QIAamp Viral RNA Mini Kit	-0.56	0.26	27.6	-0.60	0.25	25.0
	UF	TRIzol	-1.08	0.19	8.4	-0.86	0.46	13.8
	EMV	QIAamp Viral RNA Mini Kit	-2.02	0.46	1.0	-1.01	0.42	9.7
	EMV	TRIzol	-2.32	0.10	0.5	-2.05	0.15	0.9
	PEG	QIAamp Viral RNA Mini Kit	-0.29	0.24	51.4	-1.56	0.14	2.8
	PEG	**TRIzol**	**-0.11**	**0.13**	**77.6**	**-0.53**	**0.23**	**29.8**
C	UF	QIAamp Viral RNA Mini Kit	-0.78	0.44	16.5	-0.45	0.20	35.8
	UF	TRIzol	-1.26	0.10	5.2	-0.52	0.31	30.0
	EMV	QIAamp Viral RNA Mini Kit	-1.47	0.70	3.4	-1.80	0.22	1.6
	EMV	TRIzol	-2.58	0.07	0.3	-2.33	0.51	0.5
	PEG	QIAamp Viral RNA Mini Kit	-0.57	0.13	27.0	-1.53	0.09	3.0
	PEG	**TRIzol**	**-0.56**	**0.05**	**27.5**	**-0.30**	**0.31**	**49.8**

[a] Mean values of log whole process recovery ratio

[b] Standard deviation of log whole process recovery ratio

[c] Anti-logarithm of mean values of log whole process recovery ratio.

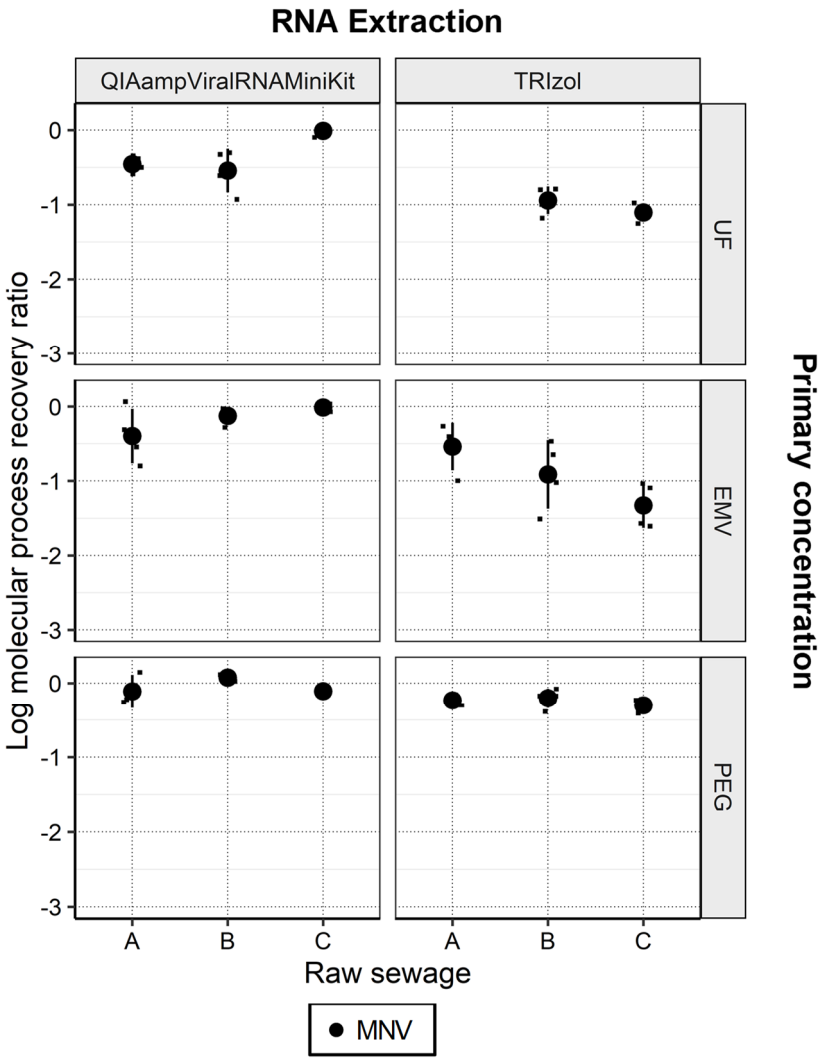

Figure 28 Molecular process (MNV) recovery ratio of each method (primary concentration + RNA extraction) as a function of the type of raw sewage

Each panel shows the MNV recovery with respect to the type of raw sewage. The black circle plot indicates mean MNV recovery The error bar indicates standard deviation (n = 4). Smaller square is jittered plots, indicating each data of recovery ratio. Note that the molecular process recovery ratio of UF+TRIzol (raw sewage A) was not available

Table 21 MNV recovery ratio of each method

Raw sewage	Primary concentration	RNA extraction kit	Mean[a]	SD[b]	Mean (%)[c]
A	UF	QIAamp Viral RNA Mini Kit	-0.45	0.11	35.1
	EMV	QIAamp Viral RNA Mini Kit	-0.40	0.37	40.0
	EMV	TRIzol	-0.54	0.32	29.0
	PEG	QIAamp Viral RNA Mini Kit	-0.02	0.26	95.2
	PEG	TRIzol	-0.23	0.08	58.5
B	UF	QIAamp Viral RNA Mini Kit	-0.54	0.29	28.6
	UF	TRIzol	-0.91	0.46	12.2
	EMV	QIAamp Viral RNA Mini Kit	-0.13	0.11	74.8
	EMV	TRIzol	-0.91	0.46	12.2
	PEG	QIAamp Viral RNA Mini Kit	0.07	0.05	118.7
	PEG	TRIzol	-0.21	0.13	62.4
C	UF	QIAamp Viral RNA Mini Kit	-0.01	0.06	97.6
	UF	TRIzol	-1.10	0.12	7.9
	EMV	QIAamp Viral RNA Mini Kit	0.04	0.12	109.9
	EMV	TRIzol	-1.33	0.30	4.7
	PEG	QIAamp Viral RNA Mini Kit	0.07	0.21	117.2
	PEG	TRIzol	-0.30	0.09	50.0

[a]Mean values of log whole process recovery ratio (n = 4)

[b]Standard deviation of log whole process recovery ratio (n=4)

[c]Antilogarithm of mean values of log whole process recovery ratio.

3.2. Achievable sample limit of detection (SLOD)

Achievable SLOD in each combination of primary concentration and RNA extraction method was shown in **Figure 29**. In this study, we adopted the observed values of concentration factor and whole process recovery ratio and assumed ALOD to be the most sensitive value theoretically possible, namely, 3 copies/5 μL (Bustin et al., 2009).

PEG + TRIzol achieved the lowest SLOD of φ6 for A [1.31 ± 0.12 log copies/mL (20 copies/mL)] and the third lowest SLOD of φ6 for B and C [1.33 ± 0.28 log copies/mL (21 copies/mL) and 1.07 ± 0.31 copies/mL (12 copies/mL), respectively]. UF + QIAamp Viral RNA Mini Kit achieved the second lowest SLOD of φ6 for A [1.47 ± 0.56 log copies/mL (30 copies/mL)] and the lowest SLOD of φ6 for B and C [0.90 ± 0.26 log (8.0 copies/mL) and 0.75 ± 0.20 (5.6 copies/mL), respectively]. UF + TRIzol achieved the second lowest SLOD of φ6 for B and C [1.16 ± 0.48 log copies/mL (14 copies/mL) and 0.79 ± 0.31 copies/mL (6.2 copies/mL), respectively]. Hence, the PEG + TRIzol, UF + QIAamp Viral RNA Mini Kit, and UF + TRIzol provided the most sensitive SLOD among the tested combination of primary concentration and RNA extraction.

Achievable SLOD depends on the concentration factor, whole process recovery ratio, and ALOD. Thus, each method still can be potentially improved by higher concentration factors (i.e., increased initial sample volume or reduced concentrate volume). For example, previous studies adopted higher initial volume for primary concentration: up to 200 mL for UF concentration (Medema et al., 2020), up to 200 mL for EMV (Haramoto et al., 2020), and up to 250 mL for PEG (La Rosa et al., 2020). It should be noted that the concentration factor and whole/molecular process recovery are generally trade-offs; highly concentrated samples contain a higher amount of inhibitor, reducing the efficiency of RT and qPCR process. Hence, the removal of inhibitory substances during RNA extraction, optimized dilution of primary concentrate, and selection of reverse transcriptase qPCR master mix resistant to inhibition will be required if the primary concentration is performed with a higher concentration factor.

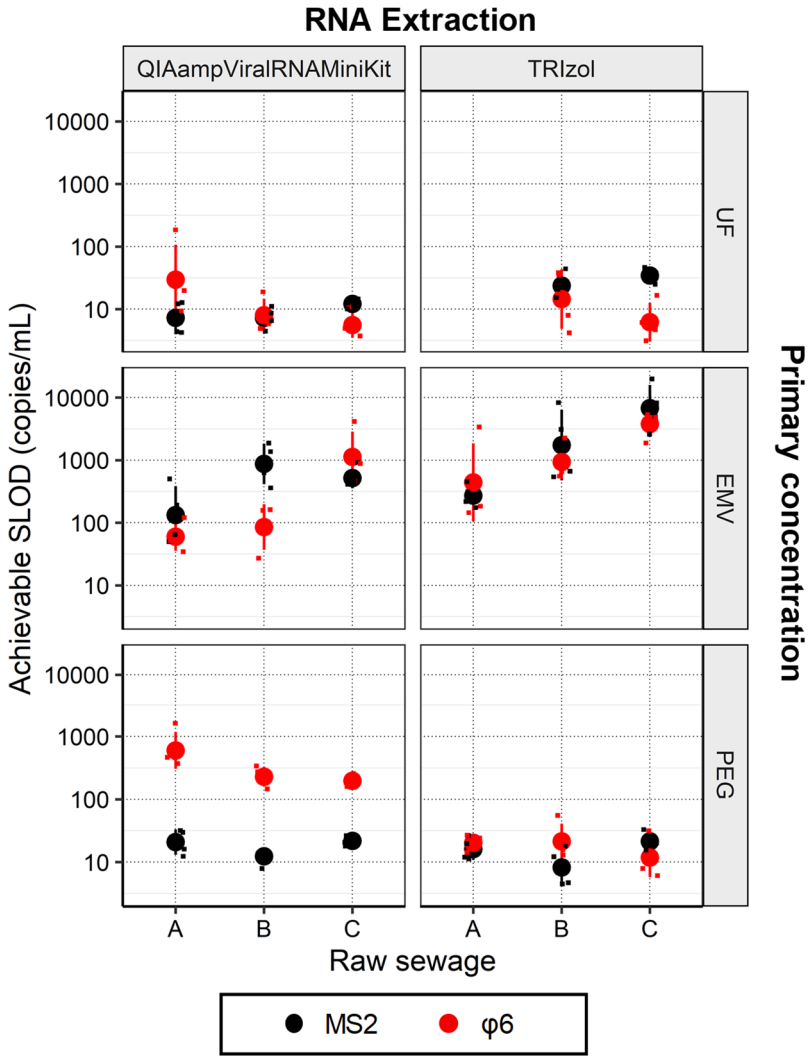

Figure 29 Sample limit of detection (SLOD) by each method (primary concentration + RNA extraction) as a function of the type of raw sewage

Each panel shows the achievable sample limit of detection (SLOD) of MS2 and φ6 with respect to the type of raw sewage. Black color indicates MS2 recovery, whereas red color indicates φ6 recovery. Circles with error bars indicate mean values and standard deviation. Smaller square is jittered plots, indicating each data of SLOD. Note that the SLOD by UF+TRIzol (raw sewage A) was not available.

3.3. Impact of RT-qPCR kit on the whole process recovery ratio

The impact of the RT-qPCR kit selection on the whole process recovery was evaluated for three primary concentration methods using raw sewage A as a test sample and QIAamp Viral RNA Mini Kit as an RNA extraction kit (Figure 30). The stored RNA extract of QIAamp Viral RNA Mini Kit was subjected to RT-qPCR process of method 2. The RT-qPCR recovery was compared between the two types of methods.

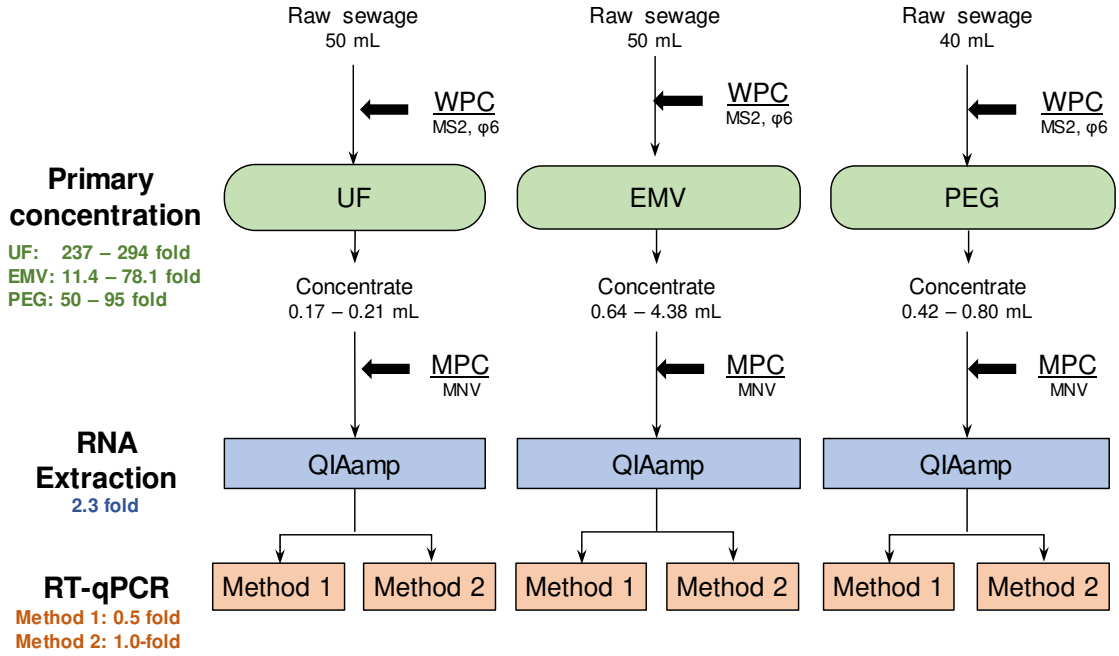

Figure 30 Flow diagram of sample processing for the comparison of whole process recovery between RT-qPCR methods (method 1 and method 2)

The concentration factor in each process was described as **-fold, below the name of the processing. Method 1 indicates two-step RT-qPCR (RT process using High-Capacity cDNA Reverse Transcription Kit and qPCR using TaqMan™ Gene Expression Master Mix); Method 2 indicates one-step qPCR (RT-qPCR process using QuantiTect Probe RT-PCR kit.

The whole process MS2 and φ6 recovery is presented in Figure 31. Method 2 provided MS2 recovery of −2.53 ± 0.32 log, −3.74 ± 0.72 log, and −1.22 ± 0.11 log and φ6 recovery of −3.38 ± 0.11 log, −2.67 ± 0.49 log, and −2.26 ± 0.16 log for UF, EMV, and PEG, respectively. For all the primary concentration methods, the whole process MS2 and φ6 recovery by method 2 were significantly lower than method 1 (paired *t*-test, $P < 0.05$). Moreover, the molecular process MNV recovery was −2.17 ± 0.54 log, −2.42 ± 0.36 log, and −0.59 ± 0.22 log for UF, EMV, and PEG, respectively (Figure 32). They were significantly lower in method 2 than method 1 (paired *t*-test, $P < 0.05$). These results indicate that method 2 was not effective for the quantification of both MS2 and φ6 from raw sewage processed by three types of primary concentration methods.

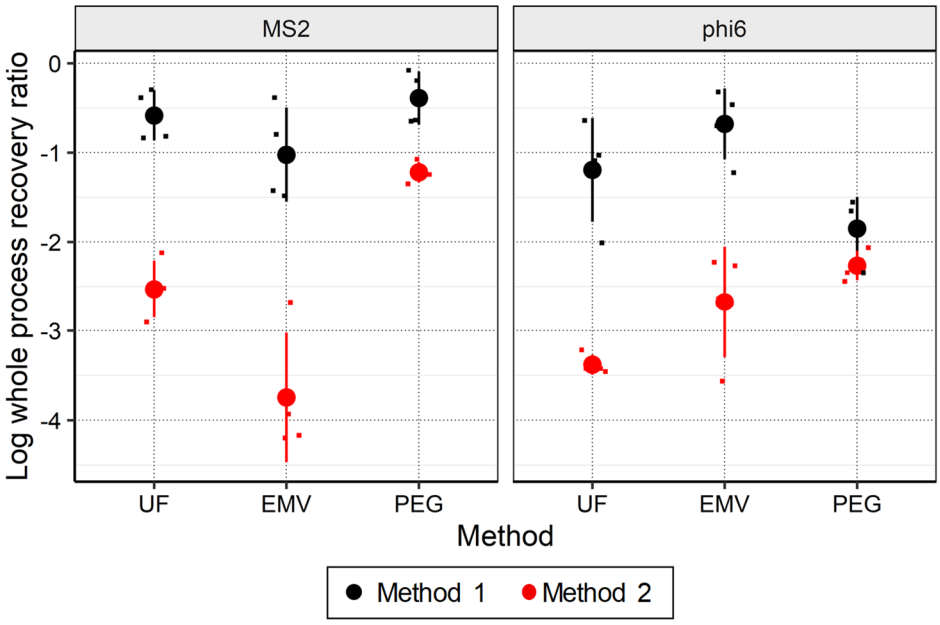

Figure 31 Whole process recovery ratio of each method (method 1 and 2) as a function of the type of primary concentration

The black circle plot indicates the mean whole process recovery. The error bar indicates the standard deviation.

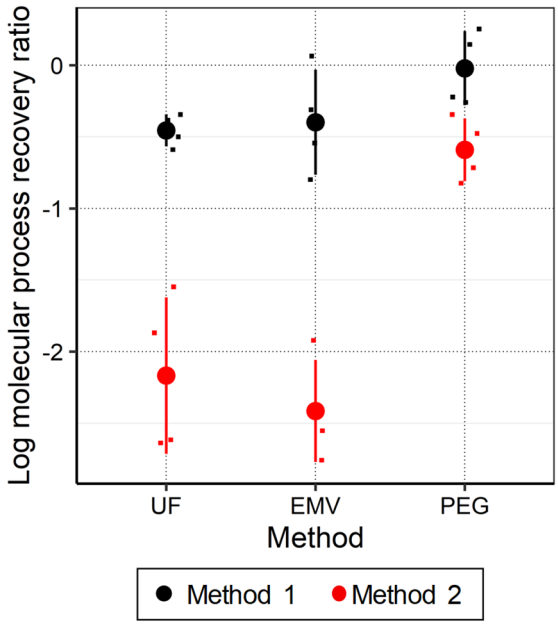

Figure 32 Molecular process recovery ratio of each method (method 1 and 2) as a function of the type of primary concentration

The black circle plot indicates the mean whole process recovery. The error bar indicates standard deviation.

The observed difference was due to the inhibition during the RT-qPCR process, as revealed by the molecular process recovery of MNV. Both methods are different in terms of master mix composition, the type of primer (method 1, random primer; method 2, specific primer), and the inclusion of RNase inhibitor (method 1, included; method 2, not included). Moreover, in method 1, 0.5-fold RNA extract was subjected to qPCR [due to the dilution in the RT process (**Figure 26**)], potentially contributing to the mitigation of PCR inhibition. A previous study reported that QIAGEN QuantiTect Probe RT-PCR Kit was susceptible to organic PCR inhibitor, such as lactoferrin, than other RT kits (Stephens et al., 2010). These results indicate that the RT-qPCR kit affects the quantification of the virus concentrate for all the methods in raw sewage. Thus, the RT-qPCR steps should also be optimized for efficient recovery.

3.4. Detection of SARS-CoV-2 RNA from raw sewage

The applicability of PEG + TRIzol + RNeasy PowerMicrobiome Kit was investigated for the detection of SARS-CoV-2 RNA from raw sewage. First, the PEG + TRIzol +

RNeasy PowerMicrobiome Kit provided the φ6 recovery ratio of −0.10 ± 0.10 (79%), −0.56 ± 0.10 (27.3%), and −0.75 ± 0.03 (17.8%) for A, B, and C, respectively, which were comparable with the PEG + TRIzol method. The SLOD was 0.72 ± 0.12 log copies/mL (5.3 copies/mL), 1.18 ± 0.09 log copies/mL (15.1 copies/mL), and 1.34 ± 0.03 log copies/mL (11.8 copies/mL). Thus, the SLOD can be slightly lowered than PEG + TRIzol.

The PEG + TRIzol + RNeasy PowerMicrobiome Kit was then applied to the detection of SARS-CoV-2 RNA from the raw sewage collected from Tokyo Metropolis. The results of four SARS-CoV-2 qPCR assays along with corresponding values of whole process recovery of φ6 were reported (Table 22). The whole process recovery of φ6 averaged −0.49 ± 0.32 log (33%). The sample limit of quantification (SLOQ), given by ALOQ (5 copies/5 μL) divided by the concentration factor and by φ6 whole process recovery ratio, averaged 4.29 ± 0.32 log copies/L (2.0×10^4 copies/L). Of the 12 grab raw sewage samples, SARS-CoV-2 RNA was detected in 4 samples, collected on July 7 (CDC N1:<4.1×10^4 copies/L), 16 (CDC N3:<6.0×10^3 copies/L), and 29 (CDC N1, <1.4×10^4 copies/L) in Plant D and on July 29 in Plant E (CDC N1, <1.1×10^4 copies/L).

The basic statistics of confirmed cases in Tokyo are presented in Table 23. All the information was cited from the official site of the Tokyo Metropolitan Government https://www.city.shinjuku.lg.jp/kusei/cln202002_kns01_me01.html and https://stopcovid19.metro.tokyo.lg.jp/ (access available on August 27. 2020). The population of Tokyo Metropolis was 14 million as of June 2020.

During the sampling period, the 7-day average of confirmed daily new cases increased in the Tokyo Metropolis (Table 23). The 7-day averages on confirmed daily new cases per 100,000 people were from 0.39 on June 30 to 2.47 on August 5. It should be noted that the death and the number of patients with severe symptoms were limited during this period. Despite the increase in infections, the SARS-CoV-2 RNA was negative or detected under SLOQ. This made it challenging for further analysis, as expected in WBE. The results of one positive well between two wells theoretically provide limited quantitative data. For example, the MPN value of one positive well per two wells, where 5 μL was template volume, is 88.6 copies/mL with a 95% confidence interval of [18.8, 1023] (Ferguson and Ihrie, 2019). This suggests a further requirement for the application of WBE in this spread of infection. For example, further refinement of primary concentration (i.e., increasing concentration factor without inhibition) is required. Other refinement includes the change of sampling method (from grab sampling to composite sampling), normalizing by the fecal viral indicator (Wu et al., 2020a). The research for

the successful application of WBE, such as capturing the trend occurrence and community prevalence of the infections, will be the scope of the future study.

Overall, the PEG + TRIzol was successfully applied to the detection of SARS-CoV-2 RNA from wastewater with a favorable whole process recovery ratio of φ6.

Table 22 Detection of SARS-CoV-2 RNA from raw sewage

Date	Plant	Concentration factor	$\log_{10}$ W[a]	SLOQ (copies/mL)	SARS-CoV-2			
					CDC N1	CDC N2	CDC N3	NIID
June 30	D	160	-0.41	16.1	Neg	Neg	Neg	Neg
	E	149	-0.76	38.5	Neg	Neg	Neg	Neg
July 7	D	152	-0.79	40.6	**Pos**[b]	Neg	Neg	Neg
	E	163	-0.65	27.5	Neg	Neg	Neg	Neg
July 16	D	152	0.04	6.0	Neg	Neg	**Pos**[c]	Neg
	E	146	-0.29	13.2	Neg	Neg	Neg	Neg
July 22	D	159	-1.14	86.6	Neg	Neg	Neg	Neg
	E	160	-0.34	13.5	Neg	Neg	Neg	Neg
July 29	D	159	-0.36	14.3	**Pos**[d]	Neg	Neg	Neg
	E	160	-0.26	11.3	**Pos**[e]	Neg	Neg	Neg
August 5	D	154	-0.2	10.4	Neg	Neg	Neg	Neg
	E	154	-0.68	31.3	Neg	Neg	Neg	Neg

Neg: negative, Pos: positive

[a]Whole process recovery ratio (*W*) of φ6 was determined at $n = 1$ for each sample.

[b]SARS-CoV-2 CDC N1 gene was positive; the Ct was 38.7 (in one of two PCR reactions)

[c]SARS-CoV-2 CDC N3 gene was positive; Ct was 38.9 (in one of two PCR reactions)

[d]SARS-CoV-2 CDC N1 gene was positive; the Ct was 40.9 (in one of two PCR reactions)

[e]SARS-CoV-2 CDC N1 gene was positive; the Ct was 37.7 (in one of two PCR reactions)

Table 23 Basic statistics of confirmed cases in Tokyo Metropolis

Date	Cumulative confirmed cases	Cumulative cases of deaths	Cumulative cases of discharged patients	Current number of hospitalized patients	Current number of patients with severe symptom	7-day average on confirmed daily new cases
June 30	6225	325	5447	264	10	55.1
July 7	6973	325	5772	427	8	106.9
July 16	8640	326	6771	760	7	195.4
July 22	10054	327	7767	916	18	242.9
July 29	11861	329	9109	1106	22	258.1
August 5	14285	333	10687	1475	21	346.3
August 12	16474	336	12526	1659	21	312.7

3.5. Implications for the wastewater-based epidemiology

The results suggest three implications for the successful application of WBE. First, to validate the quantification results of enveloped viruses, it is preferable to include enveloped surrogates. Earlier studies detecting the SARS-CoV-2 RNA used nonenveloped surrogates, such as indigenous F-RNA phages (Medema et al., 2020) and coliphage MS2 (Kumar et al., 2020), for the validation partially due to the resource limitation at that time. However, nonenveloped and enveloped surrogates can be recovered with different efficiency as highlighted in the case of PEG + QIAamp Viral RNA Mini Kit (see **Figure 27**). This indicates the danger of reliance on nonenveloped surrogates.

In addition, not only primary concentration but also the molecular process (RNA extraction and RT-qPCR) should be optimized. Our study suggested that effective primary concentration is just the first step. An appropriate molecular process (i.e., RNA extraction and RT-qPCR) is required, as was proven by the comparison between PEG + QIAamp Viral RNA Mini Kit and PEG + TRIzol (see **Figure 27**) and by the comparison between RT-qPCR methods (Figure 31).

Finally, the universal applicability of primary concentration methods cannot be judged from a single type of wastewater matrix. The results of the whole process recovery by EMV indicate that the efficiency of primary concentration differs depending on the wastewater matrix (see **Figure 27**). It may be necessary to validate the quantification process *in house* by adopting the appropriate WPC because the RNA extraction kits, RT-qPCR kits, and the water quality differ in every laboratory.

A further consideration is required for adopting φ6 as a process control to validate the quantification results of enveloped viruses. The possible rationales and limitations of adopting φ6 are presented in Table 24. Under the limited BSL facility (e.g., WWTP), the choice of φ6 will be practically best considering the broad and commercial availability compared with other enveloped bacteriophages. However, φ6 has double-stranded RNA and an envelope derived from *Pseudomonas syringae*, which might not fully reflect the properties of viruses in interest (e.g., SARS-CoV-2 and influenza). Thus, further research should confirm the comparability of the fate of φ6 during primary concentration and molecular process with the SARS-CoV-2, coronavirus surrogates (MHV, porcine epidemic diarrhea virus (Randazzo et al., 2020), bovine attenuated coronavirus (Gonzalez et al., 2020)), and ideally indigenous SARS-CoV-2 in wastewater. To the best of our

knowledge, no studies have evaluated the comparability of overall recovery efficiency of surrogate viruses. *De facto* standardization of these surrogate viruses should be avoided before the comparison conducted in the future.

Table 24 Rationales and limitations of φ6 as a process control for SARS-CoV-2

Rationales	Limitations
・Similar morphologies Having an envelope, thus showing similar adsorptive characteristics with murine hepatitis virus (MHV) (Ye et al., 2016) **・Minimal containment for laboratory** Not required for BSL2 facility (Handling of MHV and other enveloped virus surrogates required BSL2). This feature allows for on-site usages, such as a wastewater treatment plant, as a whole process control for enveloped viruses. **・Easy handling** *Pseudomonas syringae* and φ6 can be easily propagated with high concentration. The φ6 titers of 5×10^9 PFU/mL can be achieved.	**・Additional steps required for quantification** Having a double-stranded RNA. This may require an additional step (e.g., heat denaturation of dsRNA before RT step) for quantification. **・No proof of comparability to SARS-CoV-2** The structural difference between φ6 and SARS-CoV-2 and between freshly prepared enveloped viruses and indigenous SARS-CoV-2 might affect the recovery efficiency.

4. Conclusions

- Polyethylene glycol precipitation (PEG) followed by acid guanidinium thiocyanate-phenol-chloroform extraction (PEG + TRIzol) provided the highest whole process recovery ratio of *Pseudomonas* phage φ6 ranged from -0.53 to -0.30 log (29.8 – 49.8%) in three types of raw sewage.
- Ultrafiltration (UF) followed by QIAamp Viral RNA Mini Kit provided a comparable whole process recovery of φ6, ranging from -1.19 to -0.45 log (6.4 – 35.8 %), with MS2.
- Electronegative membrane vortex (EMV) provided significantly different whole process recovery of MS2 and φ6 depending on the water quality of raw sewage; the recovery was reduced in raw sewage containing higher TSS and UV_{260}.
- The successful recovery of the enveloped virus by PEG precipitation might need an appropriate RNA extraction method (e.g., acid guanidinium thiocyanate-phenol-chloroform RNA extraction). Not only primary concentration but also the following molecular process should be optimized for the efficient recovery of enveloped viruses.
- Non-enveloped surrogate (MS2 and MNV) did not necessarily validate the success of the primary concentration and molecular process of φ6 (e.g., PEG+QIAamp Viral RNA Mini Kit). This indicates enveloped viruses should be spiked to primary concentrate as whole process control and molecular process control to validate the quantification of enveloped viruses from raw sewage.
- The modified PEG + TRIzol method was successfully applied to detect SARS-CoV-2 RNA by CDC N1 and N3 assay from raw sewage collected on 7^{th},16^{th}, and 29^{th} in July 2020 in Tokyo Metropolis.

Reference

Adler, A., 2015. lamW: Lambert-W Function.

Ahmed, W., Angel, N., Edson, J., Bibby, K., Bivins, A., O'Brien, J.W., Choi, P.M., Kitajima, M., Simpson, S.L., Li, J., Tscharke, B., Verhagen, R., Smith, W.J.M., Zaugg, J., Dierens, L., Hugenholtz, P., Thomas, K. V, Mueller, J.F., 2020a. First confirmed detection of SARS-CoV-2 in untreated wastewater in Australia: A proof of concept for the wastewater surveillance of COVID-19 in the community. Sci. Total Environ. 728, 138764. https://doi.org/https://doi.org/10.1016/j.scitotenv.2020.138764

Ahmed, W., Bertsch, P., Bivins, A., Bibby, K., Farkas, K., Gathercole, A., Haramoto, E., Gyawali, P., Korajkic, A., McMinn, B.R., Mueller, J., Simpson, S., Smith, W.J.M., Symonds, E.M., Thomas, K. V, Verhagen, R., Kitajima, M., 2020b. Comparison of virus concentration methods for the RT-qPCR-based recovery of murine hepatitis virus, a surrogate for SARS-CoV-2 from untreated wastewater. Sci. Total Environ. 139960. https://doi.org/https://doi.org/10.1016/j.scitotenv.2020.139960

Amoueyan, E., Ahmad, S., Eisenberg, J.N.S., Gerrity, D., 2019. Equivalency of indirect and direct potable reuse paradigms based on a quantitative microbial risk assessment framework. Microb. Risk Anal. 12, 60–75. https://doi.org/10.1016/j.mran.2019.06.003

Araud, E., Fuzawa, M., Shisler, J.L., Li, J., Nguyen, T.H., 2020. UV Inactivation of Rotavirus and Tulane Virus Targets Different Components of the Virions. Appl. Environ. Microbiol. 86, e02436-19. https://doi.org/10.1128/AEM.02436-19

Asami, T., Katayama, H., Torrey, J.R., Visvanathan, C., Furumai, H., 2016. Evaluation of virus removal efficiency of coagulation-sedimentation and rapid sand filtration processes in a drinking water treatment plant in Bangkok, Thailand. Water Res. 101, 84–94. https://doi.org/10.1016/j.watres.2016.05.012

Asmussen, S., Jensen, J.L., Rojas-Nandayapa, L., 2016. On the Laplace Transform of the Lognormal Distribution. Methodol. Comput. Appl. Probab. 18, 441–458. https://doi.org/10.1007/s11009-014-9430-7

Bader, H., Hoigné, J., 1981. Determination of ozone in water by the indigo method. Water Res. 15, 449–456. https://doi.org/10.1016/0043-1354(81)90054-3

Beck, S.E., Rodriguez, R.A., Hawkins, M.A., Hargy, T.M., Larason, T.C., Linden, K.G., 2016. Comparison of UV-Induced Inactivation and RNA Damage in MS2 Phage across the Germicidal UV Spectrum. Appl. Environ. Microbiol. 82, 1468 LP – 1474. https://doi.org/10.1128/AEM.02773-15

Bellamy, W., Carlson, K., Pier, D., Ducoste, J., Carlson, M., 2000a. Determining disinfection needs. J. / Am. Water Work. Assoc. 92, 44–52. https://doi.org/10.1002/j.1551-8833.2000.tb08943.x

Bellamy, W., Carlson, K., Pier, D., Ducoste, J., Carlson, M., 2000b. Determining disinfection needs. J. AWWA 92, 44–52. https://doi.org/https://doi.org/10.1002/j.1551-8833.2000.tb08943.x

Bellamy, W.D., Finch, G.R., Haas, C.N., 1998. Integrated disinfection design framework. American Water Works Association.

Bergelson, J.M., Coyne, C.B., 2013. Picornavirus Entry - Viral Entry into Host Cells, in: Pöhlmann, S., Simmons, G. (Eds.), . Springer New York, New York, NY, pp. 24–41. https://doi.org/10.1007/978-1-4614-7651-1_2

Bisseux, M., Didier, D., Audrey, M., Christine, A., Hélène, P.-L., Jean-Luc, B., Cécile, H., 2020. Monitoring of enterovirus diversity in wastewater by ultra-deep sequencing: An effective complementary tool for clinical enterovirus surveillance. Water Res. 169, 115246. https://doi.org/https://doi.org/10.1016/j.watres.2019.115246

Black, S., Thurston, J.A., Gerba, C.P., 2009. Determination of Ct values for chlorine of resistant enteroviruses. J. Environ. Sci. Heal. - Part A Toxic/Hazardous Subst. Environ. Eng. 44, 336–339. https://doi.org/10.1080/10934520802659653

Boehm, A.B., Silverman, A.I., Schriewer, A., Goodwin, K., 2019. Systematic review and meta-analysis of decay rates of waterborne mammalian viruses and coliphages in surface waters. Water Res. 164, 114898. https://doi.org/https://doi.org/10.1016/j.watres.2019.114898

Bolton, J.R., Linden, K.G., 2003. Standardization of Methods for Fluence (UV Dose) Determination in Bench-Scale UV Experiments. J. Environ. Eng. 129, 209–215. https://doi.org/10.1061/(ASCE)0733-9372(2003)129:3(209)

Brinkman, N.E., Fout, G.S., Keely, S.P., 2017. Retrospective Surveillance of

Wastewater To Examine Seasonal Dynamics of Enterovirus Infections. mSphere 2, e00099-17. https://doi.org/10.1128/mSphere.00099-17

Bryan, A.W., Starner-Kreinbrink, J.L., Hosur, R., Clark, P.L., Berger, B., 2011. Structure-based prediction reveals capping motifs that inhibit β-helix aggregation. Proc. Natl. Acad. Sci. 108, 11099 LP – 11104. https://doi.org/10.1073/pnas.1017504108

Bubba, L., Broberg, E.K., Jasir, A., Simmonds, P., Harvala, H., Redlberger-Fritz, M., Nikolaeva-Glomb, L., Havlíčková, M., Rainetova, P., Fischer, T.K., Midgley, S.E., Epštein, J., Blomqvist, S., Böttcher, S., Keeren, K., Bujaki, E., Farkas, Á., Baldvinsdóttir, G.E., Morley, U., De Gascun, C., Pellegrinelli, L., Piralla, A., Martinuka, O., Zamjatina, N., Griškevičius, A., Nguyen, T., Dudman, S.G., Numanovic, S., Wieczorek, M., Guiomar, R., Costa, I., Cristina, T., Bopegamage, S., Pastuchova, K., Berginc, N., Cabrerizo, M., González-Sanz, R., Zakikhany, K., Hauzenberger, E., Benschop, K., Duizer, E., Dunning, J., Celma, C., McKenna, J., Feeney, S., Templeton, K., Moore, C., Cottrell, S., 2020. Circulation of non-polio enteroviruses in 24 EU and EEA countries between 2015 and 2017: a retrospective surveillance study. Lancet Infect. Dis. 20, 350–361. https://doi.org/10.1016/S1473-3099(19)30566-3

Buffle, M.-O., Schumacher, J., Salhi, E., Jekel, M., von Gunten, U., 2006. Measurement of the initial phase of ozone decomposition in water and wastewater by means of a continuous quench-flow system: Application to disinfection and pharmaceutical oxidation. Water Res. 40, 1884–1894. https://doi.org/10.1016/j.watres.2006.02.026

Burnham, K.P., Anderson, D.R., 2002. Model selection and multimodel inference: a practical information-theoretic approach, 2nd ed. ed. Springer, New York.

Bustin, S.A., Benes, V., Garson, J.A., Hellemans, J., Huggett, J., Kubista, M., Mueller, R., Nolan, T., Pfaffl, M.W., Shipley, G.L., 2009. The MIQE Guidelines : Minimum Information for Publication of Quantitative Real-Time PCR Experiments. Clin. Chem. 55, 611–622. https://doi.org/10.1373/clinchem.2008.112797

Casanova, L.M., Weaver, S.R., 2015a. Inactivation of an Enveloped Surrogate Virus in Human Sewage. Environ. Sci. Technol. Lett. 2, 76–78.

https://doi.org/10.1021/acs.estlett.5b00029

Casanova, L.M., Weaver, S.R., 2015b. Evaluation of eluents for the recovery of an enveloped virus from hands by whole-hand sampling. J. Appl. Microbiol. 118, 1210–1216. https://doi.org/10.1111/jam.12777

Centers for Disease Control and Prevention, 2020. CDC 2019-Novel Coronavirus (2019-nCoV) Real-Time RT-PCR Diagnostic Panel.

Cerf, O., 1977. A REVIEW Tailing of Survival Curves of Bacterial Spores. J. Appl. Bacteriol. 42, 1–19. https://doi.org/10.1111/j.1365-2672.1977.tb00665.x

Chan, M.C.W., Lee, N., Chan, P.K.S., To, K.F., Wong, R.Y.K., Ho, W.-S., Ngai, K.L.K., Sung, J.J.Y., 2011. Seasonal influenza A virus in feces of hospitalized adults. Emerg. Infect. Dis. 17, 2038–2042. https://doi.org/10.3201/eid1711.110205

Chick, H., Martin, C.J., 1908. The Principles involved in the Standardisation of Disinfectants and the Influence of Organic Matter upon Germicidal value. J. Hyg. (Lond). 8, 654–697.

Choe, J.K., Richards, D.H., Wilson, C.J., Mitch, W.A., 2015. Degradation of Amino Acids and Structure in Model Proteins and Bacteriophage MS2 by Chlorine, Bromine, and Ozone. Environ. Sci. Technol. 49, 13331–13339. https://doi.org/10.1021/acs.est.5b03813

Chomczynski, P., Sacchi, N., 1987. Single-step method of RNA isolation by acid guanidinium thiocyanate-phenol-chloroform extraction. Anal. Biochem. 162, 156–159. https://doi.org/https://doi.org/10.1016/0003-2697(87)90021-2

Collier, S., Deng, L., Adam, E., Benedict, K., Beshearse, E., Blackstock, A., Bruce, B., Derado, G., Edens, C., Fullerton, K., Gargano, J., Geissler, A., Hall, A., Havelaar, A., Hill, V., Hoekstra, R., Reddy, S., Scallan, E., Stokes, E., Yoder, J., Beach, M., 2021. Estimate of Burden and Direct Healthcare Cost of Infectious Waterborne Disease in the United States. Emerg. Infect. Dis. J. 27. https://doi.org/10.3201/eid2701.190676

Copeland, A., Lytle, D.A., 2014. Measuring the oxidation–reduction potential of important oxidants in drinking water. J. Am. Water Works Assoc. 106, E10–E20.

Cromeans, T.L., Kahler, A.M., Hill, V.R., 2010. Inactivation of adenoviruses,

enteroviruses, and murine norovirus in water by free chlorine and monochloramine. Appl. Environ. Microbiol. 76, 1028–1033. https://doi.org/10.1128/AEM.01342-09

Czekalski, N., Imminger, S., Salhi, E., Veljkovic, M., Kleffel, K., Drissner, D., Hammes, F., Bürgmann, H., von Gunten, U., 2016. Inactivation of Antibiotic Resistant Bacteria and Resistance Genes by Ozone: From Laboratory Experiments to Full-Scale Wastewater Treatment. Environ. Sci. Technol. 50, 11862–11871. https://doi.org/10.1021/acs.est.6b02640

Delignette-Muller, M.L., Dutang, C., 2015. fitdistrplus: An R Package for Fitting Distributions. J. Stat. Softw. 64, 1–34.

Dodd, M.C., 2012. Potential impacts of disinfection processes on elimination and deactivation of antibiotic resistance genes during water and wastewater treatment. J. Environ. Monit. 14, 1754–1771. https://doi.org/10.1039/C2EM00006G

Ducoste, J., Carlson, K., Bellamy, W., 2001a. The integrated disinfection design framework approach to reactor hydraulics characterization. J. Water Supply Res. Technol. 50, 245–261. https://doi.org/10.2166/aqua.2001.0021

Ducoste, J., Carlson, K., Bellamy, W., 2001b. The integrated disinfection design framework approach to reactor hydraulics characterization. J. Water Supply Res. Technol. 50, 245–261. https://doi.org/10.2166/aqua.2001.0021

Dunkin, N., Weng, S., Jacangelo, J.G., Schwab, K.J., 2017. Minimizing Bias in Virally Seeded Water Treatment Studies: Evaluation of Optimal Bacteriophage and Mammalian Virus Preparation Methodologies. Food Environ. Virol. 9, 473–486. https://doi.org/10.1007/s12560-017-9307-3

Dunkin, N., Weng, S.C., Coulter, C.G., Jacangelo, J.G., Schwab, K.J., 2018. Impacts of virus processing on human norovirus GI and GII persistence during disinfection of municipal secondary wastewater effluent. Water Res. 134, 1–12. https://doi.org/10.1016/j.watres.2018.01.053

Espinosa, M.F., Sancho, A.N., Mendoza, L.M., Mota, C.R., Verbyla, M.E., 2020. Systematic review and meta-analysis of time-temperature pathogen inactivation. Int. J. Hyg. Environ. Health 230, 113595. https://doi.org/https://doi.org/10.1016/j.ijheh.2020.113595

Ettayebi, K., Crawford, S.E., Murakami, K., Broughman, J.R., Karandikar, U., Tenge, V.R., Neill, F.H., Blutt, S.E., Zeng, X.-L., Qu, L., Kou, B., Opekun, A.R., Burrin, D., Graham, D.Y., Ramani, S., Atmar, R.L., Estes, M.K., 2016. Replication of human noroviruses in stem cell–derived human enteroids. Science (80-.). 353, 1387 LP – 1393. https://doi.org/10.1126/science.aaf5211

Fabian, P., McDevitt, J.J., Lee, W.-M., Houseman, E.A., Milton, D.K., 2009. An optimized method to detect influenza virus and human rhinovirus from exhaled breath and the airborne environment. J. Environ. Monit. 11, 314–317. https://doi.org/10.1039/B813520G

Ferguson, M., Ihrie, J., 2019. MPN: Most Probable Number and Other Microbial Enumeration Techniques.

Finch, G.R., Fairbairn, N., 1991. Comparative Inactivation of Poliovirus Type 3 and MS2 Coliphage in Demand-Free Phosphate Buffer by Using Ozone. Appl. Environ. Microbiol. 57, 3121–3126.

Fogler, H.S., 2008. Elements of Chemical Reaction Engineering, 3rd ed. Prentice Hall PTR.

Fry, E.E., Knowles, N.J., Newman, J.W.I., Wilsden, G., Rao, Z., King, A.M.Q., Stuart, D.I., 2003. Crystal Structure of Swine Vesicular Disease Virus and Implications for Host Adaptation. J. Virol. 77, 5475 LP – 5486. https://doi.org/10.1128/JVI.77.9.5475-5486.2003

Gardoni, D., Vailati, A., Canziani, R., 2012. Decay of Ozone in Water: A Review. Ozone Sci. Eng. 34, 233–242. https://doi.org/10.1080/01919512.2012.686354

Gendron, L., Verreault, D., Veillette, M., Moineau, S., Duchaine, C., 2010. Evaluation of Filters for the Sampling and Quantification of RNA Phage Aerosols. Aerosol Sci. Technol. 44, 893–901. https://doi.org/10.1080/02786826.2010.501351

Gerba, C.P., Betancourt, W.Q., 2017. Viral Aggregation: Impact on Virus Behavior in the Environment. Environ. Sci. Technol. https://doi.org/10.1021/acs.est.6b05835

Gerba, C.P., Gramos, D.M., Nwachuku, N., 2002. Comparative Inactivation of Enteroviruses and Adenovirus 2 by UV Light. Appl. Environ. Microbiol. 68, 5167

LP – 5169. https://doi.org/10.1128/AEM.68.10.5167-5169.2002

Gerba, C.P., Rose, J.B., Haas, C.N., Crabtree, K.D., 1996. Waterborne rotavirus: A risk assessment. Water Res. 30, 2929–2940. https://doi.org/10.1016/S0043-1354(96)00187-X

Gerba, P.C., Betancourt, Q.W., 2019. Assessing the Occurrence of Waterborne Viruses in Reuse Systems: Analytical Limits and Needs. Pathogens. https://doi.org/10.3390/pathogens8030107

Gomes, A.C., Nunes, J.C., Simões, R.M.S., 2010. Determination of fast ozone oxidation rate for textile dyes by using a continuous quench-flow system. J. Hazard. Mater. 178, 57–65. https://doi.org/10.1016/j.jhazmat.2010.01.043

Gonzalez, R., Curtis, K., Bivins, A., Bibby, K., Weir, M.H., Yetka, K., Thompson, H., Keeling, D., Mitchell, J., Gonzalez, D., 2020. COVID-19 surveillance in Southeastern Virginia using wastewater-based epidemiology. Water Res. 186, 116296. https://doi.org/https://doi.org/10.1016/j.watres.2020.116296

Grabow, W.O.K., 2004. Bacteriophages: update on application as models for viruses in water. Water SA.

Gyürék, L.L., Finch, G.R., 1998. Modeling Water Treatment Chemical Disinfection Kinetics. J. Environ. Eng. 124, 783–793. https://doi.org/10.1061/(ASCE)0733-9372(1998)124:9(783)

Haas, C.N., 1980. A mechanistic kinetic model for chlorine disinfection. Environ. Sci. Technol. 14, 339–340. https://doi.org/10.1021/es60163a012

Haas, C.N., Joffe, J., 1994. Disinfection under Dynamic Conditions: Modification of Hom's Model for Decay. Environ. Sci. Technol. 28, 1367–1369. https://doi.org/10.1021/es00056a028

Haas, C.N., Karra, S.B., 1984. Kinetics of microbial inactivation by chlorine—II Kinetics in the presence of chlorine demand. Water Res. 18, 1451–1454. https://doi.org/10.1016/0043-1354(84)90016-2

Hall, R.M., Sobsey, M.D., 1993. Inactivation of Hepatitis A virus and MS2 by ozone and ozone-hydrogen peroxide in buffered water. Water Sci. Technol. 27, 371–378.

Haramoto, E., Katayama, H., Asami, M., Akiba, M., 2012. Development of a novel method for simultaneous concentration of viruses and protozoa from a single water sample. J. Virol. Methods 182, 62–69. https://doi.org/https://doi.org/10.1016/j.jviromet.2012.03.011

Haramoto, E., Kitajima, M., Hata, A., Torrey, J.R., Masago, Y., Sano, D., Katayama, H., 2018. A review on recent progress in the detection methods and prevalence of human enteric viruses in water. Water Res. 135, 168–186. https://doi.org/10.1016/j.watres.2018.02.004

Haramoto, E., Kitajima, M., Katayama, H., Ito, T., Ohgaki, S., 2009. Development of virus concentration methods for detection of koi herpesvirus in water. J. Fish Dis. 32, 297–300. https://doi.org/10.1111/j.1365-2761.2008.00977.x

Haramoto, E., Malla, B., Thakali, O., Kitajima, M., 2020. First environmental surveillance for the presence of SARS-CoV-2 RNA in wastewater and river water in Japan. Sci. Total Environ. 737, 140405. https://doi.org/https://doi.org/10.1016/j.scitotenv.2020.140405

Hartard, C., Rivet, R., Banas, S., Gantzer, C., 2015. Occurrence of and Sequence Variation among F-Specific RNA Bacteriophage Subgroups in Feces and Wastewater of Urban and Animal Origins. Appl. Environ. Microbiol. 81, 6505 LP – 6515. https://doi.org/10.1128/AEM.01905-15

Hata, A., Honda, R., Hara-Yamamura, H., Meuchi, Y., 2020. Identification of SARS-CoV-2 in wastewater in Japan by multiple molecular assays-implication for wastewater-based epidemiology (WBE). medRxiv 2020.06.09.20126417. https://doi.org/10.1101/2020.06.09.20126417

Hata, A., Katayama, H., Kitajima, M., Visvanathan, C., Nol, C., Furumai, H., 2011. Validation of Internal Controls for Extraction and Amplification of Nucleic Acids from Enteric Viruses in Water Samples. Appl. Environ. Microbiol. 77, 4336–4343. https://doi.org/10.1128/AEM.00077-11

Hata, A., Kitajima, M., Katayama, H., 2013. Occurrence and reduction of human viruses, F-specific RNA coliphage genogroups and microbial indicators at a full-scale wastewater treatment plant in Japan. J. Appl. Microbiol. 114, 545–554. https://doi.org/10.1111/jam.12051

Henquell, C., Mirand, A., Richter, J., Schuffenecker, I., Böttiger, B., Diedrich,

S., Terletskaia-Ladwig, E., Christodoulou, C., Peigue-Lafeuille, H., Bailly, J.-L., 2013. Phylogenetic Patterns of Human Coxsackievirus B5 Arise from Population Dynamics between Two Genogroups and Reveal Evolutionary Factors of Molecular Adaptation and Transmission. J. Virol. 87, 12249 LP – 12259. https://doi.org/10.1128/JVI.02075-13

Herbold, K., Flehmig, B., Botzenhart, K., 1989. Comparison of ozone inactivation, in flowing water, of hepatitis A virus, poliovirus 1, and indicator organisms. Appl. Environ. Microbiol. 55, 2949 LP – 2953.

Hicks, A.L., Duffy, S., 2011. Genus-Specific Substitution Rate Variability among Picornaviruses. J. Virol. 85, 7942 LP – 7947. https://doi.org/10.1128/JVI.02535-10

Hijnen, W.A.M., Beerendonk, E.F., Medema, G.J., 2006. Inactivation credit of UV radiation for viruses, bacteria and protozoan (oo)cysts in water: A review. Water Res. 40, 3–22. https://doi.org/10.1016/j.watres.2005.10.030

Hilder, M.H., 1979. An algebraic expression for first-order reaction in laminar flow. Trans. Inst. Chem. Eng. 57, 143–144.

Hoigné, J., Bader, H., 1983. Rate constants of reactions of ozone with organic and inorganic compounds in water—II: Dissociating organic compounds. Water Res. 17, 185–194. https://doi.org/https://doi.org/10.1016/0043-1354(83)90099-4

Hom, L.W., 1972. Kinetics of chlorine disinfection in an ecosystem. ASCE J Sanit Eng Div.

Hornstra, L.M., Smeets, P.W.M.H., Medema, G.J., 2011. Inactivation of bacteriophage MS2 upon exposure to very low concentrations of chlorine dioxide. Water Res. 45, 1847–1855. https://doi.org/https://doi.org/10.1016/j.watres.2010.11.041

Hull, N.M., Linden, K.G., 2018. Synergy of MS2 disinfection by sequential exposure to tailored UV wavelengths. Water Res. 143, 292–300. https://doi.org/https://doi.org/10.1016/j.watres.2018.06.017

Hunt, N.K., Mariñas, B.J., 1997. Kinetics of Escherichia coli inactivation with ozone. Water Res. 31, 1355–1362. https://doi.org/10.1016/S0043-1354(96)00394-6

Ikner, L.A., Soto-Beltran, M., Bright, K.R., 2011. New method using a

positively charged microporous filter and ultrafiltration for concentration of viruses from tap water. Appl. Environ. Microbiol. 77, 3500–3506. https://doi.org/10.1128/AEM.02705-10

Jiang, H.J., Chen, N., Shen, Z.Q., Yin, J., Qiu, Z.G., Miao, J., Yang, Z.W., Shi, D.Y., Wang, H.R., Wang, X.W., Li, J.W., Yang, D., Jin, M., 2019. Inactivation of Poliovirus by Ozone and the Impact of Ozone on the Viral Genome. Biomed. Environ. Sci. 32, 324–333. https://doi.org/https://doi.org/10.3967/bes2019.044

Kadoya, S., Nishimura, O., Kato, H., Sano, D., 2020. Regularized regression analysis for the prediction of virus inactivation efficiency by chloramine disinfection. Environ. Sci. Water Res. Technol. 6, 3341–3350. https://doi.org/10.1039/D0EW00539H

Kahler, A.M., Cromeans, T.L., Roberts, J.M., Hill, V.R., 2011. Source water quality effects on monochloramine inactivation of adenovirus, coxsackievirus, echovirus, and murine norovirus. Water Res. 45, 1745–1751. https://doi.org/https://doi.org/10.1016/j.watres.2010.11.026

Kahler, A.M., Cromeans, T.L., Roberts, J.M., Hill, V.R., 2010. Effects of source water quality on chlorine inactivation of adenovirus, coxsackievirus, echovirus, and murine norovirus. Appl. Environ. Microbiol. 76, 5159–5164. https://doi.org/10.1128/AEM.00869-10

Katayama, H., Haramoto, E., Oguma, K., Yamashita, H., Tajima, A., Nakajima, H., Ohgaki, S., 2008. One-year monthly quantitative survey of noroviruses, enteroviruses, and adenoviruses in wastewater collected from six plants in Japan. Water Res. 42, 1441–1448. https://doi.org/10.1016/j.watres.2007.10.029

Kato, R., Asami, T., Utagawa, E., Furumai, H., Katayama, H., 2018. Pepper mild mottle virus as a process indicator at drinking water treatment plants employing coagulation-sedimentation, rapid sand filtration, ozonation, and biological activated carbon treatments in Japan. Water Res. 132, 61–70. https://doi.org/10.1016/j.watres.2017.12.068

Kazama, S., Masago, Y., Tohma, K., Souma, N., Imagawa, T., Suzuki, A., Liu, X., Saito, M., Oshitani, H., Omura, T., 2016. Temporal dynamics of norovirus determined through monitoring of municipal wastewater by pyrosequencing and virological surveillance of gastroenteritis cases. Water Res. 92, 244–253.

https://doi.org/https://doi.org/10.1016/j.watres.2015.10.024

Keegan, A., Wati, S., Robinson, B., 2012. Chlor(am)ine disinfection of human pathogenic viruses in recycled waters, Smart Water Fund.

Kim, C.K., Gentile, D.M., Sproul, O.J., 1980. Mechanism of Ozone Inactivation of Bacteriophage f2. Appl. Environ. Microbiol. 39, 210 LP – 218.

King, A.M.Q., Adams, M.J., Carsten, E.B., Lefkowitz, E.J., 2012. Virus Taxonomy: Classification and Nomenclature of Viruses. Ninth Report of the International Committee on Taxonomy of Viruses., Elsevier Inc. https://doi.org/10.1007/s13398-014-0173-7.2

Kitajima, M., Ahmed, W., Bibby, K., Carducci, A., Gerba, C.P., Hamilton, K.A., Haramoto, E., Rose, J.B., 2020. SARS-CoV-2 in wastewater: State of the knowledge and research needs. Sci. Total Environ. 139076. https://doi.org/https://doi.org/10.1016/j.scitotenv.2020.139076

Kitajima, M., Tohya, Y., Matsubara, K., Haramoto, E., Utagawa, E., Katayama, H., Ohgaki, S., 2008. Use of Murine Norovirus as a Novel Surrogate to Evaluate Resistance of Human Norovirus to Free Chlorine Disinfection in Drinking Water Supply System. Environ. Eng. Res. 45, 361–370. https://doi.org/10.11532/proes1992.45.361

Kroneman, A., Vennema, H., Deforche, K., Avoort, H. v. d., Peñaranda, S., Oberste, M.S., Vinjé, J., Koopmans, M., 2011. An automated genotyping tool for enteroviruses and noroviruses. J. Clin. Virol. 51, 121–125. https://doi.org/https://doi.org/10.1016/j.jcv.2011.03.006

Kumar, M., Patel, A.K., Shah, A. V, Raval, J., Rajpara, N., Joshi, M., Joshi, C.G., 2020. First proof of the capability of wastewater surveillance for COVID-19 in India through detection of genetic material of SARS-CoV-2. Sci. Total Environ. 746, 141326. https://doi.org/https://doi.org/10.1016/j.scitotenv.2020.141326

La Rosa, G., Iaconelli, M., Mancini, P., Bonanno Ferraro, G., Veneri, C., Bonadonna, L., Lucentini, L., Suffredini, E., 2020. First detection of SARS-CoV-2 in untreated wastewaters in Italy. Sci. Total Environ. 736, 139652. https://doi.org/https://doi.org/10.1016/j.scitotenv.2020.139652

Lee, S.-H., Kim, S.-J., 2002. Detection of infectious enteroviruses and

adenoviruses in tap water in urban areas in Korea. Water Res. 36, 248–256. https://doi.org/https://doi.org/10.1016/S0043-1354(01)00199-3

Lewis, G.D., Metcalf, T.G., 1988. Polyethylene glycol precipitation for recovery of pathogenic viruses, including hepatitis A virus and human rotavirus, from oyster, water, and sediment samples. Appl. Environ. Microbiol. 54, 1983–1988.

Li, W., Li, M., Bolton, J.R., Qiang, Z., 2016. Configuration optimization of UV reactors for water disinfection with computational fluid dynamics: Feasibility of using particle minimum UV dose as a performance indicator. Chem. Eng. J. 306, 1–8. https://doi.org/https://doi.org/10.1016/j.cej.2016.07.042

Lim, M.Y., Kim, J.-M., Lee, J.E., Ko, G., 2010. Characterization of Ozone Disinfection of Murine Norovirus. Appl. Environ. Microbiol. 76, 1120 LP – 1124. https://doi.org/10.1128/AEM.01955-09

Lodder, W.J., Buisman, A.M., Rutjes, S.A., Heijne, J.C., Teunis, P.F., de Roda Husman, A.M., 2012. Feasibility of Quantitative Environmental Surveillance in Poliovirus Eradication Strategies. Appl. Environ. Microbiol. 78, 3800 LP – 3805. https://doi.org/10.1128/AEM.07972-11

Loison, P., Majou, D., Gelhaye, E., Boudaud, N., Gantzer, C., 2016. Impact of reducing and oxidizing agents on the infectivity of Qβ phage and the overall structure of its capsid. FEMS Microbiol. Ecol. 92, 1–11. https://doi.org/10.1093/femsec/iw153

Lukashev, A.N., Vakulenko, Y.A., 2017. Molecular evolution of types in non-polio enteroviruses. J. Gen. Virol. https://doi.org/10.1099/jgv.0.000966

Lukashev, A.N., Vakulenko, Y.A., Turbabina, N.A., Deviatkin, A.A., Drexler, J.F., 2018. Molecular epidemiology and phylogenetics of human enteroviruses: Is there a forest behind the trees? Rev. Med. Virol. 28, e2002. https://doi.org/10.1002/rmv.2002

Lytle, C.D., Routson, L.B., 1995. Minimized virus binding for tests of barrier materials. Appl. Environ. Microbiol. 61, 643–649.

Maffettone, R., Manoli, K., Santoro, D., Passalacqua, K.D., Wobus, C.E., Sarathy, S., 2020. Performic Acid Disinfection of Municipal Secondary Effluent Wastewater: Inactivation of Murine Norovirus, Fecal Coliforms, and Enterococci.

Environ. Sci. Technol. https://doi.org/10.1021/acs.est.0c05144

Manoli, K., Sarathy, S., Maffettone, R., Santoro, D., 2019. Detailed modeling and advanced control for chemical disinfection of secondary effluent wastewater by peracetic acid. Water Res. 153, 251–262. https://doi.org/10.1016/j.watres.2019.01.022

Matsuura, K., Hasegawa, S., Nakayama, T., Morita, O., Uetake, H., 1984. Viral Pollution of the Rivers in Toyama City. Microbiol. Immunol. 28, 575–588. https://doi.org/10.1111/j.1348-0421.1984.tb00710.x

Mattle, M.J., Kohn, T., 2012. Inactivation and Tailing during UV254 Disinfection of Viruses: Contributions of Viral Aggregation, Light Shielding within Viral Aggregates, and Recombination. Environ. Sci. Technol. 46, 10022–10030. https://doi.org/10.1021/es302058v

Medema, G., Heijnen, L., Elsinga, G., Italiaander, R., Brouwer, A., 2020. Presence of SARS-Coronavirus-2 RNA in Sewage and Correlation with Reported COVID-19 Prevalence in the Early Stage of the Epidemic in The Netherlands. Environ. Sci. Technol. Lett. https://doi.org/10.1021/acs.estlett.0c00357

Meister, S., Verbyla, M.E., Klinger, M., Kohn, T., 2018. Variability in Disinfection Resistance between Currently Circulating Enterovirus B Serotypes and Strains. Environ. Sci. Technol. 52, 3696–3705. https://doi.org/10.1021/acs.est.8b00851

Meng, Q.S., Gerba, C.P., 1996. Comparative inactivation of enteric adenoviruses, poliovirus and coliphages by ultraviolet irradiation. Water Res. 30, 2665–2668. https://doi.org/10.1016/S0043-1354(96)00179-0

Mijatovic-Rustempasic, S., Tam, K.I., Kerin, T.K., Lewis, J.M., Gautam, R., Quaye, O., Gentsch, J.R., Bowen, M.D., 2013. Sensitive and specific quantitative detection of rotavirus A by one-step real-time reverse transcription-PCR assay without antecedent double-stranded-RNA denaturation. J. Clin. Microbiol. 51, 3047–3054. https://doi.org/10.1128/JCM.01192-13

Murakami, M., Hata, A., Honda, R., Watanabe, T., 2020. Letter to the Editor: Wastewater-Based Epidemiology Can Overcome Representativeness and Stigma Issues Related to COVID-19. Environ. Sci. Technol. 54, 5311. https://doi.org/10.1021/acs.est.0c02172

Naghavi, M., Abajobir, A.A., Abbafati, C., Abbas, K.M., Abd-Allah, F., Abera, S.F., Aboyans, V., Adetokunboh, O., Afshin, A., Agrawal, A., Ahmadi, A., Ahmed, M.B., Aichour, A.N., Aichour, M.T.E., Aichour, I., Aiyar, S., Alahdab, F., Al-Aly, Z., Alam, K., Alam, N., Alam, T., Alene, K.A., Al-Eyadhy, A., Ali, S.D., Alizadeh-Navaei, R., Alkaabi, J.M., Alkerwi, A., Alla, F., Allebeck, P., Allen, C., Al-Raddadi, R., Alsharif, U., Altirkawi, K.A., Alvis-Guzman, N., Amare, A.T., Amini, E., Ammar, W., Amoako, Y.A., Anber, N., Andersen, H.H., Andrei, C.L., Androudi, S., Ansari, H., Antonio, C.A.T., Anwari, P., Ärnlöv, J., Arora, M., Artaman, A., Aryal, K.K., Asayesh, H., Asgedom, S.W., Atey, T.M., Avila-Burgos, L., Avokpaho, E.F.G., Awasthi, A., Babalola, T.K., Bacha, U., Balakrishnan, K., Barac, A., Barboza, M.A., Barker-Collo, S.L., Barquera, S., Barregard, L., Barrero, L.H., Baune, B.T., Bedi, N., Beghi, E., Béjot, Y., Bekele, B.B., Bell, M.L., Bennett, J.R., Bensenor, I.M., Berhane, A., Bernabé, E., Betsu, B.D., Beuran, M., Bhatt, S., Biadgilign, S., Bienhoff, K., Bikbov, B., Bisanzio, D., Bourne, R.R.A., Breitborde, N.J.K., Bulto, L.N.B., Bumgarner, B.R., Butt, Z.A., Cahuana-Hurtado, L., Cameron, E., Campuzano, J.C., Car, J., Cárdenas, R., Carrero, J.J., Carter, A., Casey, D.C., Castañeda-Orjuela, C.A., Catalá-López, F., Charlson, F.J., Chibueze, C.E., Chimed-Ochir, O., Chisumpa, V.H., Chitheer, A.A., Christopher, D.J., Ciobanu, L.G., Cirillo, M., Cohen, A.J., Colombara, D., Cooper, C., Cowie, B.C., Criqui, M.H., Dandona, L., Dandona, R., Dargan, P.I., das Neves, J., Davitoiu, D. V, Davletov, K., de Courten, B., Defo, B.K., Degenhardt, L., Deiparine, S., Deribe, K., Deribew, A., Dey, S., Dicker, D., Ding, E.L., Djalalinia, S., Do, H.P., Doku, D.T., Douwes-Schultz, D., Driscoll, T.R., Dubey, M., Duncan, B.B., Echko, M., El-Khatib, Z.Z., Ellingsen, C.L., Enayati, A., Ermakov, S.P., Erskine, H.E., Eskandarieh, S., Esteghamati, A., Estep, K., Farinha, C.S. e S., Faro, A., Farzadfar, F., Feigin, V.L., Fereshtehnejad, S.-M., Fernandes, J.C., Ferrari, A.J., Feyissa, T.R., Filip, I., Finegold, S., Fischer, F., Fitzmaurice, C., Flaxman, A.D., Foigt, N., Frank, T., Fraser, M., Fullman, N., Fürst, T., Furtado, J.M., Gakidou, E., Garcia-Basteiro, A.L., Gebre, T., Gebregergs, G.B., Gebrehiwot, T.T., Gebremichael, D.Y., Geleijnse, J.M., Genova-Maleras, R., Gesesew, H.A., Gething, P.W., Gillum, R.F., Giref, A.Z., Giroud, M., Giussani, G., Godwin, W.W., Gold, A.L., Goldberg, E.M., Gona, P.N., Gopalani, S.V., Gouda, H.N., Goulart, A.C., Griswold, M., Gupta, R., Gupta, T., Gupta, V., Gupta, P.C., Haagsma, J.A., Hafezi-Nejad, N., Hailu, A.D., Hailu, G.B., Hamadeh, R.R., Hambisa, M.T., Hamidi, S., Hammami, M., Hancock, J., Handal, A.J., Hankey, G.J., Hao, Y., Harb, H.L., Hareri, H.A., Hassanvand, M.S.,

Havmoeller, R., Hay, S.I., He, F., Hedayati, M.T., Henry, N.J., Heredia-Pi, I.B., Herteliu, C., Hoek, H.W., Horino, M., Horita, N., Hosgood, H.D., Hostiuc, S., Hotez, P.J., Hoy, D.G., Huynh, C., Iburg, K.M., Ikeda, C., Ileanu, B.V., Irenso, A.A., Irvine, C.M.S., Islam, S.M.S., Jacobsen, K.H., Jahanmehr, N., Jakovljevic, M.B., Javanbakht, M., Jayaraman, S.P., Jeemon, P., Jha, V., John, D., Johnson, C.O., Johnson, S.C., Jonas, J.B., Jürisson, M., Kabir, Z., Kadel, R., Kahsay, A., Kamal, R., Karch, A., Karimi, S.M., Karimkhani, C., Kasaeian, A., Kassaw, N.A., Kassebaum, N.J., Katikireddi, S.V., Kawakami, N., Keiyoro, P.N., Kemmer, L., Kesavachandran, C.N., Khader, Y.S., Khan, E.A., Khang, Y.-H., Khoja, A.T.A., Khosravi, M.H., Khosravi, A., Khubchandani, J., Kiadaliri, A.A., Kieling, C., Kievlan, D., Kim, Y.J., Kim, D., Kimokoti, R.W., Kinfu, Y., Kissoon, N., Kivimaki, M., Knudsen, A.K., Kopec, J.A., Kosen, S., Koul, P.A., Koyanagi, A., Kulikoff, X.R., Kumar, G.A., Kumar, P., Kutz, M., Kyu, H.H., Lal, D.K., Lalloo, R., Lambert, T.L.N., Lan, Q., Lansingh, V.C., Larsson, A., Lee, P.H., Leigh, J., Leung, J., Levi, M., Li, Y., Li Kappe, D., Liang, X., Liben, M.L., Lim, S.S., Liu, P.Y., Liu, A., Liu, Y., Lodha, R., Logroscino, G., Lorkowski, S., Lotufo, P.A., Lozano, R., Lucas, T.C.D., Ma, S., Macarayan, E.R.K., Maddison, E.R., Magdy Abd El Razek, M., Majdan, M., Majdzadeh, R., Majeed, A., Malekzadeh, R., Malhotra, R., Malta, D.C., Manguerra, H., Manyazewal, T., Mapoma, C.C., Marczak, L.B., Markos, D., Martinez-Raga, J., Martins-Melo, F.R., Martopullo, I., McAlinden, C., McGaughey, M., McGrath, J.J., Mehata, S., Meier, T., Meles, K.G., Memiah, P., Memish, Z.A., Mengesha, M.M., Mengistu, D.T., Menota, B.G., Mensah, G.A., Meretoja, T.J., Meretoja, A., Millear, A., Miller, T.R., Minnig, S., Mirarefin, M., Mirrakhimov, E.M., Misganaw, A., Mishra, S.R., Mohamed, I.A., Mohammad, K.A., Mohammadi, A., Mohammed, S., Mokdad, A.H., Mola, G.L.D., Mollenkopf, S.K., Molokhia, M., Monasta, L., Montañez, J.C., Montico, M., Mooney, M.D., Moradi-Lakeh, M., Moraga, P., Morawska, L., Morozoff, C., Morrison, S.D., Mountjoy-Venning, C., Mruts, K.B., Muller, K., Murthy, G.V.S., Musa, K.I., Nachega, J.B., Naheed, A., Naldi, L., Nangia, V., Nascimento, B.R., Nasher, J.T., Natarajan, G., Negoi, I., Ngunjiri, J.W., Nguyen, C.T., Nguyen, Q. Le, Nguyen, T.H., Nguyen, G., Nguyen, M., Nichols, E., Ningrum, D.N.A., Nong, V.M., Noubiap, J.J.N., Ogbo, F.A., Oh, I.-H., Okoro, A., Olagunju, A.T., Olsen, H.E., Olusanya, B.O., Olusanya, J.O., Ong, K., Opio, J.N., Oren, E., Ortiz, A., Osman, M., Ota, E., PA, M., Pacella, R.E., Pakhale, S., Pana, A., Panda, B.K., Panda-Jonas, S., Papachristou, C., Park, E.-K., Patten, S.B., Patton, G.C., Paudel, D., Paulson, K., Pereira, D.M., Perez-Ruiz, F., Perico, N., Pervaiz, A., Petzold, M.,

Phillips, M.R., Pigott, D.M., Pinho, C., Plass, D., Pletcher, M.A., Polinder, S., Postma, M.J., Pourmalek, F., Purcell, C., Qorbani, M., Quintanilla, B.P.A., Radfar, A., Rafay, A., Rahimi-Movaghar, V., Rahman, M.H.U., Rahman, M., Rai, R.K., Ranabhat, C.L., Rankin, Z., Rao, P.C., Rath, G.K., Rawaf, S., Ray, S.E., Rehm, J., Reiner, R.C., Reitsma, M.B., Remuzzi, G., Rezaei, S., Rezai, M.S., Rokni, M.B., Ronfani, L., Roshandel, G., Roth, G.A., Rothenbacher, D., Ruhago, G.M., SA, R., Saadat, S., Sachdev, P.S., Sadat, N., Safdarian, M., Safi, S., Safiri, S., Sagar, R., Sahathevan, R., Salama, J., Salamati, P., Salomon, J.A., Samy, A.M., Sanabria, J.R., Sanchez-Niño, M.D., Santomauro, D., Santos, I.S., Santric Milicevic, M.M., Sartorius, B., Satpathy, M., Schmidt, M.I., Schneider, I.J.C., Schulhofer-Wohl, S., Schutte, A.E., Schwebel, D.C., Schwendicke, F., Sepanlou, S.G., Servan-Mori, E.E., Shackelford, K.A., Shahraz, S., Shaikh, M.A., Shamsipour, M., Shamsizadeh, M., Sharma, J., Sharma, R., She, J., Sheikhbahaei, S., Shey, M., Shi, P., Shields, C., Shigematsu, M., Shiri, R., Shirude, S., Shiue, I., Shoman, H., Shrime, M.G., Sigfusdottir, I.D., Silpakit, N., Silva, J.P., Singh, J.A., Singh, A., Skiadaresi, E., Sligar, A., Smith, D.L., Smith, A., Smith, M., Sobaih, B.H.A., Soneji, S., Sorensen, R.J.D., Soriano, J.B., Sreeramareddy, C.T., Srinivasan, V., Stanaway, J.D., Stathopoulou, V., Steel, N., Stein, D.J., Steiner, C., Steinke, S., Stokes, M.A., Strong, M., Strub, B., Subart, M., Sufiyan, M.B., Sunguya, B.F., Sur, P.J., Swaminathan, S., Sykes, B.L., Tabarés-Seisdedos, R., Tadakamadla, S.K., Takahashi, K., Takala, J.S., Talongwa, R.T., Tarawneh, M.R., Tavakkoli, M., Taveira, N., Tegegne, T.K., Tehrani-Banihashemi, A., Temsah, M.-H., Terkawi, A.S., Thakur, J.S., Thamsuwan, O., Thankappan, K.R., Thomas, K.E., Thompson, A.H., Thomson, A.J., Thrift, A.G., Tobe-Gai, R., Topor-Madry, R., Torre, A., Tortajada, M., Towbin, J.A., Tran, B.X., Troeger, C., Truelsen, T., Tsoi, D., Tuzcu, E.M., Tyrovolas, S., Ukwaja, K.N., Undurraga, E.A., Updike, R., Uthman, O.A., Uzochukwu, B.S.C., van Boven, J.F.M., Vasankari, T., Venketasubramanian, N., Violante, F.S., Vlassov, V.V., Vollset, S.E., Vos, T., Wakayo, T., Wallin, M.T., Wang, Y.-P., Weiderpass, E., Weintraub, R.G., Weiss, D.J., Werdecker, A., Westerman, R., Whetter, B., Whiteford, H.A., Wijeratne, T., Wiysonge, C.S., Woldeyes, B.G., Wolfe, C.D.A., Woodbrook, R., Workicho, A., Xavier, D., Xiao, Q., Xu, G., Yaghoubi, M., Yakob, B., Yano, Y., Yaseri, M., Yimam, H.H., Yonemoto, N., Yoon, S.-J., Yotebieng, M., Younis, M.Z., Zaidi, Z., Zaki, M.E.S., Zegeye, E.A., Zenebe, Z.M., Zerfu, T.A., Zhang, A.L., Zhang, X., Zipkin, B., Zodpey, S., Lopez, A.D., Murray, C.J.L., 2017. Global, regional, and national age-sex specific mortality for 264 causes of death, 1980-2016: a systematic analysis for

the Global Burden of Disease Study 2016. Lancet 390, 1151–1210. https://doi.org/10.1016/S0140-6736(17)32152-9

Nikogosyan, D.N., 1990. Two-quantum UV Photochemistry of Nucleic Acids: Comparison with Conventional Low-intensity UV Photochemistry and Radiation Chemistry. Int. J. Radiat. Biol. 57, 233–299. https://doi.org/10.1080/09553009014552411

Nuanualsuwan, S., Cliver, D.O., 2003. Capsid functions of inactivated human picornaviruses and feline calicivirus. Appl. Environ. Microbiol. https://doi.org/10.1128/AEM.69.1.350-357.2003

Oberste, M.S., Maher, K., Kilpatrick, D.R., Pallansch, M.A., 1999. Molecular Evolution of the Human Enteroviruses: Correlation of Serotype with VP1 Sequence and Application to Picornavirus Classification. J. Virol. 73, 1941 LP – 1948.

Oberste, M.S., Nix, W.A., Maher, K., Pallansch, M.A., 2003. Improved molecular identification of enteroviruses by RT-PCR and amplicon sequencing. J. Clin. Virol. 26, 375–377. https://doi.org/https://doi.org/10.1016/S1386-6532(03)00004-0

Oh, C., Sun, P.P., Araud, E., Nguyen, T.H., 2020. Mechanism and efficacy of virus inactivation by a microplasma UV lamp generating monochromatic UV irradiation at 222 nm. Water Res. 186, 116386. https://doi.org/https://doi.org/10.1016/j.watres.2020.116386

Olivieri, A.W., Crook, J., Anderson, M.A., Bull, R.J., Drewes, J.E., Haas, C.N., Jakubowski, W., McCarty, P.L., Nelson, K.L., Rose, J.B., Sedlak, D.L., Wade, T.J., 2016. Expert Panel Final Report: Evaluation of the Feasibility of Developing Uniform Water Recycling Criteria for Direct Potable Reuse. Sacramento, CA.

Payment, P., Tremblay, M., Trudel, M., 1985a. Relative resistance to chlorine of poliovirus and coxsackievirus isolates from environmental sources and drinking water. Appl. Environ. Microbiol. 49, 981–983.

Payment, P., Trudel, M., Plante, R., 1985b. Elimination of viruses and indicator bacteria at each step of treatment during preparation of drinking water at seven water treatment plants. Appl. Environ. Microbiol. 49.

Pecson, B.M., Ackermann, M., Kohn, T., 2011. Framework for using quantitative PCR as a nonculture based method to estimate virus infectivity. Environ. Sci. Technol. https://doi.org/10.1021/es103488e

R Core Team, 2019. R: A Language and Environment for Statistical Computing.

Rachmadi, A.T., Kitajima, M., Kato, T., Kato, H., Okabe, S., Sano, D., 2020. Required Chlorination Doses to Fulfill the Credit Value for Disinfection of Enteric Viruses in Water: A Critical Review. Environ. Sci. Technol. https://doi.org/10.1021/acs.est.9b01685

Randazzo, W., Truchado, P., Cuevas-Ferrando, E., Simón, P., Allende, A., Sánchez, G., 2020. SARS-CoV-2 RNA in wastewater anticipated COVID-19 occurrence in a low prevalence area. Water Res. 181, 115942. https://doi.org/https://doi.org/10.1016/j.watres.2020.115942

Rice, J., Westerhoff, P., 2015. Spatial and Temporal Variation in De Facto Wastewater Reuse in Drinking Water Systems across the U.S.A. Environ. Sci. Technol. 49, 982–989. https://doi.org/10.1021/es5048057

Rockey, N., Young, S., Kohn, T., Pecson, B., Wobus, C.E., Raskin, L., Wigginton, K.R., 2020. UV Disinfection of Human Norovirus: Evaluating Infectivity Using a Genome-Wide PCR-Based Approach. Environ. Sci. Technol. https://doi.org/10.1021/acs.est.9b05747

Roy, D., Englebrecht, R.S., Chian, E.S.K., 1982. Comparative inactivation of six enteroviruses by ozone. J. Am. Water Works Assoc. 74, 660–664.

Roy, D., Wong, P.K., Engelbrecht, R.S., Chian, E.S., 1981. Mechanism of enteroviral inactivation by ozone. Appl. Environ. Microbiol. 41, 718 LP – 723.

Rusiñol, M., Martínez-Puchol, S., Forés, E., Itarte, M., Girones, R., Bofill-Mas, S., 2020. Concentration methods for the quantification of coronavirus and other potentially pandemic enveloped virus from wastewater. Curr. Opin. Environ. Sci. Heal. https://doi.org/https://doi.org/10.1016/j.coesh.2020.08.002

Sanjuan, R., Nebot, M.R., Chirico, N., Mansky, L.M., Belshaw, R., 2010. Viral Mutation Rates. J. Virol. https://doi.org/10.1128/JVI.00694-10

Sano, D., Amarasiri, M., Hata, A., Watanabe, T., Katayama, H., 2016. Risk management of viral infectious diseases in wastewater reclamation and reuse:

Review. Environ. Int. 91, 220–229. https://doi.org/10.1016/j.envint.2016.03.001

Severin, B.F., Suidan, M.T., Engelbrecht, R.S., 1983. Kinetic modeling of U.V. disinfection of water. Water Res. 17, 1669–1678. https://doi.org/https://doi.org/10.1016/0043-1354(83)90027-1

Sherchan, S.P., Shahin, S., Ward, L.M., Tandukar, S., Aw, T.G., Schmitz, B., Ahmed, W., Kitajima, M., 2020. First detection of SARS-CoV-2 RNA in wastewater in North America: A study in Louisiana, USA. Sci. Total Environ. 140621. https://doi.org/https://doi.org/10.1016/j.scitotenv.2020.140621

Shi, H., Xagoraraki, I., Parent, K.N., Bruening, M.L., Tarabara, V. V, 2016. Elution Is a Critical Step for Recovering Human Adenovirus 40 from Tap Water and Surface Water by Cross-Flow Ultrafiltration. Appl. Environ. Microbiol. 82, 4982 LP – 4993. https://doi.org/10.1128/AEM.00870-16

Shin, G.-A., Sobsey, M.D., 2003. Reduction of Norwalk Virus, Poliovirus 1, and Bacteriophage MS2 by Ozone Disinfection of Water. Appl. Environ. Microbiol. 69, 3975 LP – 3978. https://doi.org/10.1128/AEM.69.7.3975-3978.2003

Shirasaki, N., Matsushita, T., Matsui, Y., Koriki, S., 2020. Suitability of pepper mild mottle virus as a human enteric virus surrogate for assessing the efficacy of thermal or free-chlorine disinfection processes by using infectivity assays and enhanced viability PCR. Water Res. 186, 116409. https://doi.org/https://doi.org/10.1016/j.watres.2020.116409

Shirato, K., Nao, N., Katano, H., Takayama, I., Saito, S., Kato, F., Katoh, H., Sakata, M., Nakatsu, Y., Mori, Y., Kageyama, T., Matsuyama, S., Takeda, M., 2020. Development of Genetic Diagnostic Methods for Novel Coronavirus 2019 (nCoV-2019) in Japan. Jpn. J. Infect. Dis. advpub. https://doi.org/10.7883/yoken.JJID.2020.061

Sigmon, C., Shin, G.-A., Mieog, J., Linden, K.G., 2015. Establishing Surrogate-Virus Relationships for Ozone Disinfection of Wastewater. Environ. Eng. Sci. 32, 451–460. https://doi.org/10.1089/ees.2014.0496

Sigstam, T., Gannon, G., Cascella, M., Pecson, B.M., Wigginton, K.R., Kohn, T., 2013. Subtle differences in virus composition affect disinfection kinetics and mechanisms. Appl. Environ. Microbiol. 79, 3455–3467. https://doi.org/10.1128/AEM.00663-13

Sigstam, T., Rohatschek, A., Zhong, Q., Brennecke, M., Kohn, T., 2014. On the cause of the tailing phenomenon during virus disinfection by chlorine dioxide. Water Res. 48, 82–89. https://doi.org/10.1016/j.watres.2013.09.023

Simonet, J., Gantzer, C., 2006. Inactivation of Poliovirus 1 and F-Specific RNA Phages and Degradation of Their Genomes by UV Irradiation at 254 Nanometers. Appl. Environ. Microbiol. 72, 7671 LP – 7677. https://doi.org/10.1128/AEM.01106-06

Smeets, P.W.M.H., van der Helm, A.W.C., Dullemont, Y.J., Rietveld, L.C., van Dijk, J.C., Medema, G.J., 2006. Inactivation of Escherichia coli by ozone under bench-scale plug flow and full-scale hydraulic conditions. Water Res. 40, 3239–3248. https://doi.org/10.1016/j.watres.2006.06.025

Sobsey, M.D., Fuji, T., Shields, P.A., 1988. Inactivation of hepatitis A virus and model viruses in water by free choline and monochloramine. Water Sci. Technol. 20, 385–391.

Soller, J.A., Eftim, S.E., Nappier, S.P., 2019. Comparison of Predicted Microbiological Human Health Risks Associated with de Facto, Indirect, and Direct Potable Water Reuse. Environ. Sci. Technol. 53, 13382–13389. https://doi.org/10.1021/acs.est.9b02002

Soller, J.A., Eftim, S.E., Nappier, S.P., 2018. Direct potable reuse microbial risk assessment methodology: Sensitivity analysis and application to State log credit allocations. Water Res. 128, 286–292. https://doi.org/https://doi.org/10.1016/j.watres.2017.10.034

Stephens, K.W., Hutchins, R.J., Dauphin, L.A., 2010. Cross-platform evaluation of commercial real-time reverse transcription PCR master mix kits using a quantitative 5′nuclease assay for Ebola virus. Mol. Cell. Probes 24, 370–375. https://doi.org/https://doi.org/10.1016/j.mcp.2010.08.004

Templeton, M.R., Andrews, R.C., Hofmann, R., 2008. Particle-Associated Viruses in Water: Impacts on Disinfection Processes. Crit. Rev. Environ. Sci. Technol. 38, 137–164. https://doi.org/10.1080/10643380601174764

Teunis, P.F.M., Moe, C.L., Liu, P., Miller, S.E., Lindesmith, L., Baric, R.S., Pendu, J. Le, Calderon, R.L., 2008. Norwalk Virus: How Infectious is It? J. Med. Virol. 80. https://doi.org/10.1002/jmv

Thurston-Enriquez, J.A., Haas, C.N., Jacangelo, J., Gerba, C.P., 2005. Inactivation of enteric adenovirus and feline calicivirus by ozone. Water Res. 39, 3650–3656. https://doi.org/10.1016/j.watres.2005.06.006

Thurston-Enriquez, J.A., Haas, C.N., Jacangelo, J., Gerba, C.P., 2003. Chlorine Inactivation of Adenovirus Type 40 and Feline Calicivirus. Appl. Environ. Microbiol. 69, 3979 LP – 3985. https://doi.org/10.1128/AEM.69.7.3979-3985.2003

Title 22 and 17 California Code of Regulations, 2015. Regulations related to recycled water state water resources control board. Division of Drinking Water. July 16, 2015.

Torii, S., Hashimoto, T., Do, A.T., Furumai, H., Katayama, H., 2019a. Impact of repeated pressurization on virus removal by reverse osmosis membranes for household water treatment. Environ. Sci. Water Res. Technol. 5, 910–919. https://doi.org/10.1039/C8EW00944A

Torii, S., Hashimoto, T., Do, A.T., Furumai, H., Katayama, H., 2019b. Repeated pressurization as a potential cause of deterioration in virus removal by aged reverse osmosis membrane used in households. Sci. Total Environ. 695, 133814. https://doi.org/10.1016/j.scitotenv.2019.133814

Torii, S., Itamochi, M., Katayama, H., 2020. Inactivation kinetics of waterborne virus by ozone determined by a continuous quench flow system. Water Res. 186, 116291. https://doi.org/10.1016/j.watres.2020.116291

Torrey, J., von Gunten, U., Kohn, T., 2019. Differences in viral disinfection mechanisms as revealed by quantitative transfection of Echovirus 11 genomes. Appl. Environ. Microbiol. AEM.00961-19. https://doi.org/10.1128/AEM.00961-19

Tracy, S., Chapman, N.M., Mahy, B.W.J., 2013. Group B Coxsackieviruses, Current Topics in Microbiology and Immunology. Springer Berlin Heidelberg.

USEPA, 2016. Six-Year Review 3 Technical Support Document for Microbial Contaminant Regulations.

USEPA, 2010. Long Term 2 Enhanced Surface Water Treatment Rule: Toolbox Guidance Manual.

USEPA, 2006. Ultraviolet Disinfection Guidance Manual for the Final Long Term 2 Enhanced Surface Water Treatment Rule. Washington, DC.

USEPA, 1999. Disinfection Profiling and Benchmarking Guidance Manual.

USEPA, 1991. Guidance Manual for Compliance With the Filtration and Disinfection Requirements for Public Water Systems Using Surface Water Sources.

von Gunten, U., 2018. Oxidation Processes in Water Treatment: Are We on Track? Environ. Sci. Technol. 52, 5062–5075. https://doi.org/10.1021/acs.est.8b00586

von Sonntag, C., von Gunten, U., 2012. Chemistry of Ozone in Water and Wastewater Treatment: From Basic Principles to Applications. https://doi.org/10.2166/9781780400839

Waldman, P., Meseguer, A., Lucas, F., Moulin, L., Wurtzer, S., 2017. Interaction of Human Enteric Viruses with Microbial Compounds: Implication for Virus Persistence and Disinfection Treatments. Environ. Sci. Technol. 51, 13633–13640. https://doi.org/10.1021/acs.est.7b03875

Wati, S., Robinson, B.S., Mieog, J., Blackbeard, J., Keegan, A.R., 2018. Chlorine inactivation of coxsackievirus B5 in recycled water destined for non-potable reuse. J. Water Health wh2018393–wh2018393.

Watson, H.E., 1908. A Note on the Variation of the Rate of Disinfection with Change in the Concentration of the Disinfectant. J. Hyg. (Lond). 8, 536–542.

Wigginton, K.R., Kohn, T., 2012. Virus disinfection mechanisms: the role of virus composition, structure, and function. Curr. Opin. Virol. 2, 84–89. https://doi.org/10.1016/j.coviro.2011.11.003

Wigginton, K.R., Pecson, B.M., Sigstam, T., Bosshard, F., Kohn, T., 2012. Virus inactivation mechanisms: Impact of disinfectants on virus function and structural integrity. Environ. Sci. Technol. 46, 12069–12078. https://doi.org/10.1021/es3029473

Wolf, C., Pavese, A., von Gunten, U., Kohn, T., 2019. Proxies to monitor the inactivation of viruses by ozone in surface water and wastewater effluent. Water Res. 166, 115088. https://doi.org/10.1016/j.watres.2019.115088

Wolf, C., von Gunten, U., Kohn, T., 2018. Kinetics of Inactivation of Waterborne Enteric Viruses by Ozone. Environ. Sci. Technol. 52, 2170–2177.

https://doi.org/10.1021/acs.est.7b05111

Wolf, S., Hewitt, J., Greening, G.E., 2010. Viral multiplex quantitative PCR assays for tracking sources of fecal contamination. Appl. Environ. Microbiol. 76, 1388–1394. https://doi.org/10.1128/AEM.02249-09

Wölfel, R., Corman, V.M., Guggemos, W., Seilmaier, M., Zange, S., Müller, M.A., Niemeyer, D., Jones, T.C., Vollmar, P., Rothe, C., Hoelscher, M., Bleicker, T., Brünink, S., Schneider, J., Ehmann, R., Zwirglmaier, K., Drosten, C., Wendtner, C., 2020. Virological assessment of hospitalized patients with COVID-2019. Nature 581, 465–469. https://doi.org/10.1038/s41586-020-2196-x

World Health Organization, 2020. Transmission of SARS-CoV-2: implications for infection prevention precautions [WWW Document]. URL https://www.who.int/news-room/commentaries/detail/transmission-of-sars-cov-2-implications-for-infection-prevention-precautions (accessed 1.13.20).

World Health Organization, 2017. Safely managed drinking water - thematic report on drinking water 2017. Geneva, Switzerland.

World Health Organization, 2016. Quantitative Microbial Risk Assessment: Application for Water Safety Management. https://doi.org/10.1002/9781118910030

World Health Organization, 2011. Chapter 7: Microbial aspects, Guidelines for drinking-water quality, fourth edition 2011. Geneva, Switzerland.

Wu, F., Xiao, A., Zhang, J., Moniz, K., Endo, N., Armas, F., Bonneau, R., Brown, M.A., Bushman, M., Chai, P.R., Duvallet, C., Erickson, T.B., Foppe, K., Ghaeli, N., Gu, X., Hanage, W.P., Huang, K.H., Lee, W.L., Matus, M., McElroy, K.A., Nagler, J., Rhode, S.F., Santillana, M., Tucker, J.A., Wuertz, S., Zhao, S., Thompson, J., Alm, E.J., 2020a. SARS-CoV-2 titers in wastewater foreshadow dynamics and clinical presentation of new COVID-19 cases. medRxiv 2020.06.15.20117747. https://doi.org/10.1101/2020.06.15.20117747

Wu, F., Zhang, J., Xiao, A., Gu, X., Lee, W.L., Armas, F., Kauffman, K., Hanage, W., Matus, M., Ghaeli, N., Endo, N., Duvallet, C., Poyet, M., Moniz, K., Washburne, A.D., Erickson, T.B., Chai, P.R., Thompson, J., Alm, E.J., 2020b. SARS-CoV-2 Titers in Wastewater Are Higher than Expected from Clinically Confirmed Cases. mSystems 5, e00614-20.

https://doi.org/10.1128/mSystems.00614-20

Ye, Y., Chang, P.H., Hartert, J., Wigginton, K.R., 2018. Reactivity of Enveloped Virus Genome, Proteins, and Lipids with Free Chlorine and UV254. Environ. Sci. Technol. 52, 7698–7708. https://doi.org/10.1021/acs.est.8b00824

Ye, Y., Ellenberg, R.M., Graham, K.E., Wigginton, K.R., 2016. Survivability, Partitioning, and Recovery of Enveloped Viruses in Untreated Municipal Wastewater. Environ. Sci. Technol. 50, 5077–5085. https://doi.org/10.1021/acs.est.6b00876

Zhong, Q., Carratalà, A., Ossola, R., Bachmann, V., Kohn, T., 2017a. Cross-resistance of UV- or chlorine dioxide-resistant echovirus 11 to other disinfectants. Front. Microbiol. 8. https://doi.org/10.3389/fmicb.2017.01928

Zhong, Q., Carratalà, A., Shim, H., Bachmann, V., Jensen, J.D., Kohn, T., 2017b. Resistance of Echovirus 11 to ClO2Is Associated with Enhanced Host Receptor Use, Altered Entry Routes, and High Fitness. Environ. Sci. Technol. https://doi.org/10.1021/acs.est.7b03288

Acknowledgments

First of all, I would like to express my greatest appreciation to my mentor, Prof. Hiroyuki Katayama, who have continuously supervised and guided me for five years to peruse my Master and PhD degree in the University of Tokyo. He provided me with a tremendous amount of exciting opportunities, such as collaborative research projects (with Toyama Institute of Health, Kitasato University, Department of Chemistry and Biotechnology, the University of Tokyo), international activities (e.g., sampling in Vietnam and Indonesia, international conferences, and research visits in Switzerland, France, Sweden, and the USA), outreach activities (e.g., Water Forum in Todai) and, more importantly, drinking parties with our and his colleagues. I believe these experiences greatly enhanced my attitude toward researches and expanded my viewpoints. I would also like to thank Prof. Hiroaki Furumai, Assoc. Prof. Futoshi Kurisu, and Assoc. Prof. Ikuro Kasuga and Assist. Prof. Takashi Hashimoto for their supervision and comments on my research.

I would like to greatly appreciate all the committee members, Prof. Hiroaki Furumai, Assoc. Prof. Kumiko Oguma, Assist. Prof. Takashi Hashimoto, and Asssist. Prof. Takashi Hashimoto for their valuable comments and suggestions to improve this dissertation.

I deeply appreciate all the co-authors, Dr. Fuminari Miura at Center for Marine Environmental Studies, Ehime University, Dr. Masae Itamochi at Toyama Institute of Health, Japan, Dr. Kei Haga and Prof. Kazuhiko Katayama at Kitasato University, for helping us with publishing our research results. Dr. Miura is my senior in the current department, Department of Urban Engineering. He provided me with fundamental mathematical knowledge and greatly helped with developing the disinfection model in Chapter 5. Additionally, he always gives me nice advice regarding my private life, overseas life, and career plan. Dr. Itamochi kindly provided us with environmental isolates of *Enterovirus B*, used in Chapters 3 and 5, and advised on our manuscript from a virological viewpoint. Dr. Haga kindly instructed the protocols of RNA sequencing and bioinformatics. Prof. K Katayama supervised and instructed me and provided an environment to perform sequencing during the research stay at Kitasato University. Dr. Haga and Prof. K Katayama provided me with a fruitful comment on our manuscript.

I also would like to appreciate continuous supports from my seniors, juniors, and staff in our laboratory. Dr. Akihiko Hata provided me with a lot of helpful advice and comments on my research and my career. Especially, I greatly acknowledge him for training us for an oral presentation at the international conference in Airbnb house in

Arizona. The experience greatly enhanced my confidence in my presentation skills. Dr. Vu Duc Canh is my senior in our laboratory. We were in the same graduate students room for five years. I was very happy to encourage each other and work together in our laboratory. Ms. Nakagawa kindly helped me with her technical assistance and fruitful advice on everything, including my private life. Ms. Kakimoto kindly helped me with an administration issues regarding any research activities.

I would like to thank Japan Student Services Organization (JASSO), the School of Engineering, the University of Tokyo, Nishihara Cultural Foundation, Iwadare Scholarship Foundation, and Japan Society for the Promotion of Science (JSPS) for their financial support and housing. These supports enabled me to intensively work on research activities and to pursue PhD degree.

I am greatly appreciated all the faculty members, staff members and students of the Department of Urban Engineering, the University of Tokyo, for their kind supports in my academic and social life.

Finally, I would like to express my greatest gratitude to my family, my wife and my friends for continuous encouragement and inspiration throughout the years.

February 16, 2021

Shotaro TORII